Supporting Information

Tris(pentafluoroethyl)difluorophosphorane for Fluoride Abstraction and Ligand Exchange Reactions of *N*-Heterocyclic Carbene and Cyclic Alkyl(amino)carbene Copper(I) Fluorides

Melanie Riethmann,[a] Steffen A. Föhrenbacher,[a] Christian Luz,[a]] Nikolai V. Ignat'ev,[a,b,c] Maik Finze[a,b]* and Udo Radius[a]*

[a] M. Riethmann, S. A. Föhrenbacher, C. Luz, Prof. Dr. M. Finze, Prof. Dr. U. Radius
Institute of Inorganic Chemistry, Julius-Maximilians-Universität Würzburg
Am Hubland, 97074 Würzburg, Germany
maik.finze@uni-wuerzburg.de, u.radius@uni-wuerzburg.de.
http://www.ak-radius.de; http://go.uniwue.de/finze-group

[b] Institute for Sustainable Chemistry & Catalysis with Boron (ICB), Julius-Maximilians-Universität Würzburg
Am Hubland, 97074 Würzburg, Germany

[c] Consultant, Merck KGaA, Frankfurter Straße 250, 64293 Darmstadt, Germany

Contents

1) Crystallographic Details

Crystal data were collected on a Bruker X8 Apex-2 diffractometer with a CCD area detector and graphite monochromated Mo−Kα radiation or a Rigaku XtaLAB Synergy-DW diffractometer with an Hy-Pix-6000HE detector and monochromated Cu−Kα radiation equipped with an Oxford Cryo 800 cooling unit. Crystals were immersed in a film of perfluoropolyether oil on a glass fiber MicroMount™ (MiTeGen) and data were collected at 100 K. Images were processed with Bruker or CrySalis software packages and equivalent reflections were merged. Corrections for Lorentz-polarization effects and absorption were performed if necessary and the structures were solved by direct methods. Subsequent difference Fourier syntheses revealed the positions of all other non-hydrogen atoms. Structures were solved by using the ShelXTL software package.[1] All non-hydrogen atoms were refined anisotropically. All hydrogen atoms were assigned to idealized geometric positions and were included in structure factors calculations.

Crystallographic data for the structures reported in this paper have been deposited with the Cambridge Crystallographic Data Centre as supplementary publication no.s CCDC 2444352 (**1**), CCDC 2444336 (**3**), CCDC 2444351 (**5**), CCDC 2444348 (**6**), CCDC 2444349 (**7**), CCDC 2444343 (**10**), CCDC 2444350 (**11**), CCDC 2444347 (**12**), CCDC 2444346 (**16**), CCDC 2444340 (**17**), CCDC 2444345 (**19**), CCDC 2444342 (**20**), CCDC 2444338 (**21**), CCDC 2444341 (**23**), CCDC 2444344 (**24**), CCDC 2444339 (**26**), CCDC 2444337 (**27**). Copies of the data can be obtained free of charge on application to CCDC.

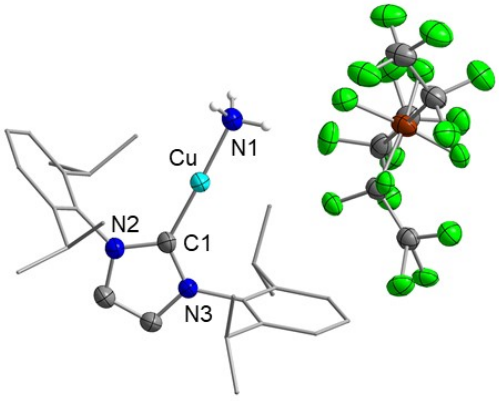

Figure S1. Molecular structure of [(IDipp)Cu(NH_3)]$^+$**FAP**$^-$ (**1**) in the solid state (ellipsoids set at the 50% probability level; Dipp substituents are shown as wire-and-stick models). Hydrogen atoms except the ones directly bound to N1 and co-crystallized solvent molecule are omitted for clarity. Only one of two independent molecules in the asymmetric unit is shown. Selected bond lengths [Å] and angles [°]: Cu−C1 1.882(3), Cu−N1 1.908(3), N2−C1 1.360(4), N3−C1 1.353(43); C1−Cu−N1 177.19(15).

Crystal Data for [(IDipp)Cu(NH_3)]$^+$FAP$^-$ (1): $C_{67}H_{79}Cl_3Cu_2F_{36}N_6P_2$, M_r = 1947.73, T = 100.00(2) K, λ = 1.54184 Å, colorless block, 0.200×0.290×0.400 mm^3, triclinic space group $P\bar{1}$, a = 12.7224(2) Å, b = 16.7168(2) Å, c = 21.0326(2) Å, α = 98.6100(10)°, β = 107.3470(10)°, γ = 95.1630(10)°, V = 4178.42(10) Å^3, Z = 2, ρ_{calcd} = 1.548 g·cm^{-3}, μ = 2.990 mm^{-1}, F(000) = 1972, 84475 reflections,

-16 ≤ h ≤ 16, -21 ≤ k ≤ 19, -26 ≤ l ≤ 26, 2.240° < θ < 80.839°, completeness 97.6%, 17912 independent reflections, 15317 reflections observed with [I > 2***23*** (I)], 1552 parameters, 1638 restraints, *R* indices (all data) R_1 = 0.0981, wR_2 = 0.2629, final *R* indices [I > 2σ(I)] R_1 = 0.0904, wR_2 = 0.2520, largest difference peak and hole 1.380 and −1.053 e Å^{-3}, GooF = 1.034.

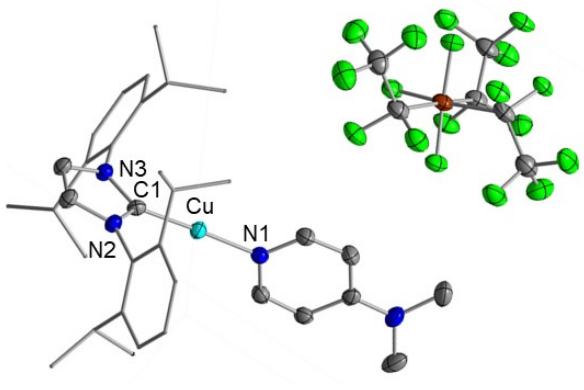

Figure S2. Molecular structure of [(IDipp)Cu($C_7H_{10}N_2$)]$^+$**FAP**$^-$ (**3**) in the solid state (ellipsoids set at the 50% probability level; Dipp substituents are shown as wire-and-stick models). Hydrogen atoms and co-crystallized solvent molecule are omitted for clarity. Only one of two independent molecules in the asymmetric unit is shown. Selected bond lengths [Å] and angles [°]: Cu−C1 1.875(2), Cu−N1 1.8785(19), N2−C1 1.357(3), N3−C1 1.355(3); C1−Cu−N1 175.45(9).

Crystal Data for [(IDipp)Cu($C_7H_{10}N_2$)]$^+$FAP$^-$ (3): $C_{81}H_{93}Cl_3Cu_2F_{36}N_8P_2$, M_r = 2158.00, T = 100.00(2) K, λ = 1.54184 Å, colorless block, 0.117×0.196×0.283 mm^3, triclinic space group $P\bar{1}$, a = 11.33150(10) Å, b = 19.5059(2) Å, c = 23.4078(3)°, α = 102.6080(10)°, β = 99.0610(10)°, γ = 102.3770(10)°, V = 4817.16(9) Å^3, Z = 2, ρ_{calcd} = 1.488 g·cm^{-3}, μ = 2.660 mm^{-1}, F(000) = 2196, 70913 reflections, −14 ≤ h ≤ 14, −24 ≤ k ≤ 23, −28 ≤ l ≤ 29, 1.980° < θ < 74.501°, completeness 98.5%, 19406 independent reflections, 17127 reflections observed with [I > 2σ(I)], 1655 parameters, 2541 restraints, *R* indices (all data) R_1 = 0.0584, wR_2 = 0.1571, final *R* indices [I > 2σ(I)] R_1 = 0.0533, wR_2 = 0.1519, largest difference peak and hole 1.562 and −1.211 e Å^{-3}, GooF = 1.063.

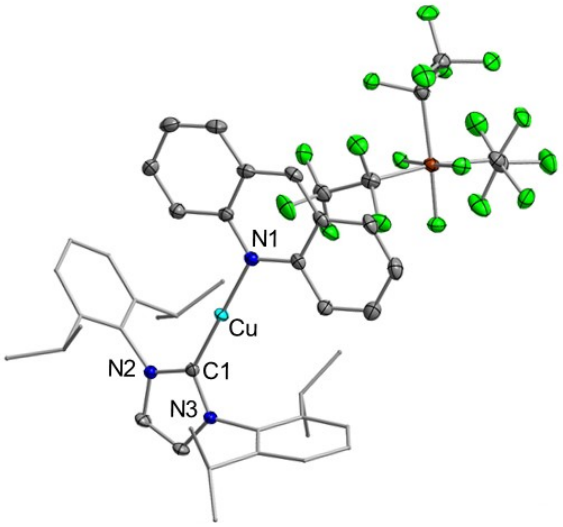

Figure S3. Molecular structure of [(IDipp)Cu($C_{13}H_9N$)]$^+$**FAP**$^-$ (**5**) in the solid state (ellipsoids set at the 50% probability level; Dipp substituents are shown as wire-and-stick models). Hydrogen atoms are omitted for clarity. Selected bond lengths [Å] and angles [°]: Cu−C1 1.8789(18), Cu−N1 1.9038(15), N2−C1 1.359(2), N3−C1 1.358(2); C1−Cu−N1 179.62(7).

Crystal Data for [(IDipp)Cu($C_{13}H_9N$)]$^+$FAP$^-$ (5): $C_{46}H_{45}CuF_{18}N_3P$, M_r = 1076.36, T = 100.00(2) K, λ = 0.71073 Å, colorless block, 0.070×0.160×0.240 mm^3, monoclinic space group $P2_1/c$, a = 16.1433(4) Å, b = 16.7833(3) Å, c = 17.5037(4) Å, β = 103.057(3)°, V = 4619.80(18) Å^3, Z = 4, ρ_{calcd} = 1.548 g·cm^{-3}, μ = 0.618 mm^{-1}, F(000) = 2192, 53839 reflections, −22 ≤ h ≤ 20, −21 ≤ k ≤ 24, −23 ≤ l ≤ 24, 1.969° < θ < 31.243°, completeness 81.8%, 12308 independent reflections, 9039 reflections observed with [I > 2σ(I)], 630 parameters, 0 restraints, *R* indices (all data) R_1 = 0.0657, wR_2 = 0.1047, final *R* indices [I > 2σ(I)] R_1 = 0.0399, wR_2 = 0.0939, largest difference peak and hole 0.608 and −0.548 e Å^{-3}, GooF = 1.016.

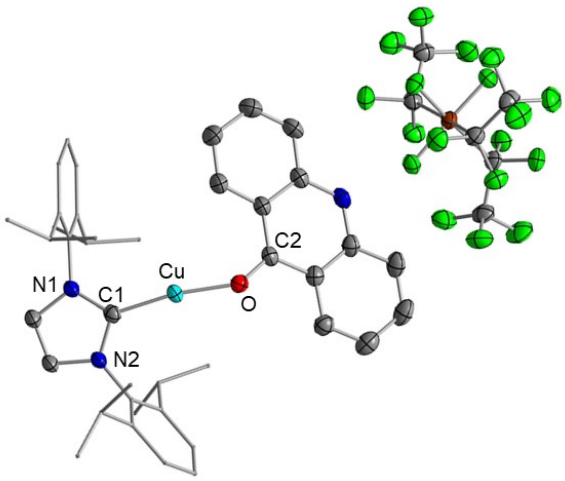

Figure S4. Molecular structure of [(IDipp)Cu(η^1-O=$C_{13}H_9N$)]$^+$**FAP**$^-$ (**6**) in the solid state (ellipsoids set at the 50% probability level; Dipp substituents are shown as wire-and-stick models). Hydrogen atoms and a co-crystallized solvent molecule are omitted for clarity. Selected bond lengths [Å] and angles [°]: Cu−C1 1.863(2), Cu−O 1.8313(16), N1−C1 1.356(3), N2−C1 1.352(3), C1−Cu−O 169.58(9), Cu−O−C2 139.64(16).

Crystal Data for [(IDipp)Cu(η^1-O=$C_{13}H_9N$)]$^+$FAP$^-$ (6): $C_{49}H_{52}CuF_{18}N_3OP$, M_r = 1135.44, T = 100.00(2) K, λ = 1.54184 Å, colorless block, 0.150×0.170×0.480 mm^3, triclinic space group $P\bar{1}$, a = 12.70530(10) Å, b = 13.77550(10) Å, c = 16.5290(2) Å, α = 73.0900(10)°, β = 68.1900(10)°, γ = 86.4690(10)°, V = 2566.21(5) Å^3, Z = 2, ρ_{calcd} = 1.469 g·cm^{-3}, μ = 1.837mm^{-1}, F(000) = 1162, 53129 reflections, −16 ≤ h ≤ 13, −17 ≤ k ≤ 17, −20 ≤ l ≤ 20, 3.008° < θ < 79.995°, completeness 97.9%, 10954 independent reflections, 9734 reflections observed with [I > 2σ(I)], 656 parameters, 0 restraints, *R* indices (all data) R_1 = 0.0572, wR_2 = 0.1495, final *R* indices [I > 2σ(I)] R_1 = 0.0522, wR_2 = 0.1450, largest difference peak and hole 1.034 and −0.991 e Å^{-3}, GooF = 1.075.

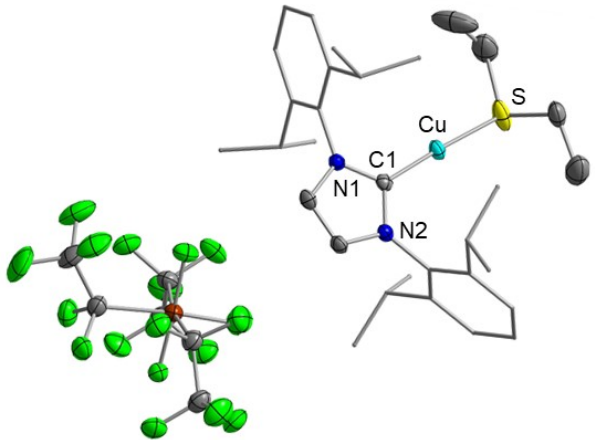

Figure S5. Molecular structure of [(IDipp)Cu($C_4H_{10}S$)]$^+$**FAP**$^-$ (**7**) in the solid state (ellipsoids set at the 50% probability level; Dipp substituents are shown as wire-and-stick models). Hydrogen atoms are omitted for clarity. Selected bond lengths [Å] and angles [°]: Cu−C1 1.887(3), Cu−S 2.1705(8), N1−C1 1.351(3), N2−C1 1.353(3); C1−Cu−S 176.49(8).

Crystal Data for [(IDipp)Cu($C_4H_{10}S$)]$^+$FAP$^-$ (7): $C_{37}H_{46}CuF_{18}N_2PS$, M_r = 987.33, T = 100.00(2) K, λ = 1.54184 Å, colorless block, 0.099×0.193×0.362 mm^3, monoclinic space group $P2_1/n$, a = 15.3271(2) Å, b = 16.1495(2) Å, c = 17.9666(3) Å, β = 101.9160(10)°, V = 4351.35(11) Å^3, Z = 4, ρ_{calcd} = 1.507 g·cm^{-3}, μ = 2.481 mm^{-1}, F(000) = 2016, 33531 reflections, −19 ≤ h ≤ 18, −20 ≤ k ≤ 11, −22 ≤ l ≤ 20, 3.456° < θ < 74.496°, completeness 98.4%, 8751 independent reflections, 7643 reflections observed with [I > 2σ(I)], 551 parameters, 0 restraints, R indices (all data) R_1 = 0.0635, wR_2 = 0.1589, final R indices [I > 2σ(I)] R_1 = 0.0572, wR_2 = 0.1531, largest difference peak and hole 1.802 and −1.040 e Å^{-3}, GooF = 1.053.

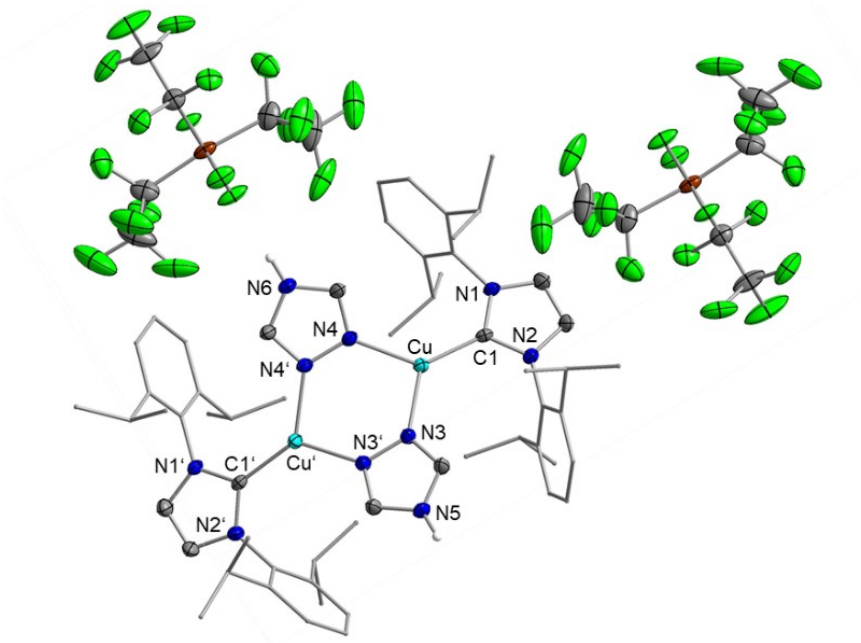

Figure S6. Molecular structure of $[\{(IDipp)Cu\}_2(C_2N_3H_3)_2]^{2+}$**2FAP**$^-$ (**10**) in the solid state (ellipsoids set at the 50% probability level; Dipp substituents are shown as wire-and-stick models). Hydrogen atoms except the ones bound to H5 and N6 and a co-crystallized solvent molecule are omitted for clarity. Selected bond lengths [Å] and angles [°]: Cu−C1 1.937(6), Cu−N3 2.038(5), Cu−N4 2.035(4), N1−C1 1.350(7), N2−C1 1.354(7), C1−Cu−N3 128.50(19), C1−Cu−N4 132.12(19).

Crystal Data for $[\{(IDipp)Cu\}_2(C_2N_3H_3)_2]^{2+}2FAP^-$ (10): $C_{73}H_{81}Cl_9Cu_2F_{36}N_{10}P_2$, M_r = 2290.54, T = 100.00(2) K, λ = 1.54184 Å, colorless block, 0.130×0.190×0.260 mm^3, monoclinic space group $P2_1/m$, a = 14.6881(2) Å, b = 21.2716(5) Å, c = 14.9560(3) Å, β = 91.888(2)°, V = 4670.31(16) Å^3, Z = 2, ρ_{calcd} = 1.629 g·cm^{-3}, μ = 4.331 mm^{-1}, F(000) = 2308, 48516 reflections, −18 ≤ h ≤ 18, −26 ≤ k ≤ 26, −19 ≤ l ≤ 14, 2.956° < θ < 80.331°, completeness 98.6%, 48516 independent reflections, 40756 reflections observed with [I > 2σ(I)], 721 parameters, 654 restraints, *R* indices (all data) R_1 = 0.1142, wR_2 = 0.2842, final *R* indices [I > 2σ(I)] R_1 = 0.1028, wR_2 = 0.2751, largest difference peak and hole 2.562 and −2.645 e Å^{-3}, GooF = 1.041.

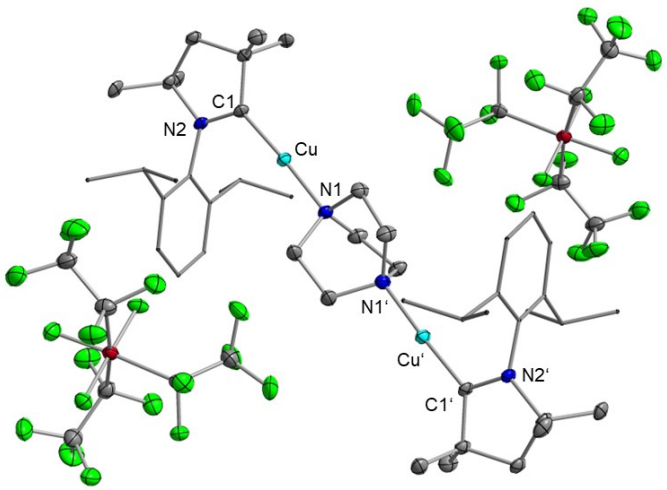

Figure S7. Molecular structure of $[\{(cAAC^{Me})Cu\}_2\{C_6H_{12}N_2\}]^{2+}$**2FAP**$^-$ (**11**) in the solid state (ellipsoids set at the 50% probability level; Dipp substituents are shown as wire-and-stick models). Hydrogen atoms are omitted for clarity. Selected bond lengths [Å] and angles [°]: Cu−C1 1.900(4), Cu−N1 1.927(3), N2−C1 1.306(5); C1−Cu−N1 176.68(15).

Crystal Data for [{(cAAC^{Me})Cu}$_2${$C_6H_{12}N_2$}]$^{2+}$2FAP$^-$ (11): $C_{58}H_{74}Cu_2F_{36}N_4P_2$, M_r = 1700.23, T = 100.00(2) K, λ = 0.71073 Å, colorless block, 0.120×0.180×0.330 mm^3, monoclinic space group $P2_1/n$, a = 13.8496(4) Å, b = 17.3310(5) Å, c = 14.6695(4) Å, β = 101.873(2)°, V = 3445.75(17) Å^3, Z = 2, ρ_{calcd} = 1.639 g·cm^{-3}, μ = 0.802 mm^{-1}, F(000) = 1724, 41410 reflections, −17 ≤ h ≤ 16, −25 ≤ k ≤ 21, −20 ≤ l ≤ 18, 2.185° < θ < 31.270°, completeness 80.2%, 9022 independent reflections, 6872 reflections observed with [I > 2σ(I)], 931 parameters, 2055 restraints, *R* indices (all data) R_1 = 0.0566, wR_2 = 0.0948, final *R* indices [I > 2σ(I)] R_1 = 0.0367, wR_2 = 0.0860, largest difference peak and hole 0.471 and −0.322 e Å^{-3}, GooF = 1.036.

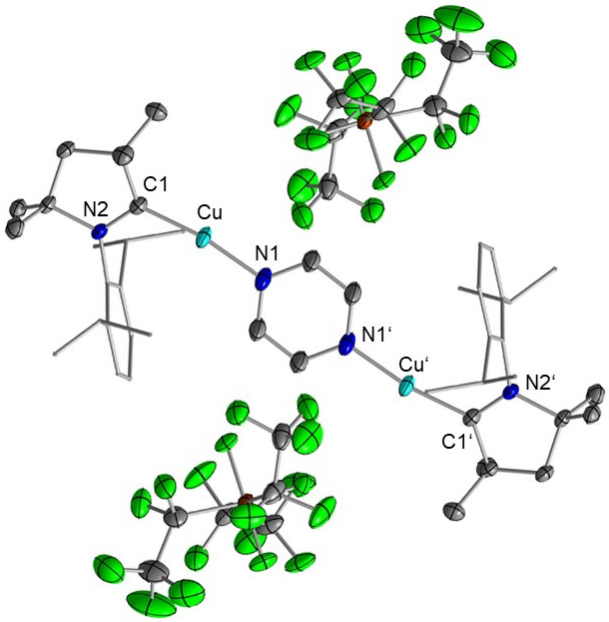

Figure S8. Molecular structure [{(cAAC^{Me})Cu}$_2${$C_4H_4N_2$}]$^{2+}$**2FAP**$^-$ (**12**) in the solid state (ellipsoids set at the 50% probability level; Dipp substituents are shown as wire-and-stick models). Hydrogen atoms are omitted for clarity. Selected bond lengths [Å] and angles [°]: Cu−C1 1.890(3), Cu−N1 1.906(2), N2−C1 1.299(4); C1−Cu−N1 170.45(12).

Crystal Data for [{(cAAC^{Me})Cu}$_2${$C_4H_4N_2$}]$^{2+}$2FAP$^-$ (12): $C_{56}H_{66}Cu_2F_{36}N_4P_2$, M_r = 1668.14, T = 100.00(2) K, λ = 1.54184 Å, yellow block, 0.090×0.160×0.220 mm^3, monoclinic space group $P2_1/n$, a = 13.98110(10) Å, b = 17.2021(2) Å, c = 14.09990(10) Å, β = 102.6220(10)°, V = 3309.13(5) Å^3, Z = 2, ρ_{calcd} = 1.674 g·cm^{-3}, μ = 2.562 mm^{-1}, F(000) = 1684, 34985 reflections, −11 ≤ h ≤ 17, −21 ≤ k ≤ 21, −17 ≤ l ≤ 18, 4.034° < θ < 79.988°, completeness 97.8%, 7062 independent reflections, 6386 reflections observed with [I > 2σ(I)], 685 parameters, 720 restraints, *R* indices (all data) R_1 = 0.0666, wR_2 = 0.1852, final *R* indices [I > 2σ(I)] R_1 = 0.0625, wR_2 = 0.0625, largest difference peak and hole 1.232 and −0.425 e Å^{-3}, GooF = 1.058.

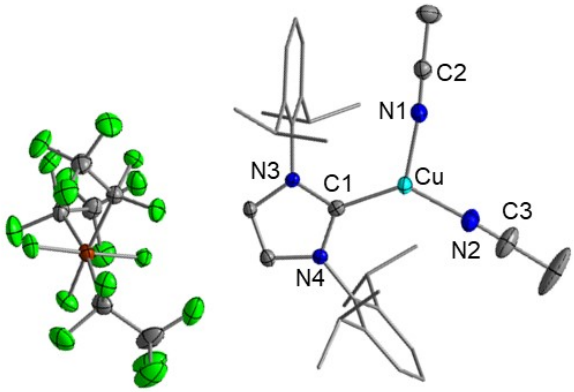

Figure S9. Molecular structure of [(IDipp)Cu(N≡CMe)$_2$]$^+$**FAP**$^-$ (**16**) in the solid state (ellipsoids set at the 50% probability level; Dipp substituents are shown as wire-and-stick models). Hydrogen atoms are omitted for clarity. Selected bond lengths [Å] and angles [°]: Cu−C1 1.909(2), Cu−N1 1.967(2), Cu−N2 1.938(2), N3−C1 1.360(3), N4−C1 1.358(3), N1−C2 1.133(3), N2−C3 1.123(4); C1−Cu−N1 121.11(9), C1−Cu−N2 131.08(10), N1−Cu−N2 107.71(9).

Crystal Data for [(IDipp)Cu(N≡CMe)$_2$]$^+$FAP$^-$ (16): $C_{37}H_{42}CuF_{18}N_4P$, M_r = 979.25, T = 100.00(10) K, λ = 1.54184 Å, colorless block, 0.116×0.146×0.249 mm^3, monoclinic space group $P2_1/c$, a = 12.60010(10) Å, b = 22.0470(2) Å, c = 16.4358(2) Å, β = 106.5990(10)°, V = 4375.51(8) Å^3, Z = 4, ρ_{calcd} = 1.487 g·cm^{-3}, μ = 2.044 mm^{-1}, F(000) = 1992, 45059 reflections, −15 ≤ h ≤ 15, −26 ≤ k ≤ 27, −19 ≤ l ≤ 20, 3.449° < θ < 74.500°, completeness 99.3%, 8901 independent reflections, 7750 reflections observed with [I > 2σ(I)], 560, parameters, 0 restraints, *R* indices (all data) R_1 = 0.0602, wR_2 = 0.1113, final *R* indices [I > 2σ(I)] R_1 = 0.0503, wR_2 = 0.1064, largest difference peak and hole 0.478 and −0.501 e Å^{-3}, GooF = 0.928.

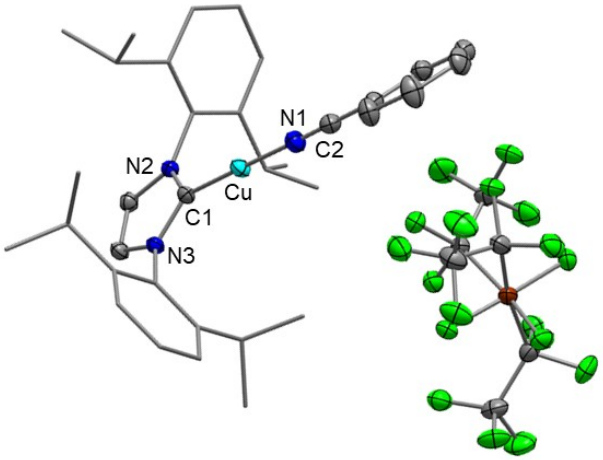

Figure S10. Molecular structure of [(IDipp)Cu(N≡CPh)]$^+$**FAP**$^-$ (**17**) in the solid state (ellipsoids set at the 50% probability level; Dipp substituents are shown as wire-and-stick models). Hydrogen atoms are omitted for clarity. Selected bond lengths [Å] and angles [°]: Cu−C1 1.8848(15), Cu−N1 1.8453(14), N2−C1 1.350(2), N3−C1 1.3503(19), N1−C2 1.141(2); C1−Cu−N1 178.03(7), Cu−N1−C2 176.85(15).

Crystal Data for [(IDipp)Cu(N≡CPh)]$^+$FAP$^-$ (17): $C_{40}H_{41}CuF_{18}N_3P$, M_r = 1000.27, T = 99.99(10) K, λ = 1.54184 Å, colorless block, 0.178×0.203×0.294 mm^3, monoclinic space group $P2_1/c$, a = 13.9829(2) Å, b = 17.2015(3) Å, c = 18.1556(3) Å, β = 96.7310(10)°, V = 4336.81(12) Å^3, Z = 4, ρ_{calcd} = 1.532 g·cm^{-3}, μ = 2.071 mm^{-1}, F(000) = 2032, 32423 reflections, −17 ≤ h ≤ 16, −21 ≤ k ≤ 19,

−21 ≤ l ≤ 22, 3.551° < θ < 74.494°, completeness 98.0%, 8700 independent reflections, 7608 reflections observed with [I > 2σ(I)], 576 parameters, 0 restraints, *R* indices (all data) R_1 = 0.0378, wR_2 = 0.0865, final *R* indices [I > 2σ(I)] R_1 = 0.0320, wR_2 = 0.0835, largest difference peak and hole 0.399 and −0.559 e Å^{-3}, GooF = 1.072.

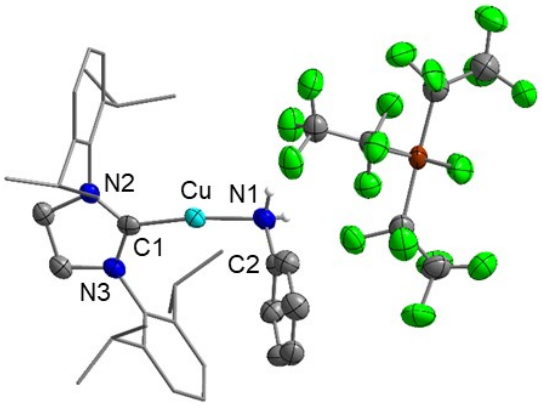

Figure S11. Molecular structure of [(SIDipp)Cu(NH_2Ph)]$^+$**FAP**$^-$ (**19**) in the solid state (ellipsoids set at the 50% probability level; Dipp substituents are shown as wire-and-stick models). Hydrogen atoms except these of the nitrogen atom of the aniline ligand and a co-crystallized solvent molecule are omitted for clarity. Only one of two independent molecules in the asymmetric unit is shown. Selected bond lengths [Å] and angles [°] (average out of two independent molecules in the asymmetric unit): Cu−C1 1.893(3), Cu−N1 1.935(3), N2−C1 1.331(4), N3−C1 1.335(4), N1−C2 1.452(4); C1−Cu−N1 171.88(13), Cu−N1−C2 110.9(2).

Crystal Data for [(SIDipp)Cu(NH_2Ph)]$^+$FAP$^-$ (19): $C_{85}H_{98}Cu_2F_{36}N_6P_2$, M_r = 2076.71, T = 99.98(12) K, λ = 1.54184 Å, colorless block, 0.220×0.111×0.080 mm^3, monoclinic space group $P2_1/c$, a = 10.93360(10) Å, b = 43.2109(5) Å, c = 19.8400(2) Å, β = 98.0870(10)°, V = 9280.21(17) Å^3, Z = 4, ρ_{calcd} = 1.486 Mg/m^3, μ = 1.956 mm^{-1}, F(000) = 4248, 67731 reflections, −13 ≤ h ≤ 13, −54 ≤ k ≤ 53, −24 ≤ l ≤ 15, 2.471° < θ < 74.499°, completeness 97.6%, 18532 independent reflections, 15520 reflections observed with [I > 2σ(I)], 1714 parameters, 3349 restraints, *R* indices (all data) R_1 = 0.0650, wR_2 = 0.1577, final *R* indices [I > 2σ(I)] R_1 = 0.0770, wR_2 = 0.1653, largest difference peak and hole 1.153 and −0.486 e Å^{-3}, GooF = 1.051.

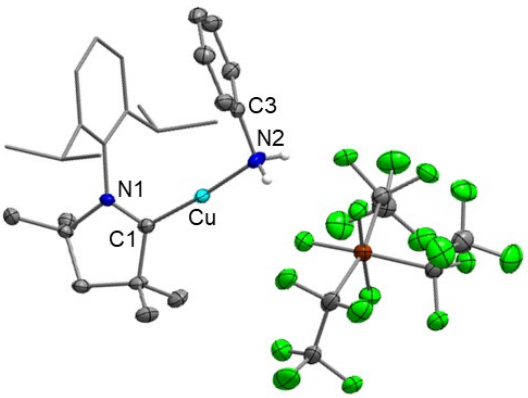

Figure S12. Molecular structure of [(cAAC^{Me})Cu(NH_2Ph)]$^+$**FAP**$^-$ (**20**) in the solid state (ellipsoids set at the 50% probability level; the Dipp substituent is shown as a wire-and-stick model). Hydrogen atoms except these of the nitrogen atom of the aniline ligand are omitted for clarity. Selected bond lengths [Å] and angles [°]: Cu−C1 1.882(3), Cu−N1 1.942(3), N1−C3 1.457(4); C1−Cu−N1 175.47(12), Cu−N1−C3 109.99(18).

Crystal Data for [(cAAC^{Me})Cu(NH$_2$Ph)]$^+$FAP$^-$ (20): $C_{32}H_{38}CuF_{18}N_2P$, M_r = 887.15, T = 99.98(10) K, λ = 1.54184 Å, colorless block, 0.092×0.172×0.215 mm^3, monoclinic space group $P2_1/c$, a = 13.91300(10) Å, b = 15.00150(10) Å, c = 17.89340(10) Å, β = 96.1210(10)°, V = 3713.34(4) Å^3, Z = 4, ρ_{calcd} = 1.587 g·cm^{-3}, μ = 2.323 mm^{-1}, F(000) = 1800, 40061 reflections, −17 ≤ h ≤ 17, −18 ≤ k ≤ 18, −22 ≤ l ≤ 16, 3.833° < θ < 74.503°, completeness 100%, 7610 independent reflections, 6946 reflections observed with [I > 2σ(I)], 495 parameters, 0 restraints, *R* indices (all data) R_1 = 0.0652, wR_2 = 0.1750, final *R* indices [I > 2σ(I)] R_1 = 0.0614, wR_2 = 0.1705, largest difference peak and hole 2.251 and −0.847 e Å^{-3}, GooF = 1.034.

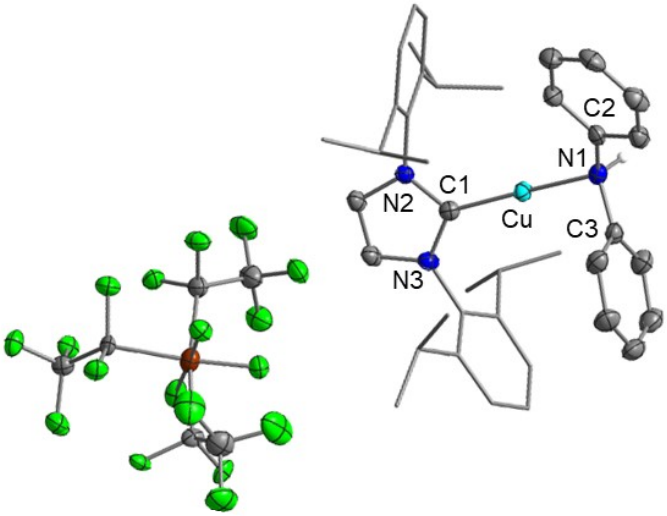

Figure S13. Molecular structure of [(IDipp)Cu(NHPh$_2$)]$^+$**FAP**$^-$ (**21**) in the solid state (ellipsoids set at the 50% probability level; Dipp substituents are shown as wire-and-stick models). Hydrogen atoms except these of the nitrogen atom of the diphenylamine ligand are omitted for clarity. Selected bond lengths [Å] and angles [°]: Cu−C1 1.8716(17), Cu−N1 1.9492(15), N2−C1 1.358(2), N3−C1 1.353(2), N1−C2 1.471(2), N1−C2 1.471(2), N1−C3 1.461(2); C1−Cu−N1 175.97(7), Cu−N1−C2 113.95(11), Cu−N1−C3 95.36(10), C2−N1−C3 118.09(4).

Crystal Data for [(IDipp)Cu(NHPh$_2$)]$^+$FAP$^-$ (21): $C_{45}H_{47}CuF_{18}N_3P$, M_r = 1066.36, T = 99.9(5) K, λ = 1.54184 Å, colorless block, 0.063×0.090×0.189 mm^3, monoclinic space group $P2_1/c$, a = 12.75280(10) Å, b = 21.8800(2) Å, c = 16.76400(10) Å, β = 96.4180(10)°, V = 4648.36(6) Å^3, Z = 4, ρ_{calcd} = 1.524 g·cm^{-3}, μ = 1.971 mm^{-1}, F(000) = 2176, 69991 reflections, −14 ≤ h ≤ 15, −27 ≤ k ≤ 26, −20 ≤ l ≤ 20, 3.334° < θ < 74.498°, completeness 99.8%, 9467 independent reflections, 8483 reflections observed with [I > 2σ(I)], 847 parameters, 1182 restraints, R indices (all data) R_1 = 0.0416, wR_2 = 0.0996, final R indices [I > 2σ(I)] R_1 = 0.0375, wR_2 = 0.0970, largest difference peak and hole 0.848 and −0.397 e Å^{-3}, GooF = 1.049.

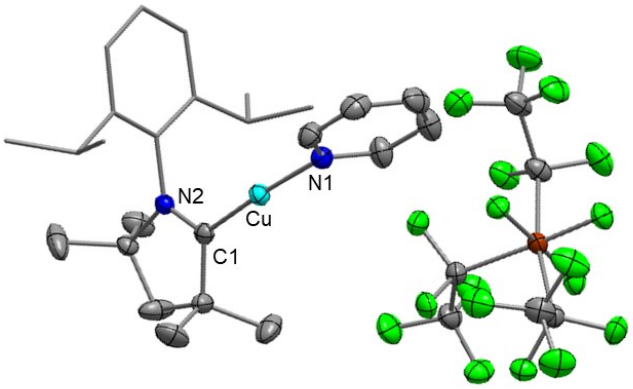

Figure S14. Molecular structure of [(cAAC^{Me})Cu(NC$_5$H$_5$)]$^+$**FAP**$^-$ (**23**) in the solid state (ellipsoids set at the 50% probability level; the Dipp substituent is shown as a wire-and-stick model). Hydrogen atoms are omitted for clarity. Selected bond lengths [Å] and angles [°]: Cu−C1 1.8853(17), Cu−N1 1.9038(15), N2−C1 1.300(2); C1−Cu−N1 174.25(6).

Crystal Data for [(cAAC^{Me})Cu(NC$_5$H$_5$)]$^+$FAP$^-$ (23): $C_{31}H_{36}CuF_{18}N_2P$, M_r = 873.13, T = 99.9(3) K, λ = 1.54184 Å, colorless block, 0.124×0.198×0.211 mm^3, monoclinic space group $P2_1/c$, a = 14.05780(10) Å, b = 16.1196(2) Å, c = 15.84600(10) Å, β = 94.2150(10)°, V = 3581.09(6) Å^3, Z = 4, ρ_{calcd} = 1.619 g·cm^{-3}, μ = 2.398 mm^{-1}, F(000) = 1768, 52927 reflections, −17 ≤ h ≤ 17, −20 ≤ k ≤ 20, −19 ≤ l ≤ 17, 3.917° < θ < 74.504°, completeness 99.8%, 7311 independent reflections, 6579 reflections observed with [I > 2σ(I)], 723 parameters, 1341 restraints, *R* indices (all data) R_1 = 0.0382, wR_2 = 0.0946, final *R* indices [I > 2σ(I)] R_1 = 0.0345, wR_2 = 0.0916, largest difference peak and hole 0.378 and −0.277 e Å^{-3}, GooF = 1.052.

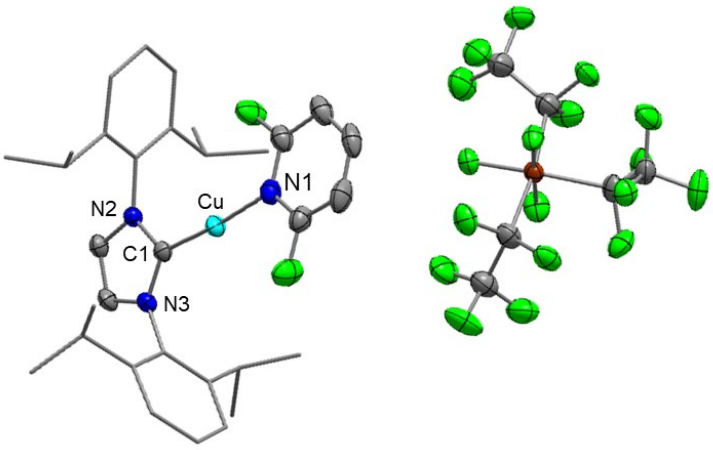

Figure S15. Molecular structure of [(IDipp)Cu(NC$_5$H$_3$F$_2$)]$^+$**FAP**$^-$ (**24**) in the solid state (ellipsoids set at the 50% probability level; Dipp substituents are shown as wire-and-stick models). Hydrogen atoms are omitted for clarity. Selected bond lengths [Å] and angles [°]: Cu−C1 1.878(2), Cu−N1 1.916(2), N2−C1 1.357(3), N3−C1 1.351(3); C1−Cu−N1 172.2(1).

Crystal Data for [(IDipp)Cu(NC$_5$H$_3$F$_2$)]$^+$FAP$^-$ (24): $C_{38}H_{39}CuF_{20}N_3P$, M_r = 1012.23, T = 99.99(10) K, λ = 1.54184 Å, colorless block, 0.162×0.234×0.298 mm^3, orthorhombic space group *Pbca*, a = 18.63510(10) Å, b = 20.20240(10) Å, c = 23.25420(10) Å, V = 8754.60(7) Å^3, Z = 8, ρ_{calcd} = 1.536 g·cm^{-3}, μ = 2.126 mm^{-1}, F(000) = 4096, 89464 reflections, −23 ≤ h ≤ 23, −24 ≤ k ≤ 25, −25 ≤ l ≤ 29, 3.745° < θ < 74.503°, completeness 100%, 8953 independent reflections, 8252 reflections

observed with [I > 2σ(I)], 802 parameters, 1293 restraints, *R* indices (all data) R_1 = 0.0559, wR_2 = 0.1470, final *R* indices [I > 2σ(I)] R_1 = 0.0529, wR_2 = 0.1442, largest difference peak and hole 0.922 and −0.488 e Å^{-3}, GooF = 1.032.

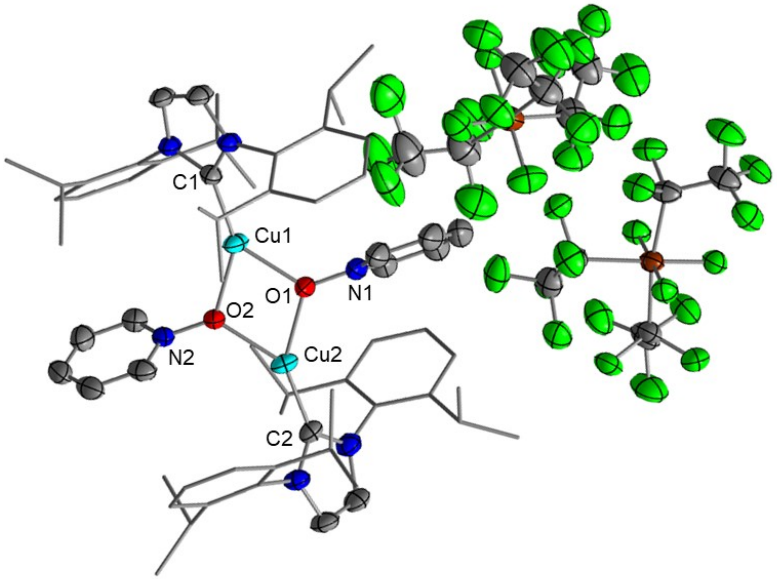

Figure S16. Molecular structure of [{(IDipp)Cu(μ-ONC$_5$H$_5$)}$_2$]$^{2+}$**2FAP**$^-$ (**26**) in the solid state (ellipsoids set at the 50% probability level; Dipp substituents are shown as wire-and-stick models). Hydrogen atoms and two co-crystallized solvent molecules are omitted for clarity. Selected bond lengths [Å] and angles [°]: Cu1−C1 1.873(3), Cu2−C2 1.876(3), Cu1−O1 2.054(2), Cu2−O1 2.027(2), Cu1−O2 2.028(2), Cu2−O2 2.070(2), Cu1−Cu2 3.3117(8), O1−N1 1.357(4), O2−N2 1.348(3); C1−Cu1−O1 142.16(11), C1−Cu1−O2 145.85(11), C2−Cu2−O1 144.71(12), C2−Cu2−O2 143.59(11), Cu1−O1−Cu2 108.47(11), Cu1−O2−Cu2 107.84(10).

Crystal Data for [{(IDipp)Cu(μ-ONC$_5$H$_5$)}$_2$]$^{2+}$2FAP$^-$ (26): $C_{88}H_{90}Cu_2F_{40}N_6O_2P_2$, M_r = 2212.67, T = 99.98(11) K, λ = 1.54184 Å, colorless block, 0.143×0.209×0.424 mm^3, triclinic space group $P\bar{1}$, a = 15.15180(10) Å, b = 15.53180(10) Å, c = 22.82480(10) Å, α = 90.2190(10)°, β = 103.7860(10)°, γ = 112.7070(10)°, V = 4784.79(6) Å^3, Z = 2, ρ_{calcd} = 1.536 Mg/m^3, μ = 2.016 mm^{-1}, F(000) = 2248, 197077 reflections, −18 ≤ h ≤ 18, −19 ≤ k ≤ 19, −28 ≤ l ≤ 25, 3.102° < θ < 74.503°, completeness 100%, 19494 independent reflections, 17389 reflections observed with [I > 2σ(I)], 1520 parameters, 1830 restraints, *R* indices (all data) R_1 = 0.0829, wR_2 = 0.2530, final *R* indices [I > 2σ(I)] R_1 = 0.0778, wR_2 = 0.2293, largest difference peak and hole 1.881 and −1.060 e Å^{-3}, GooF = 1.069.

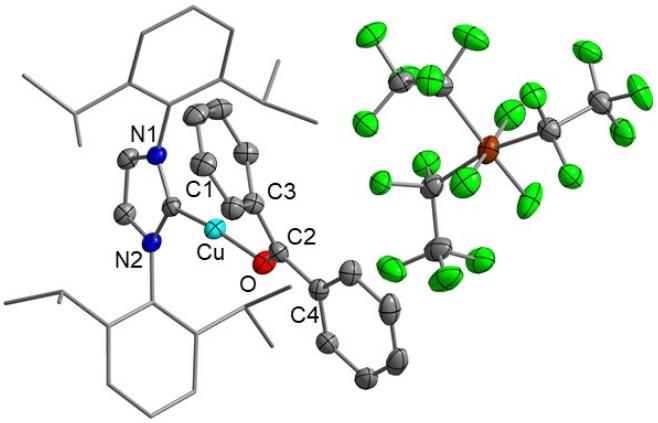

Figure S17. Molecular structure of [(IDipp)Cu(η^1-O=CPh$_2$)]$^+$**FAP**$^-$ (**27**) in the solid state (ellipsoids set at the 50% probability level; Dipp substituents are shown as wire-and-stick models). Hydrogen atoms are omitted for clarity. Selected bond lengths [Å] and angles [°]: Cu−C1 1.866(3), Cu−O 1.8624(19), N1−C1 1.352(3), N2−C1 1.359(2), O−C2 1.246(3); C1−Cu−O 167.61(9), Cu−O−C2 133.48(18), C3−C2−C4 123.0(2), O−C2−C3 119.1(2), O−C2−C4 117.9(2).

Crystal Data for [(IDipp)Cu(η^1-O=CPh$_2$)]$^+$FAP$^-$ (27): $C_{46}H_{46}CuF_{18}N_2OP$, M_r = 1079.36, T = 100.00(10) K, λ = 1.54184 Å, colorless block, 0.179×0.206×0.225 mm^3, monoclinic space group $P2_1/c$, a = 14.08110(10) Å, b = 19.34660(10) Å, c = 17.91920(10) Å, β = 96.8600(10)°, V = 4846.63(5) Å^3, Z = 4, ρ_{calcd} = 1.479 g·cm^{-3}, μ = 1.909 mm^{-1}, F(000) = 2200, 73441 reflections, −17 ≤ h ≤ 14, −24 ≤ k ≤ 24, −22 ≤ l ≤ 21, 3.375° < θ < 74.499°, completeness 99.7%, 9877 independent reflections, 8944 reflections observed with [I > 2σ(I)], 688 parameters, 282 restraints, *R* indices (all data) R_1 = 0.0609, wR_2 = 0.1517, final *R* indices [I > 2σ(I)] R_1 = 0.0565, wR_2 = 0.1478, largest difference peak and hole 1.371 and −1.070 e Å^{-3}, GooF = 1.044.

2) NMR spectra of compounds

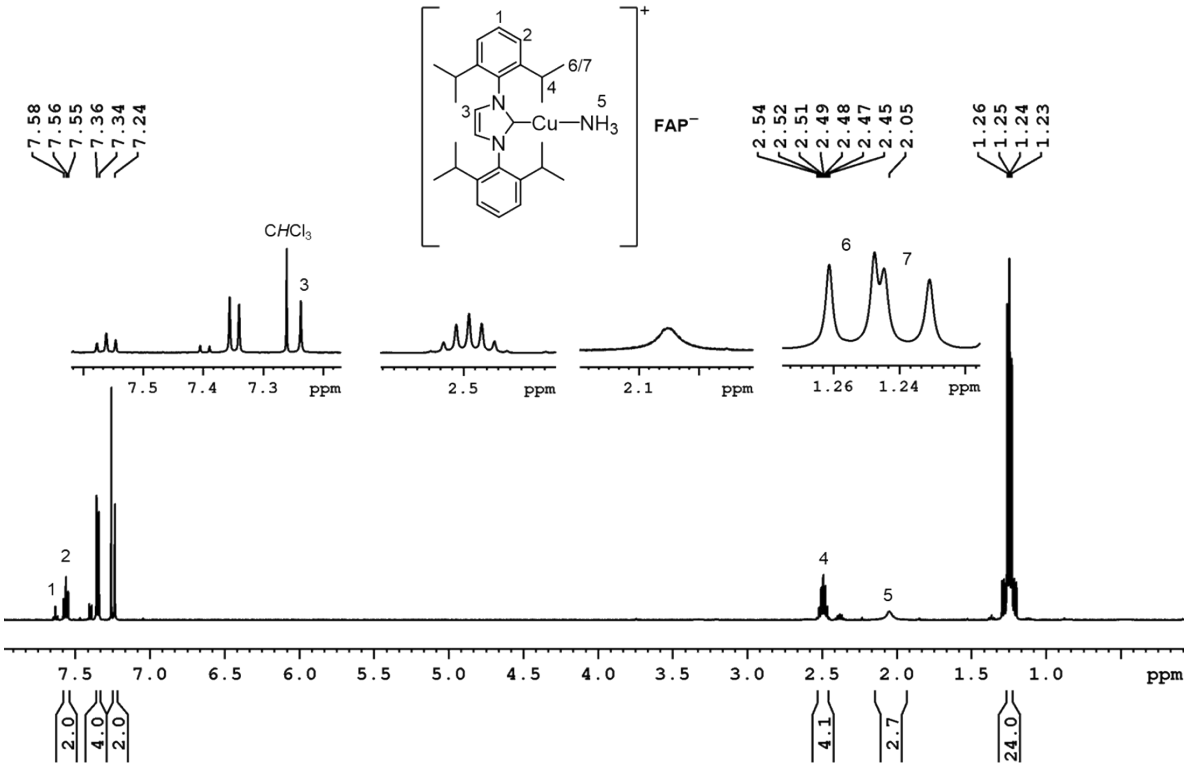

Figure S18. ^{1}H NMR spectrum (500.1 MHz) of **1** recorded in $CDCl_3$.

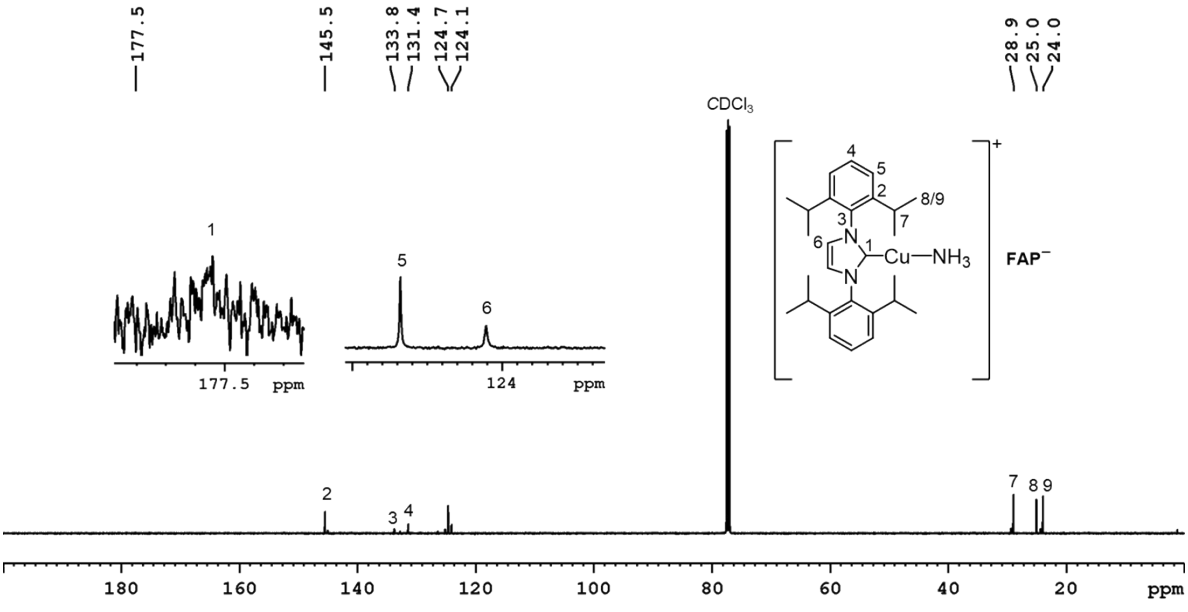

Figure S19. $^{13}C\{^{1}H\}$ NMR spectrum (125.8 MHz) of **1** recorded in $CDCl_3$.

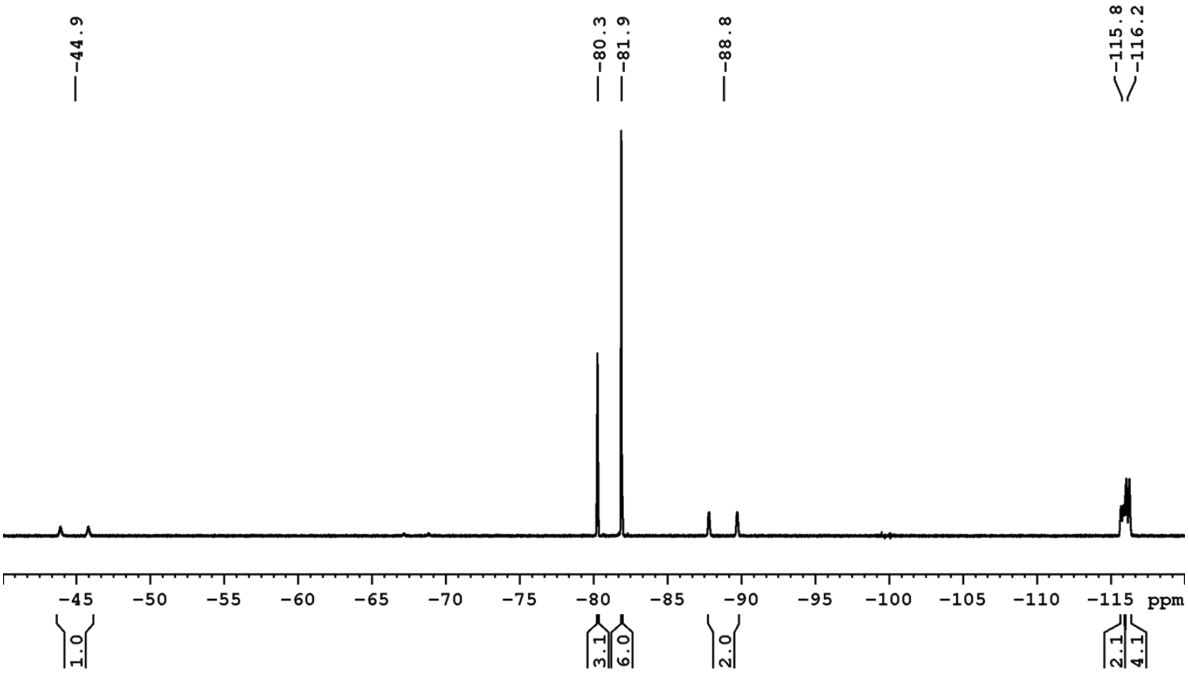

Figure S20. ^{19}F NMR spectrum (470.5 MHz) of **1** recorded in $CDCl_3$.

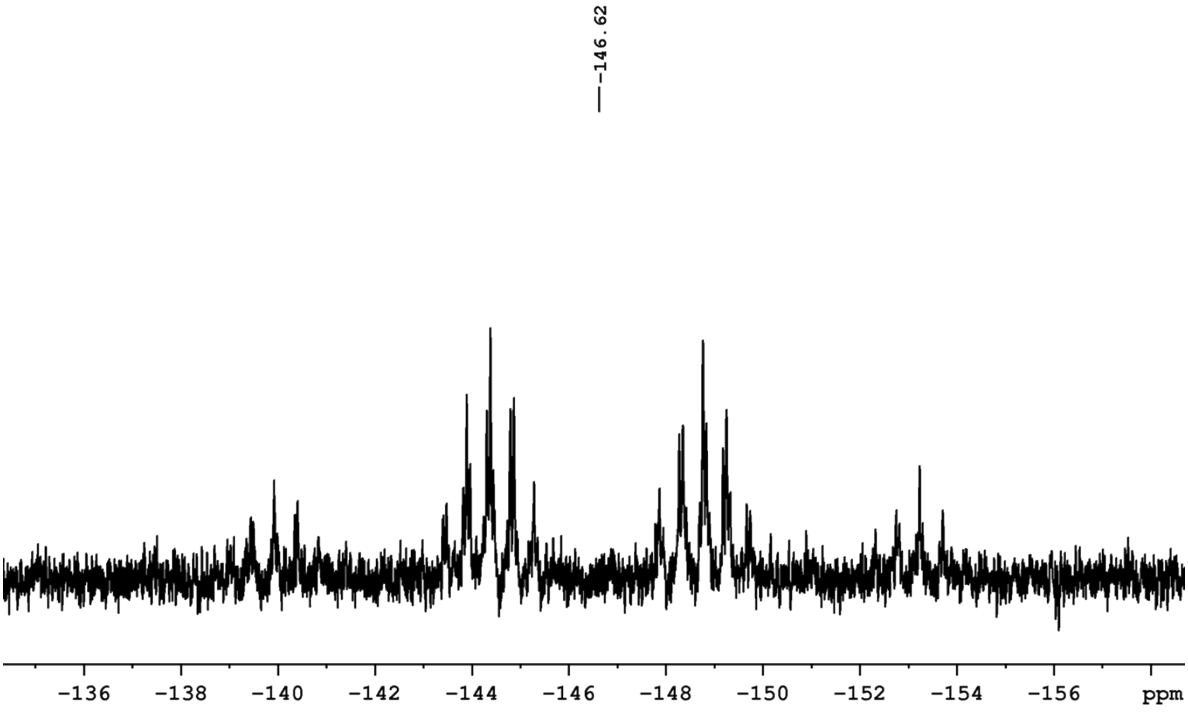

Figure S21. ^{31}P NMR spectrum (202.4 MHz) of **1** recorded in $CDCl_3$.

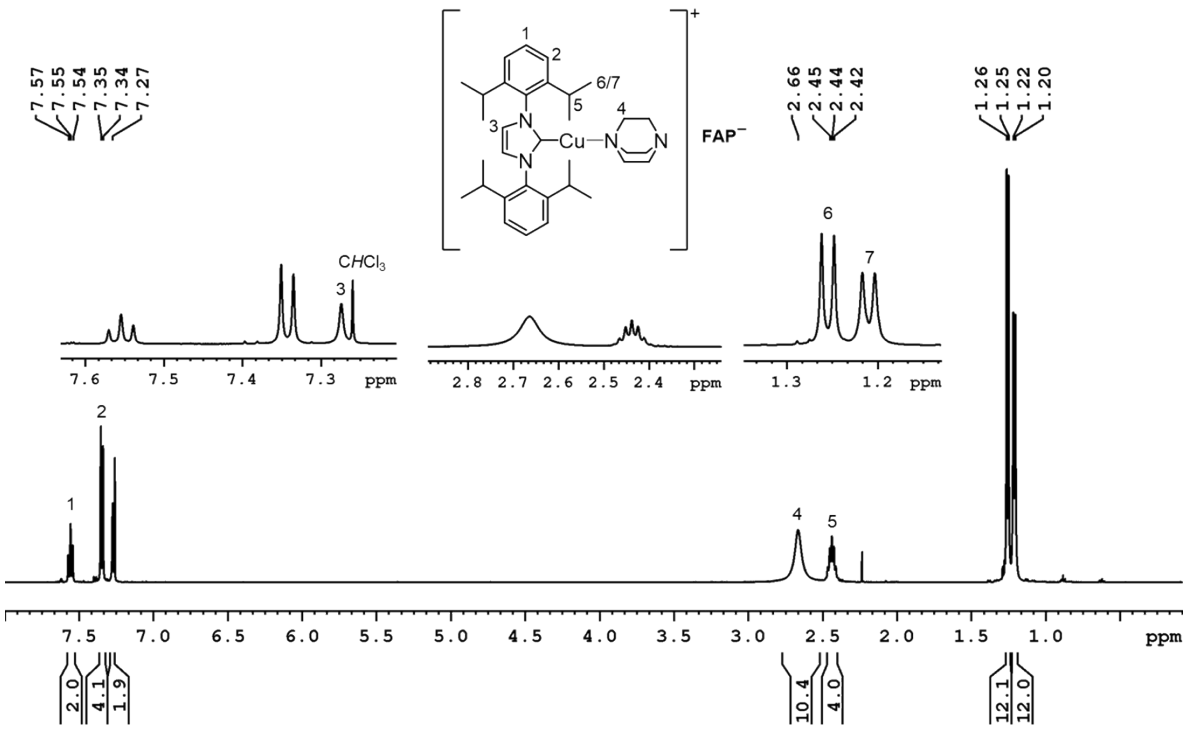

Figure S22. ^{1}H NMR spectrum (500.1 MHz) of **2** recorded in $CDCl_3$.

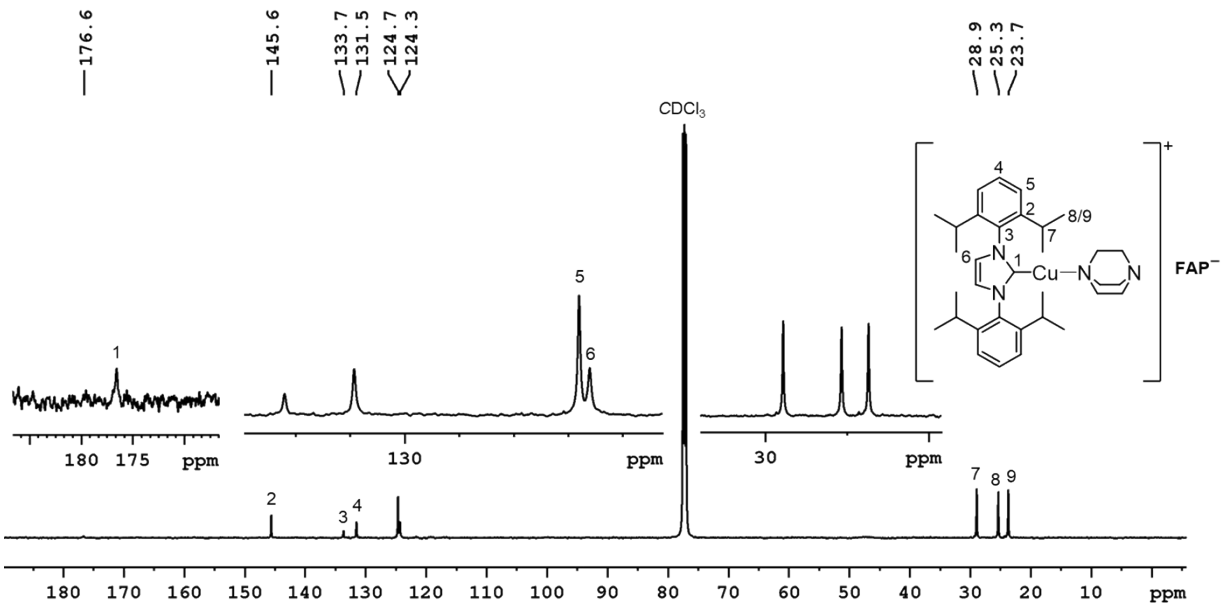

Figure S23. $^{13}C\{^{1}H\}$ NMR spectrum (125.8 MHz) of **2** recorded in $CDCl_3$.

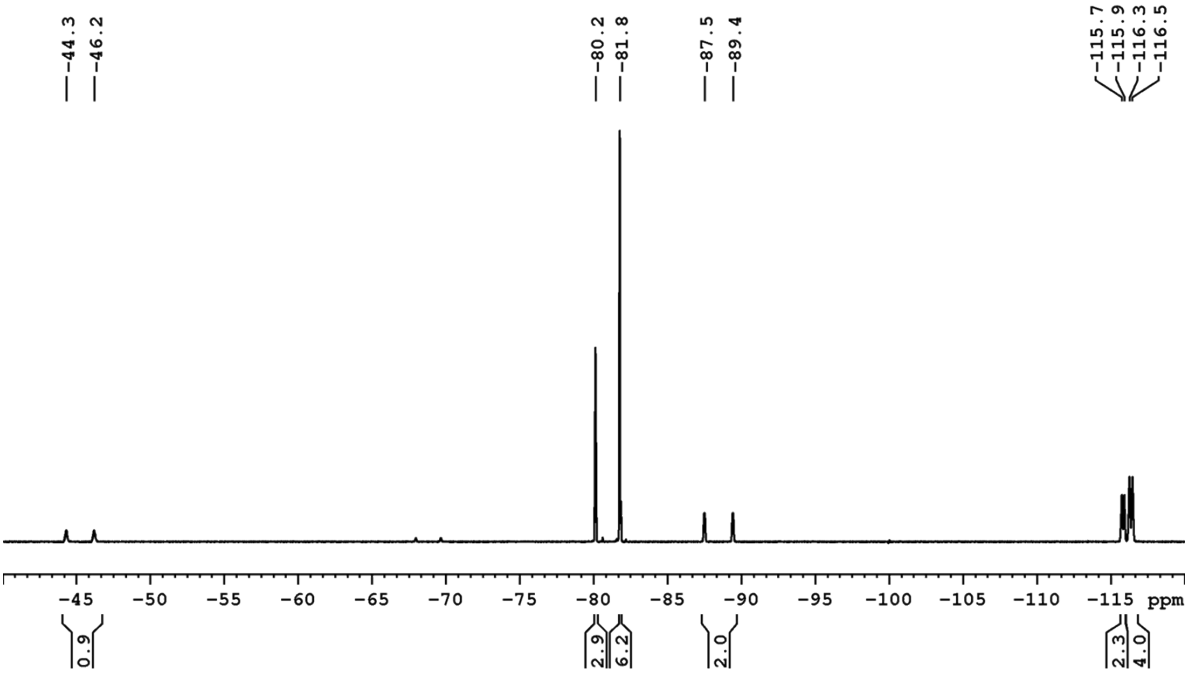

Figure S24. ^{19}F NMR spectrum (470.5 MHz) of **2** recorded in $CDCl_3$.

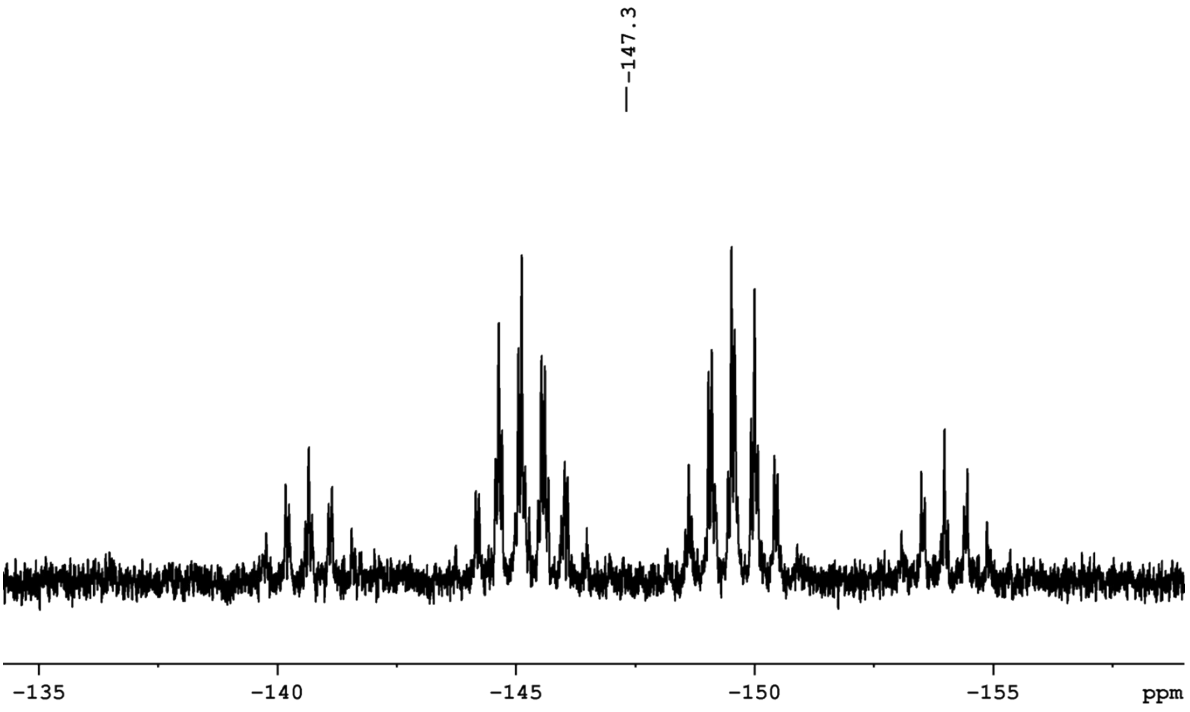

Figure S25. ^{31}P NMR spectrum (202.4 MHz) of **2** recorded in $CDCl_3$.

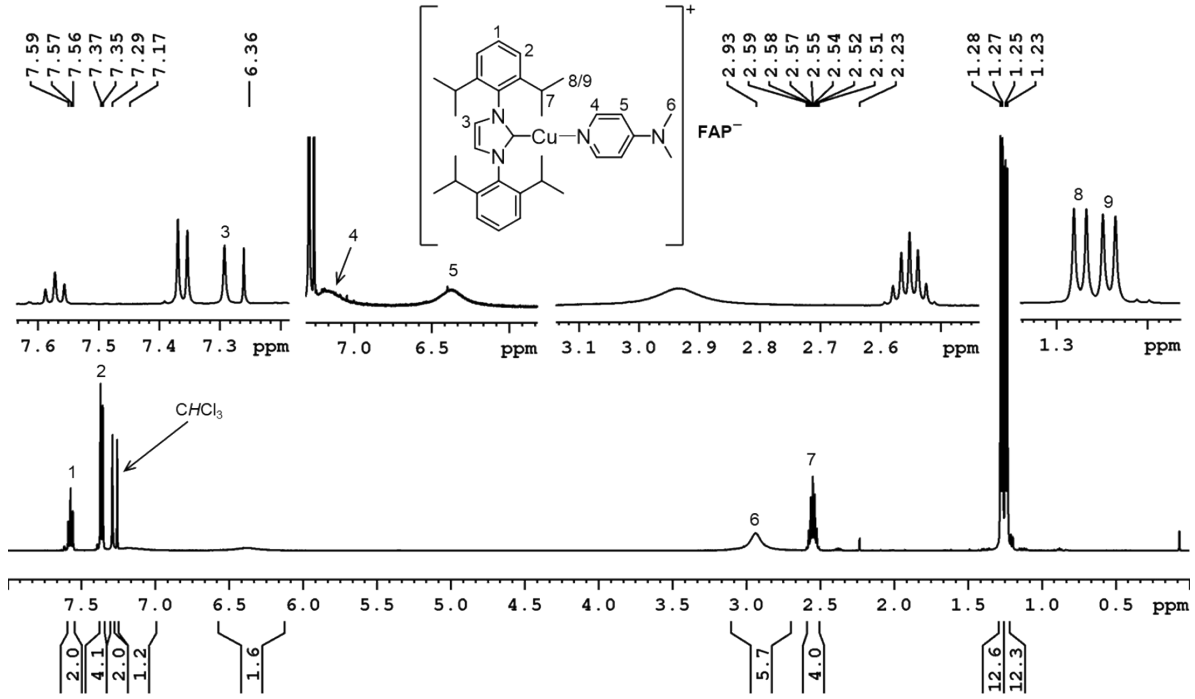

Figure S26. ^{1}H NMR spectrum (500.1 MHz) of **3** recorded in $CDCl_3$.

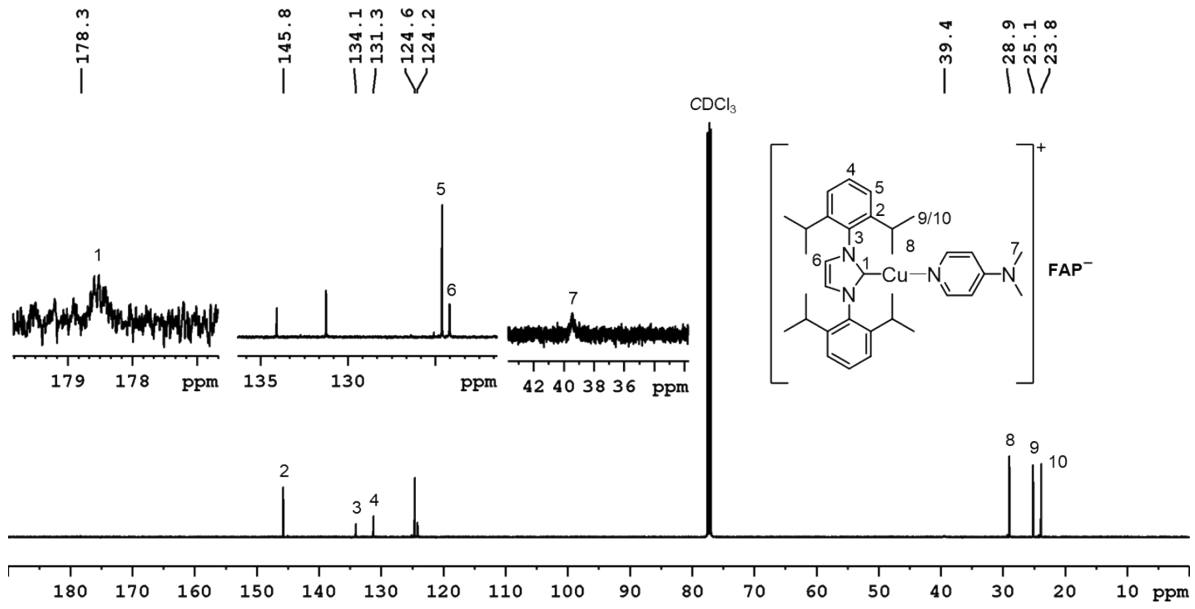

Figure S27. $^{13}C\{^{1}H\}$ NMR spectrum (125.8 MHz) of **3** recorded in $CDCl_3$.

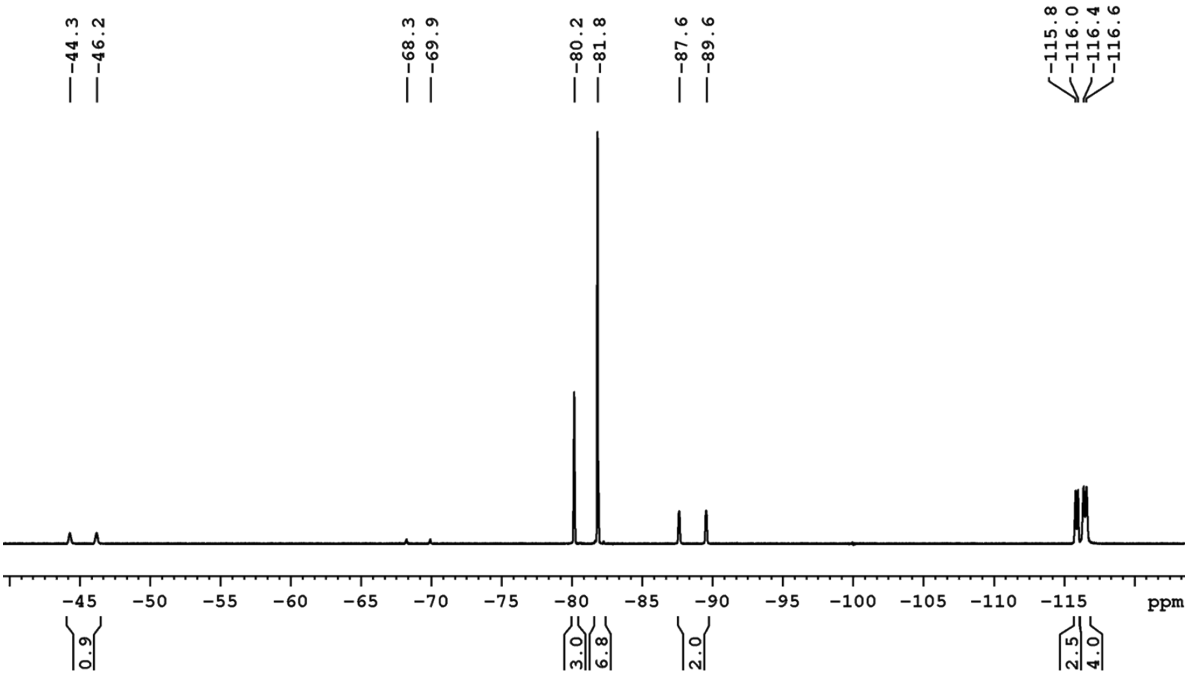

Figure S28. ^{19}F NMR spectrum (470.5 MHz) of **3** recorded in $CDCl_3$.

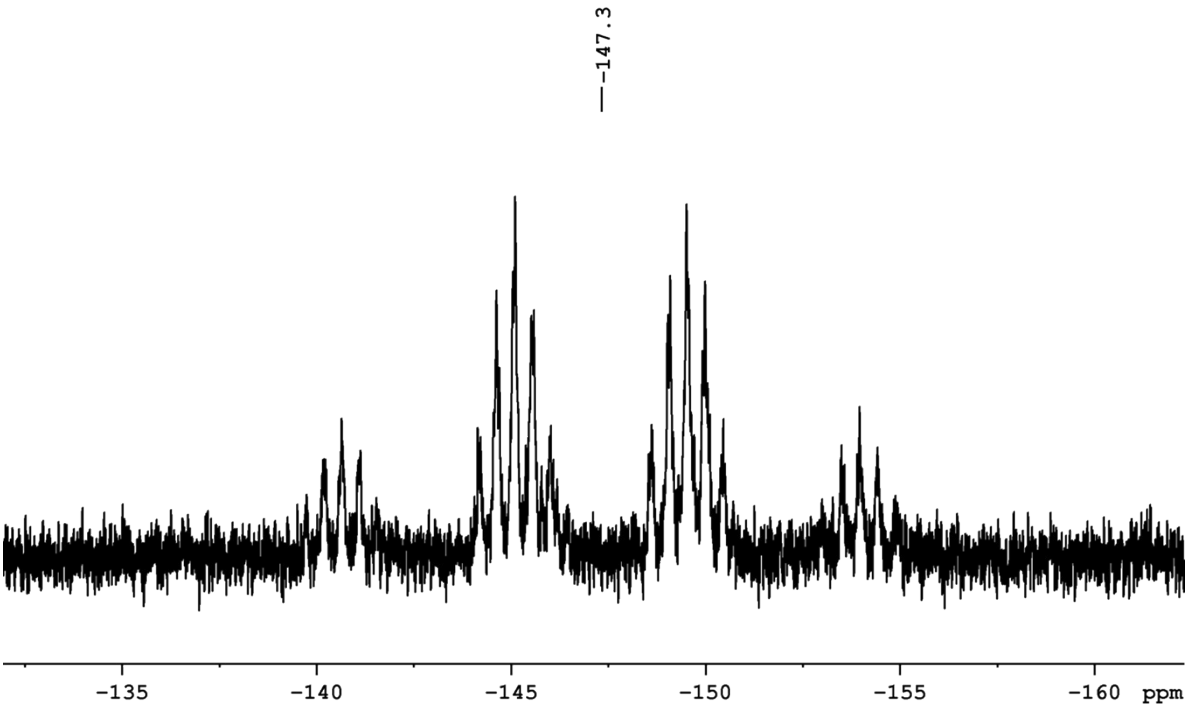

Figure S29. ^{31}P NMR spectrum (202.4 MHz) of **3** recorded in $CDCl_3$.

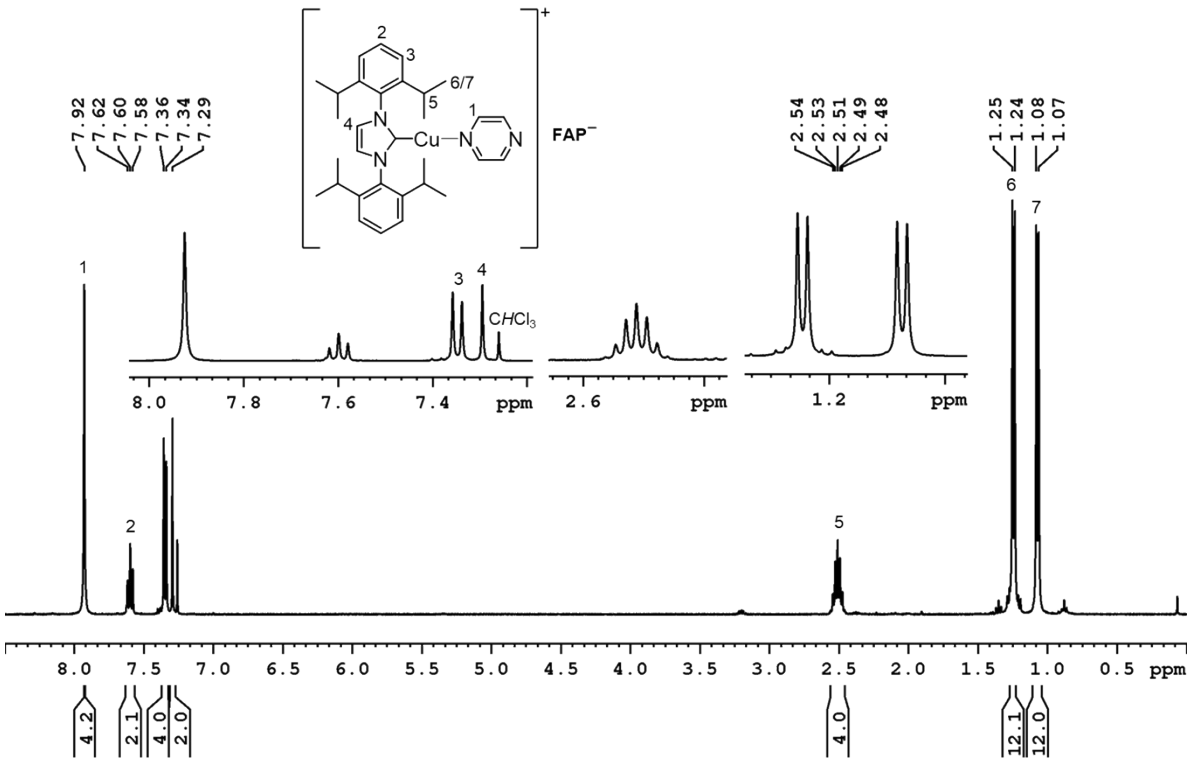

Figure S30. ^{1}H NMR spectrum (400.1 MHz) of **4** recorded in $CDCl_3$.

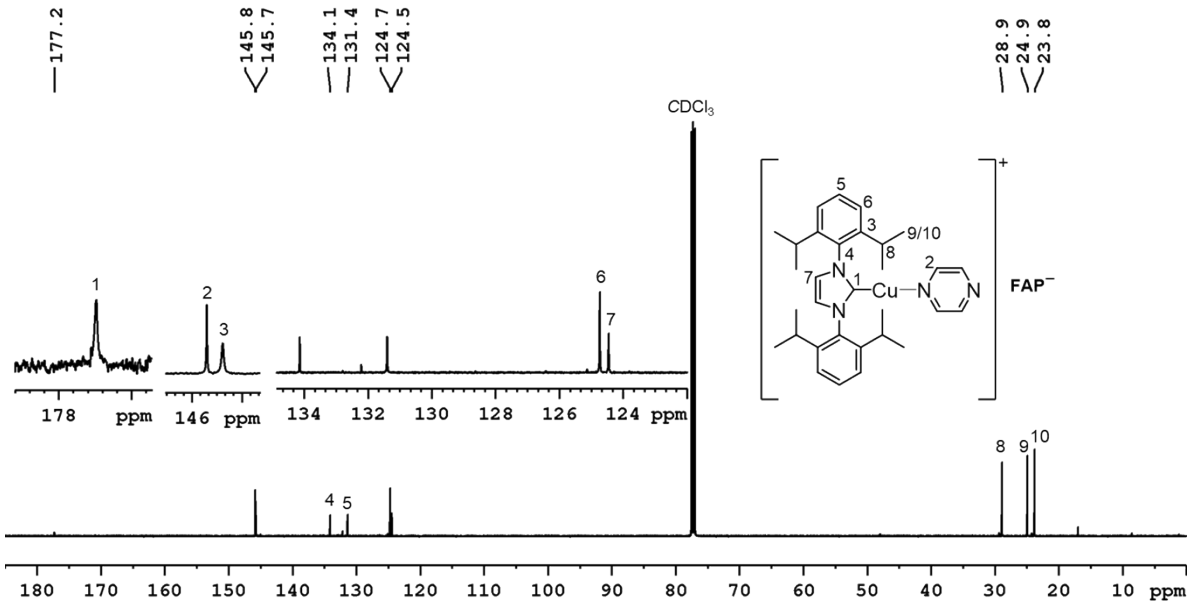

Figure S31. $^{13}C\{^{1}H\}$ NMR spectrum (125.8 MHz) of **4** recorded in $CDCl_3$.

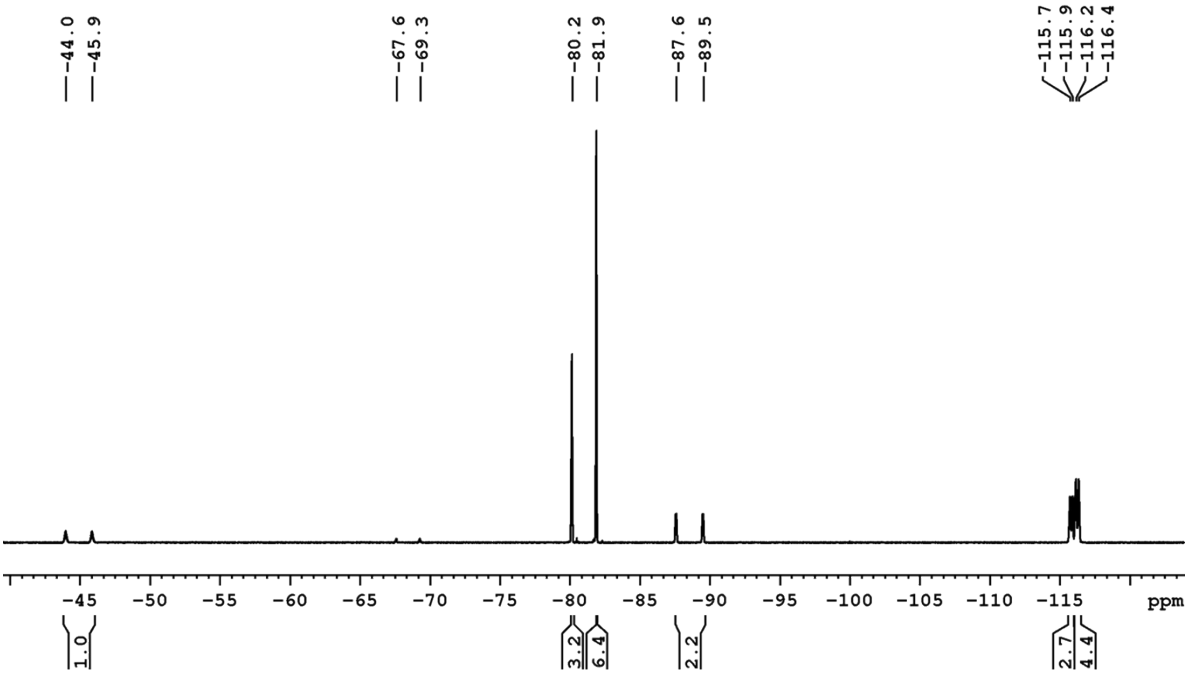

Figure S32. ^{19}F NMR spectrum (470.5 MHz) of **4** recorded in $CDCl_3$.

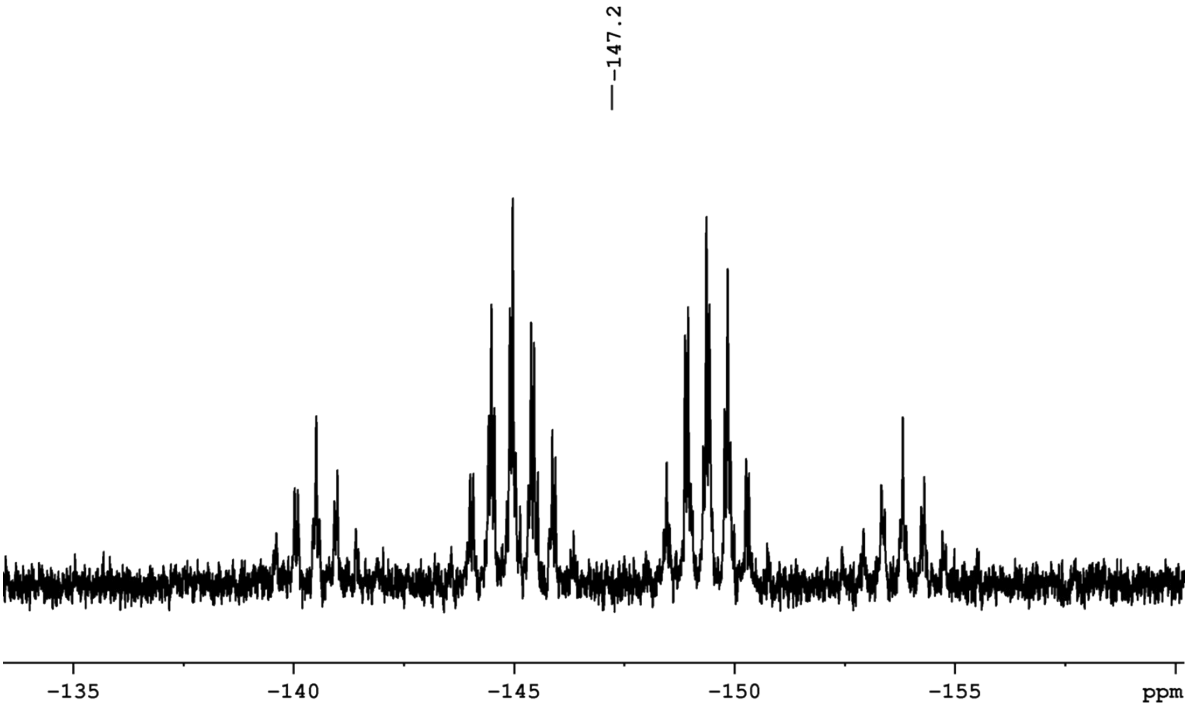

Figure S33. ^{31}P NMR spectrum (202.4 MHz) of **4** recorded in $CDCl_3$.

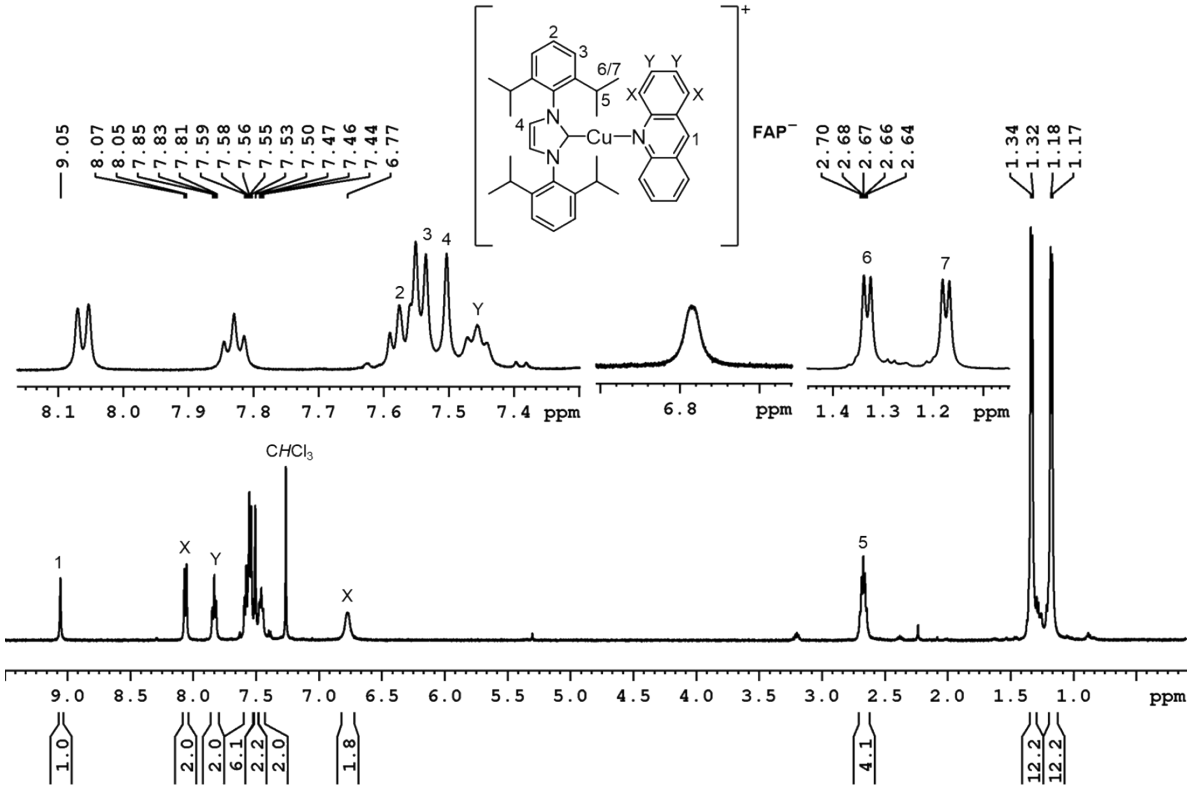

Figure S34. ^{1}H NMR spectrum (500.1 MHz) of **5** recorded in $CDCl_3$.

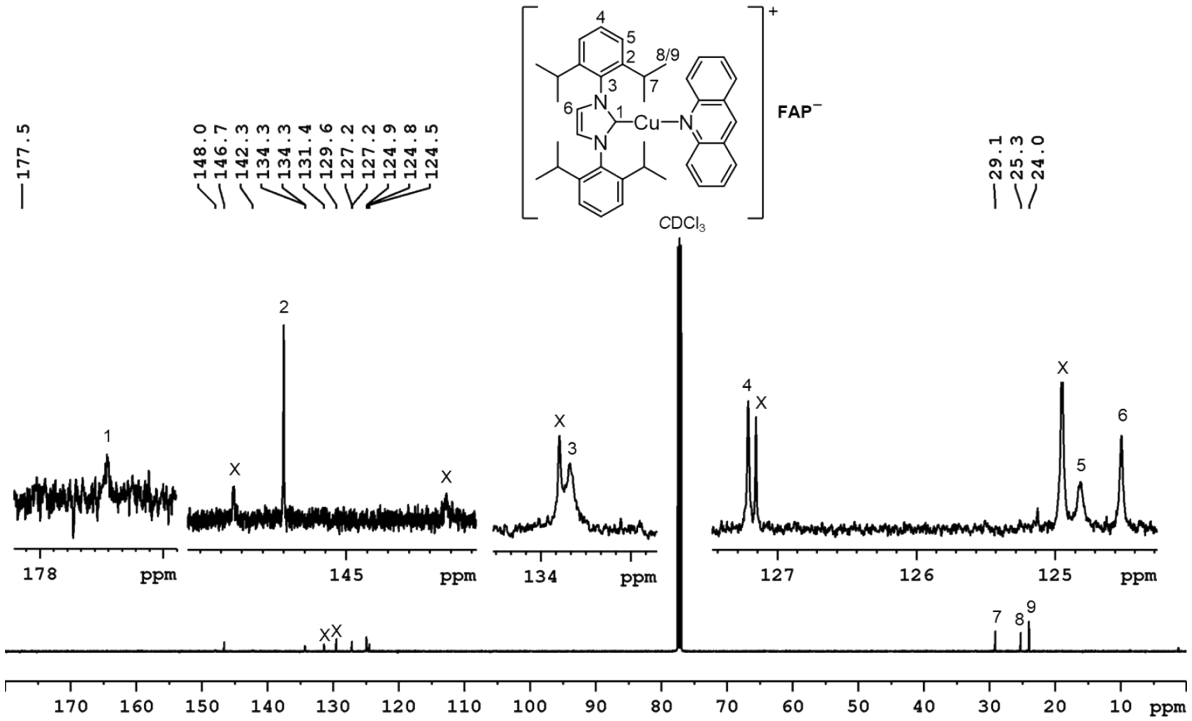

Figure S35. $^{13}C\{^{1}H\}$ NMR spectrum (125.8 MHz) of **5** recorded in $CDCl_3$ (X: signals for acridine ligand).

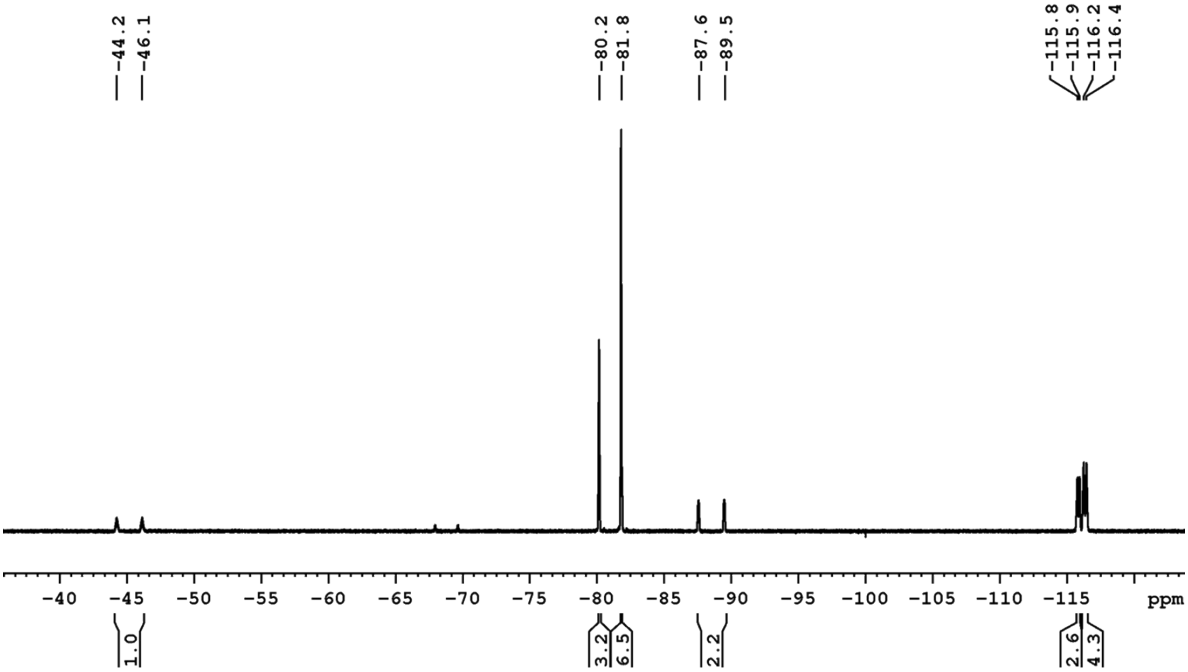

Figure S36. ^{19}F NMR spectrum (470.5 MHz) of **5** recorded in $CDCl_3$.

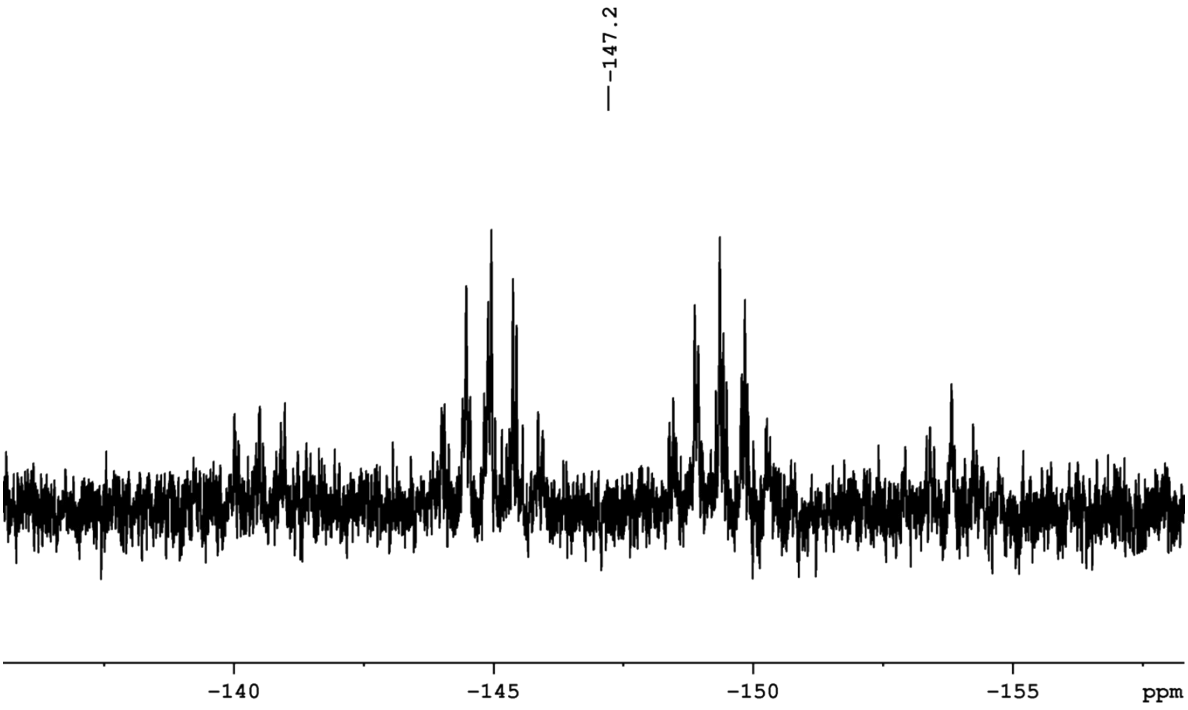

Figure S37. ^{31}P NMR spectrum (202.4 MHz) of **5** recorded in $CDCl_3$.

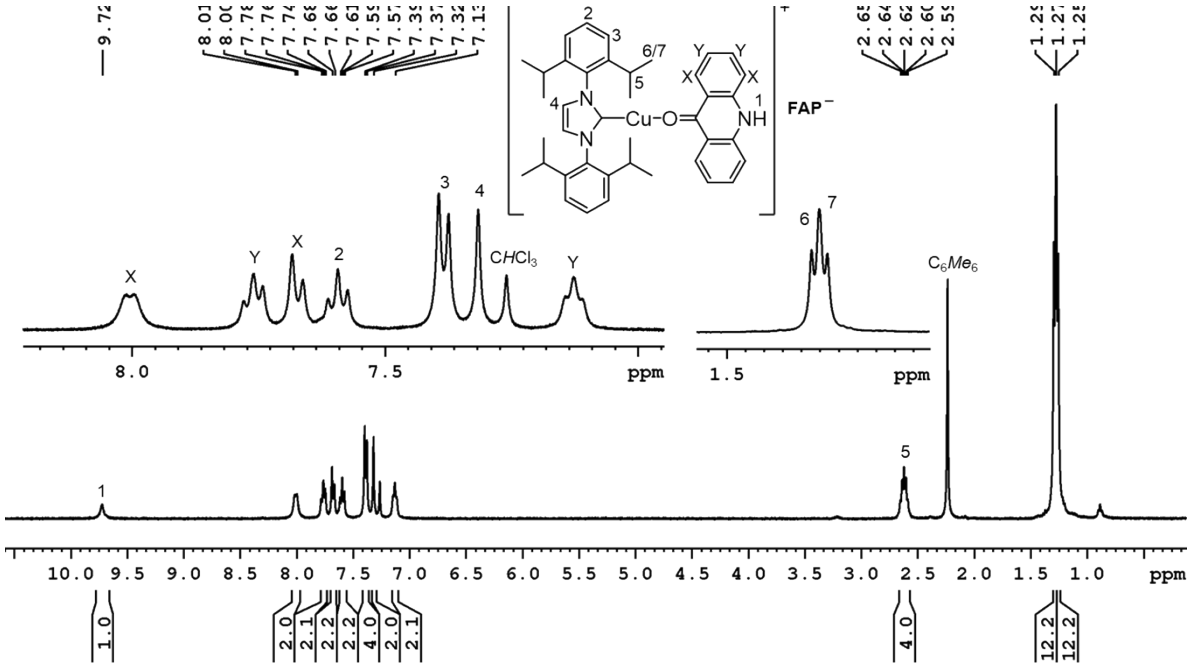

Figure S38. ^{1}H NMR spectrum (400.1 MHz) of **6** recorded in $CDCl_3$.

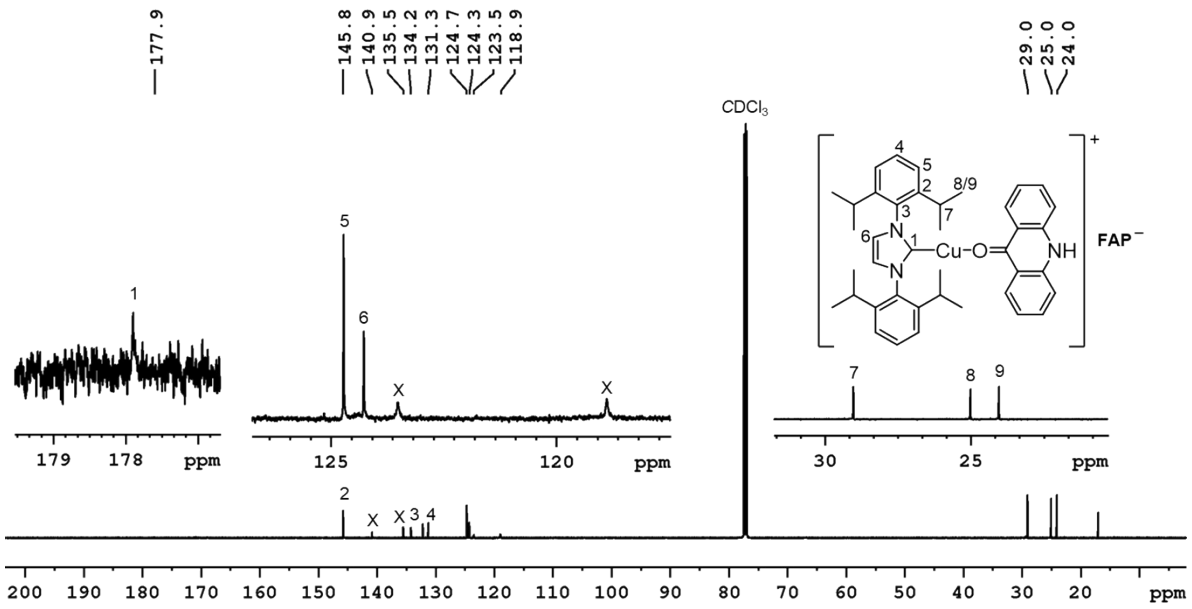

Figure S39. $^{13}C\{^{1}H\}$ NMR spectrum (125.8 MHz) of **6** recorded in $CDCl_3$ (X: signals for acridone ligand).

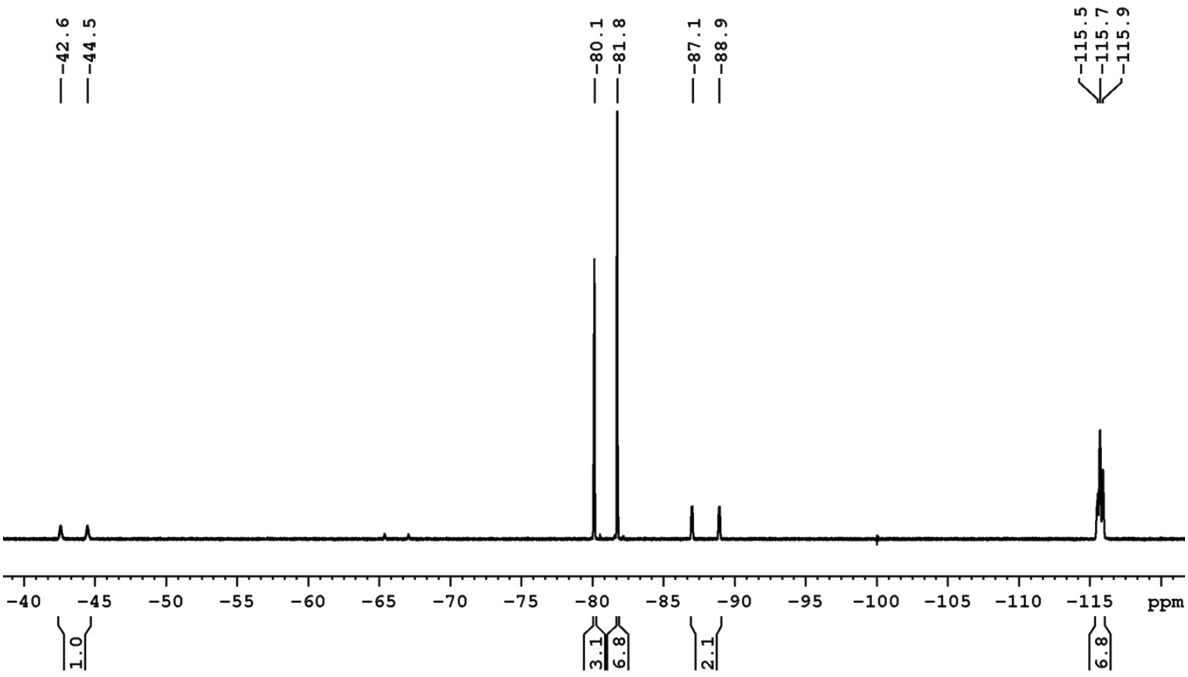

Figure S40. ^{19}F NMR spectrum (470.5 MHz) of **6** recorded in $CDCl_3$.

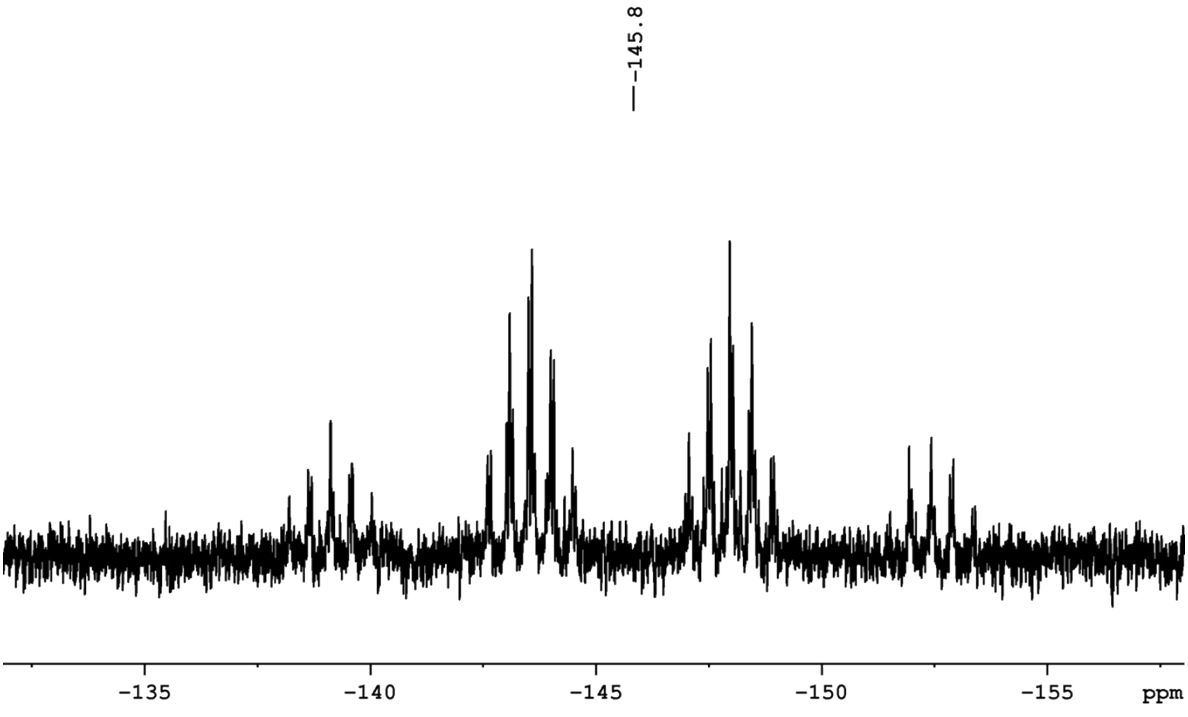

Figure S41. ^{31}P NMR spectrum (202.4 MHz) of **6** recorded in $CDCl_3$.

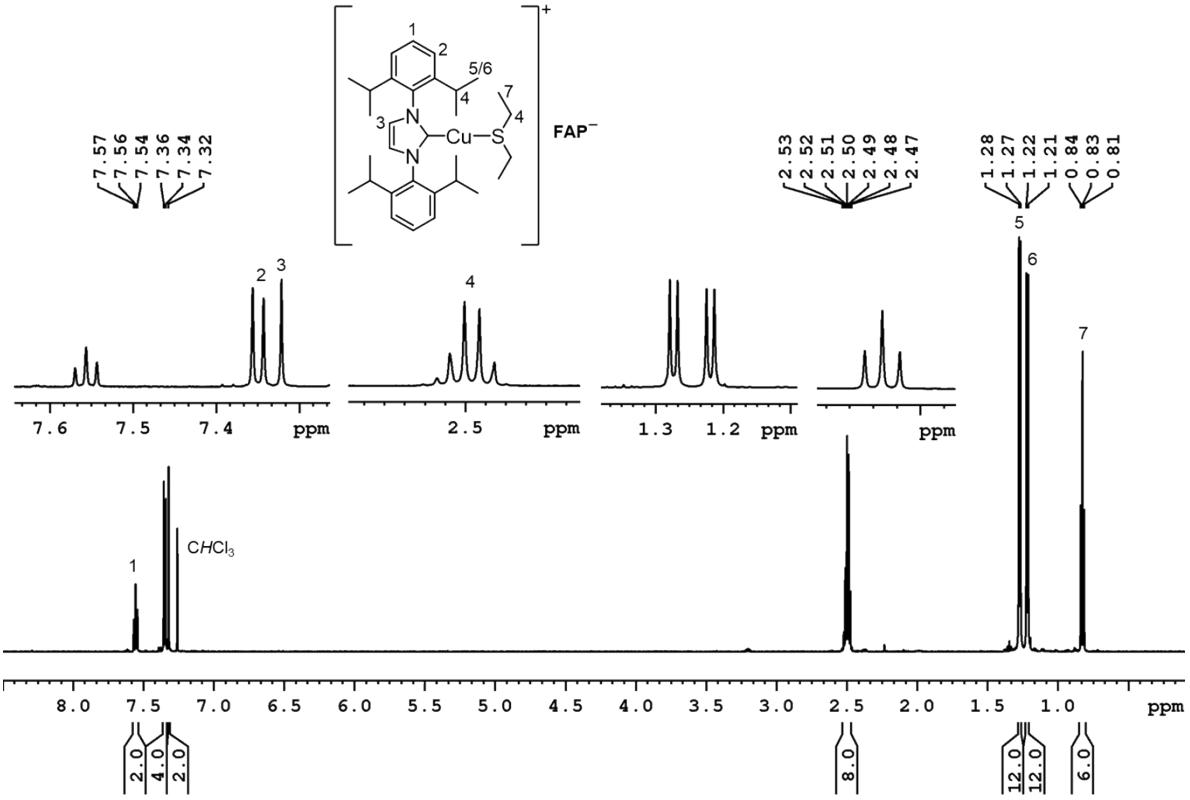

Figure S42. ^{1}H NMR spectrum (600.2 MHz) of **7** recorded in $CDCl_3$.

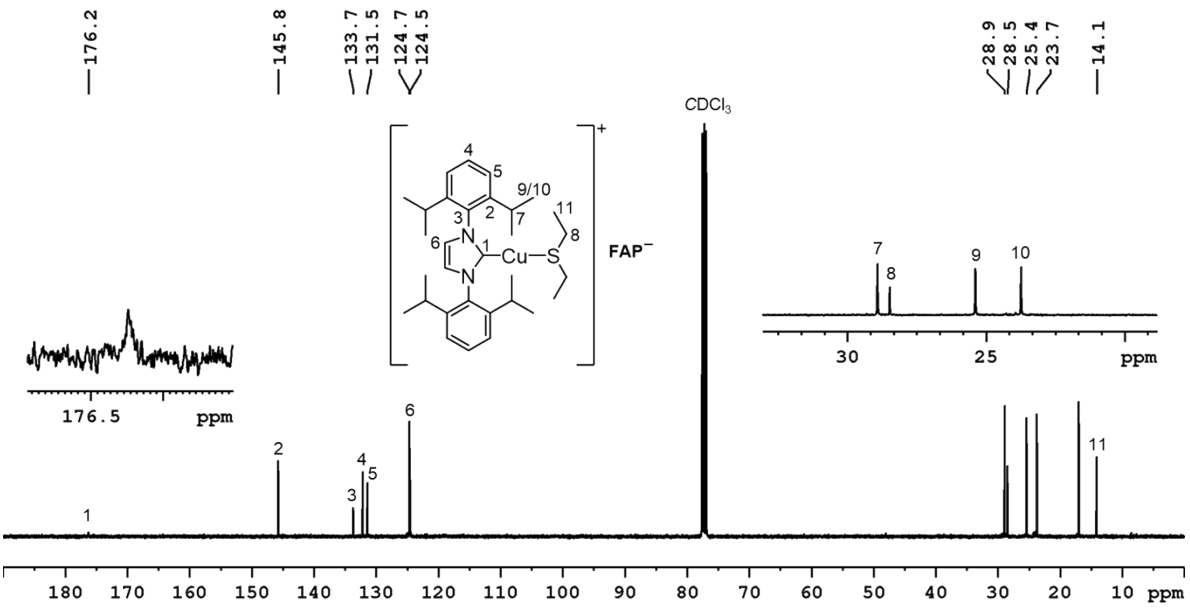

Figure 43. $^{13}C\{^{1}H\}$ NMR spectrum (100.6 MHz) of **7** recorded in $CDCl_3$.

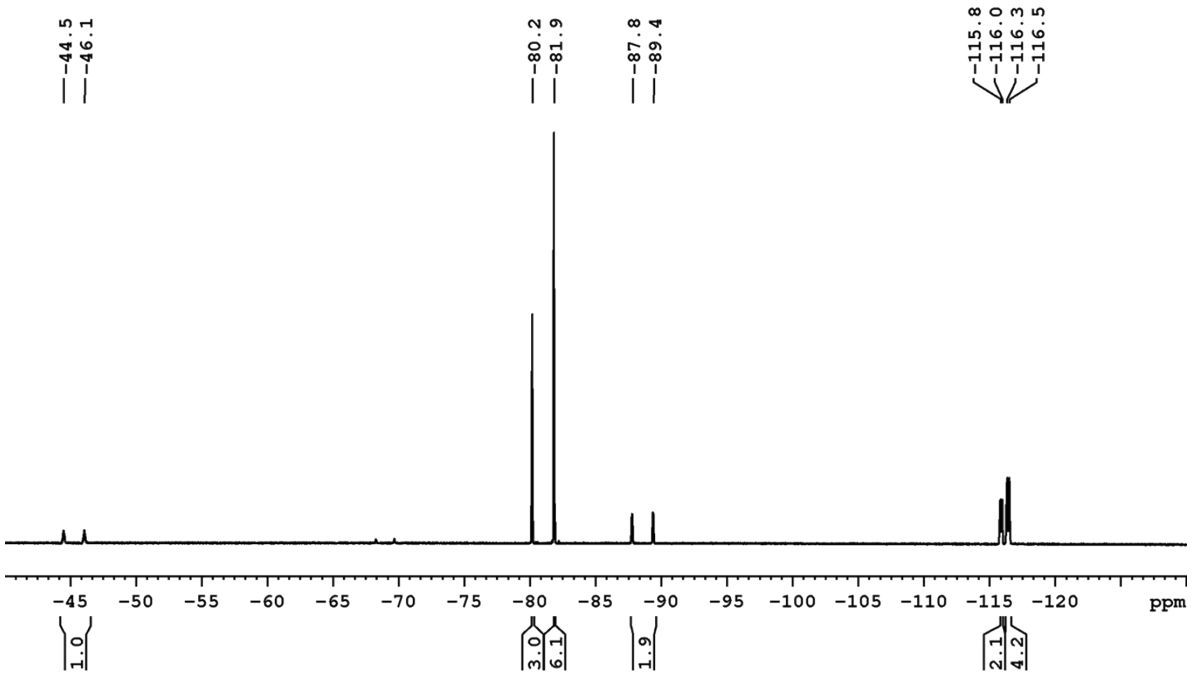

Figure S44. ^{19}F NMR spectrum (470.5 MHz) of **7** recorded in $CDCl_3$.

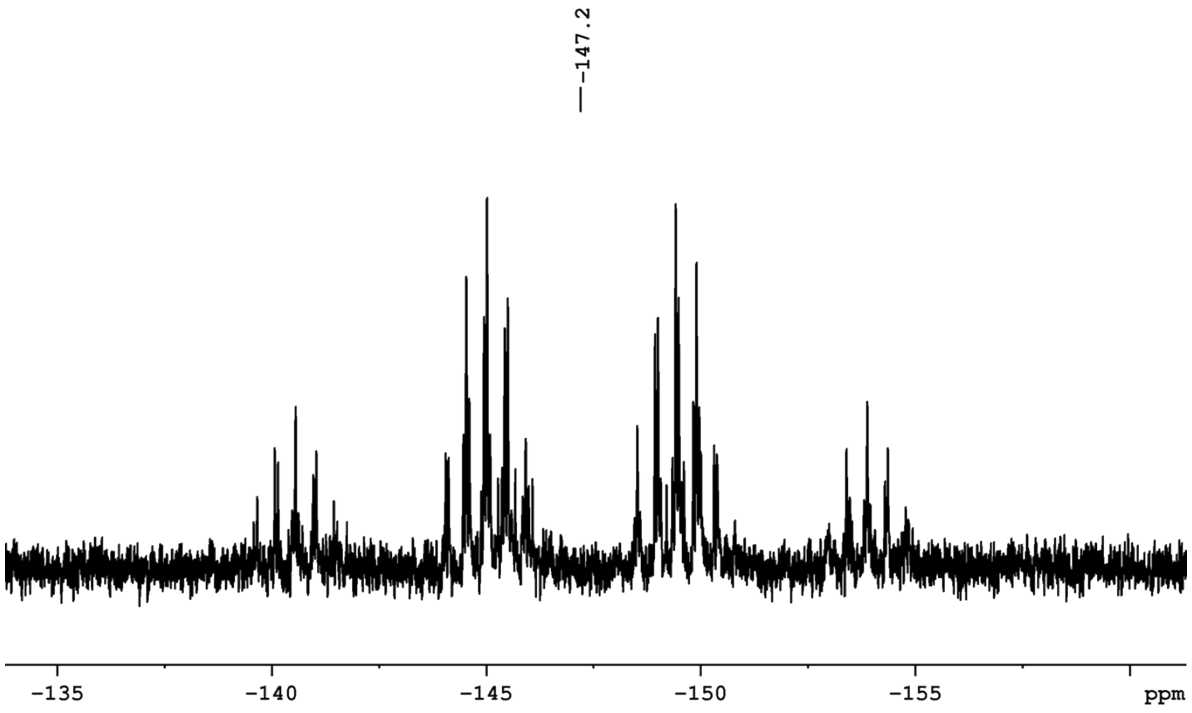

Figure S45. ^{31}P NMR spectrum (202.4 MHz) of **7** recorded in $CDCl_3$.

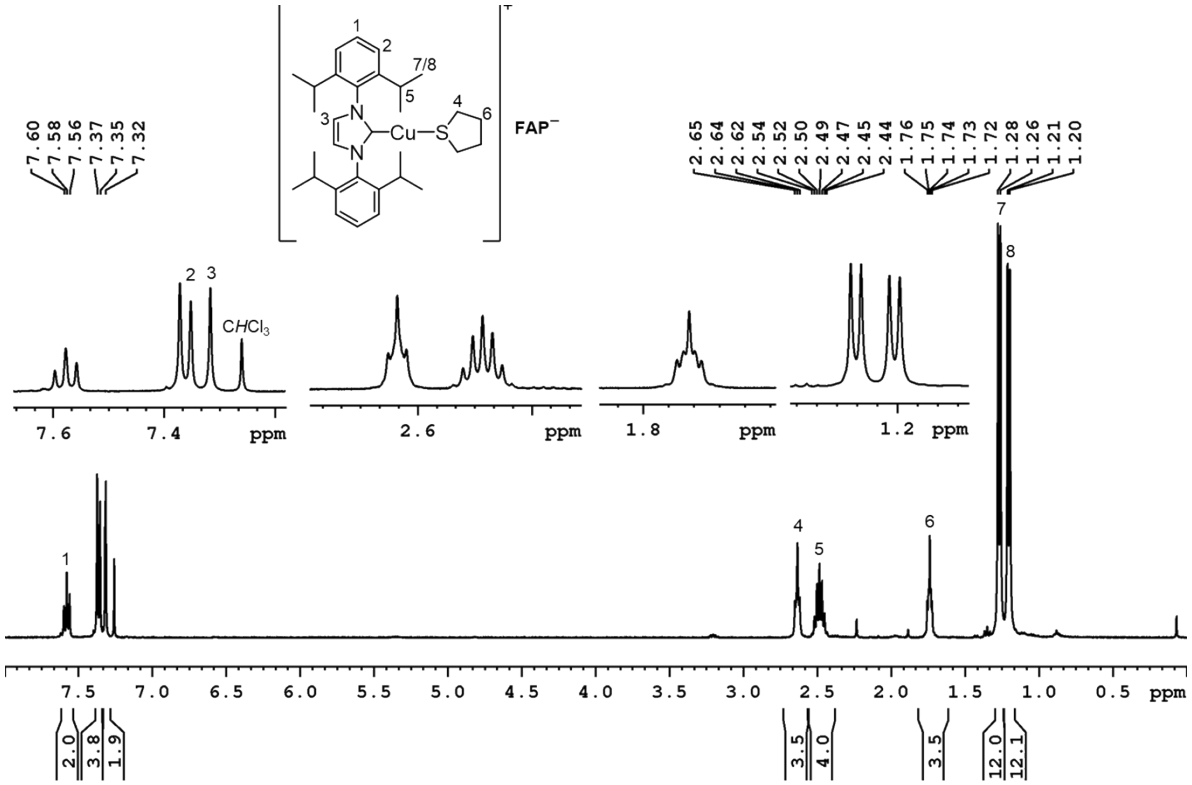

Figure S46. ^{1}H NMR spectrum (500.1 MHz) of **8** recorded in $CDCl_3$.

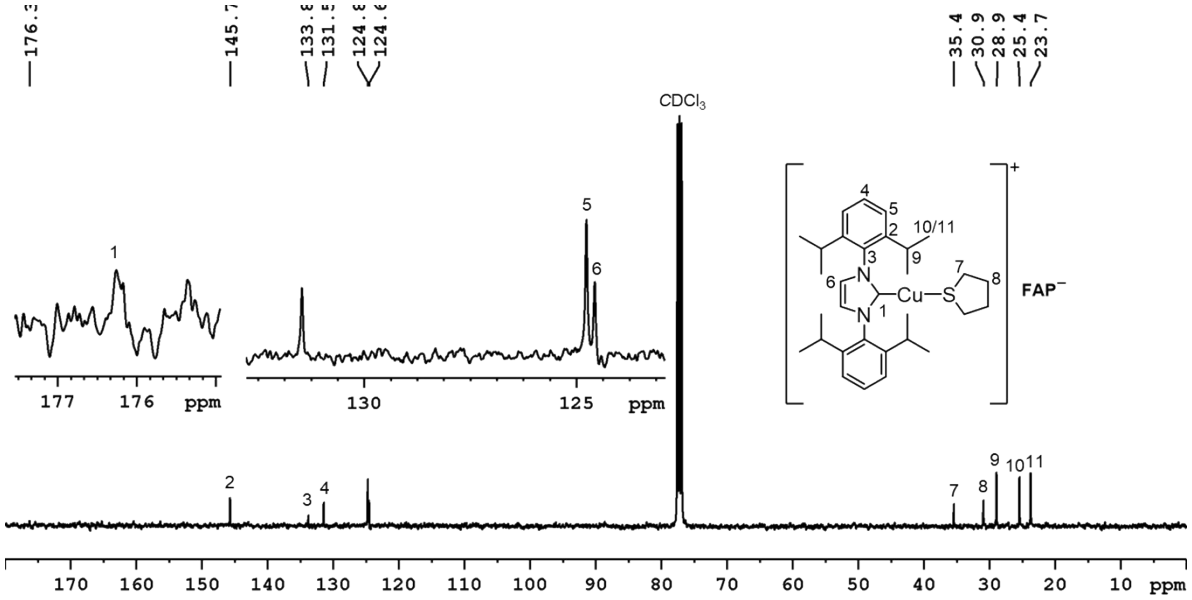

Figure S47. $^{13}C\{^{1}H\}$ NMR spectrum (100.6 MHz) of **8** recorded in $CDCl_3$.

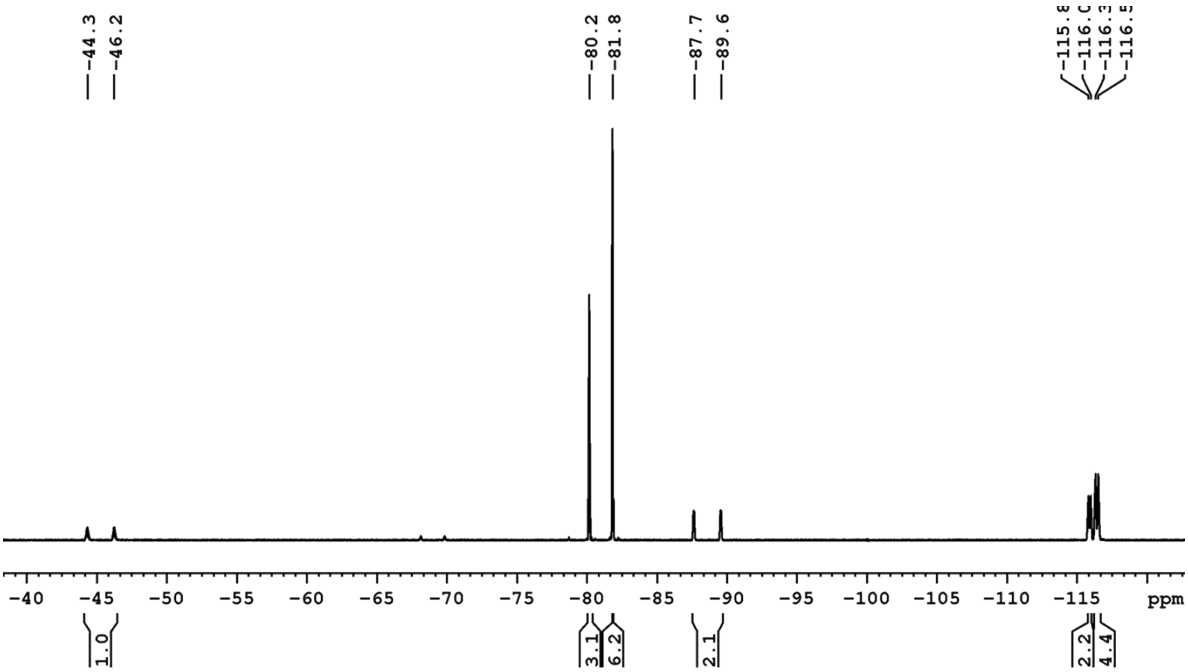

Figure S48. ^{19}F NMR spectrum (470.5 MHz) of **8** recorded in $CDCl_3$.

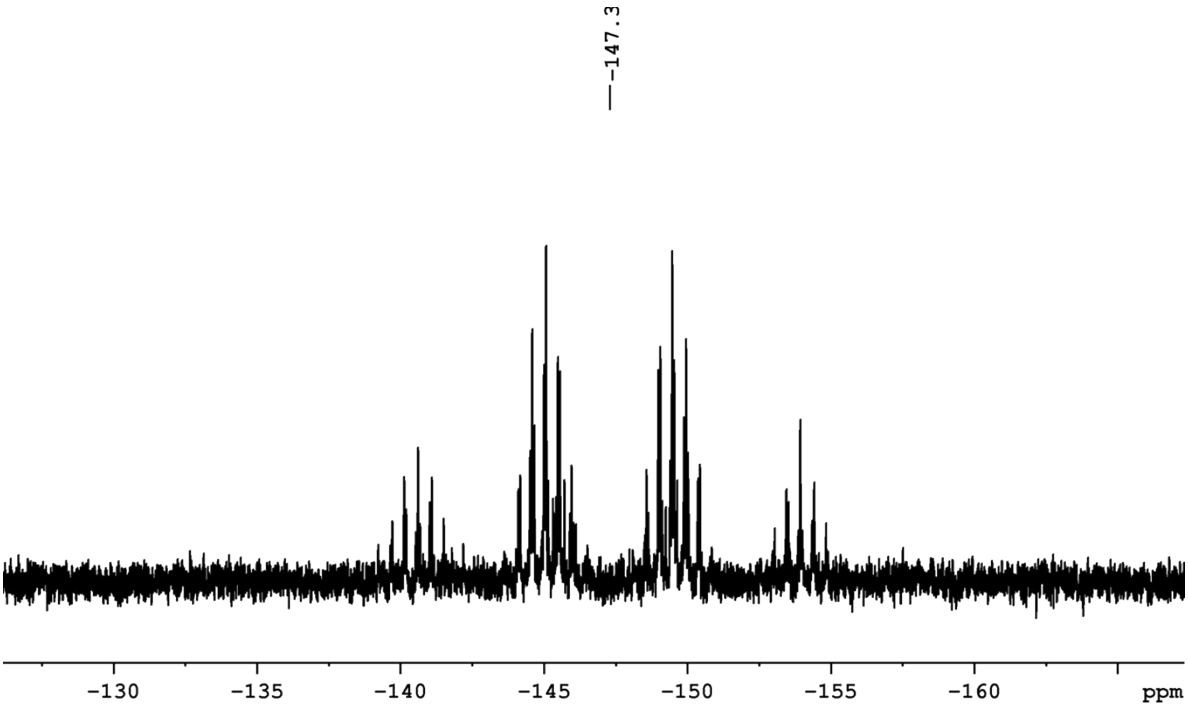

Figure S49. ^{31}P NMR spectrum (202.4 MHz) of **8** recorded in $CDCl_3$.

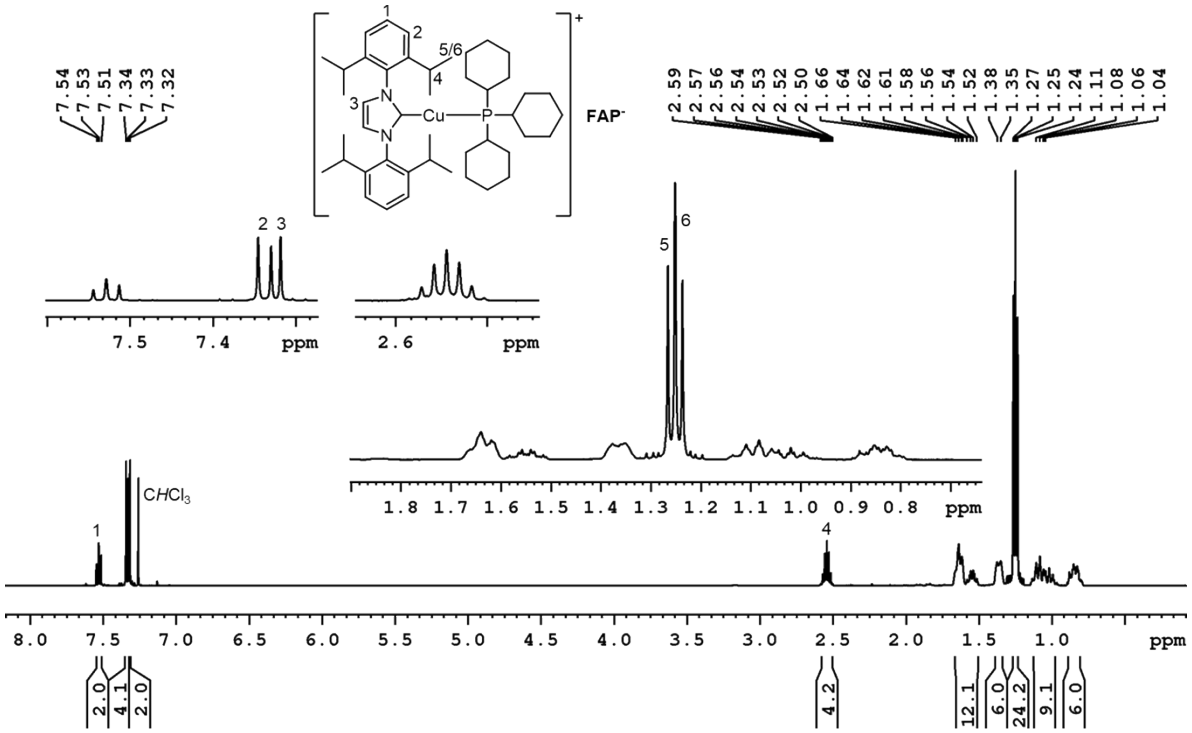

Figure S50. ^{1}H NMR spectrum (500.1 MHz) of **9** recorded in $CDCl_3$.

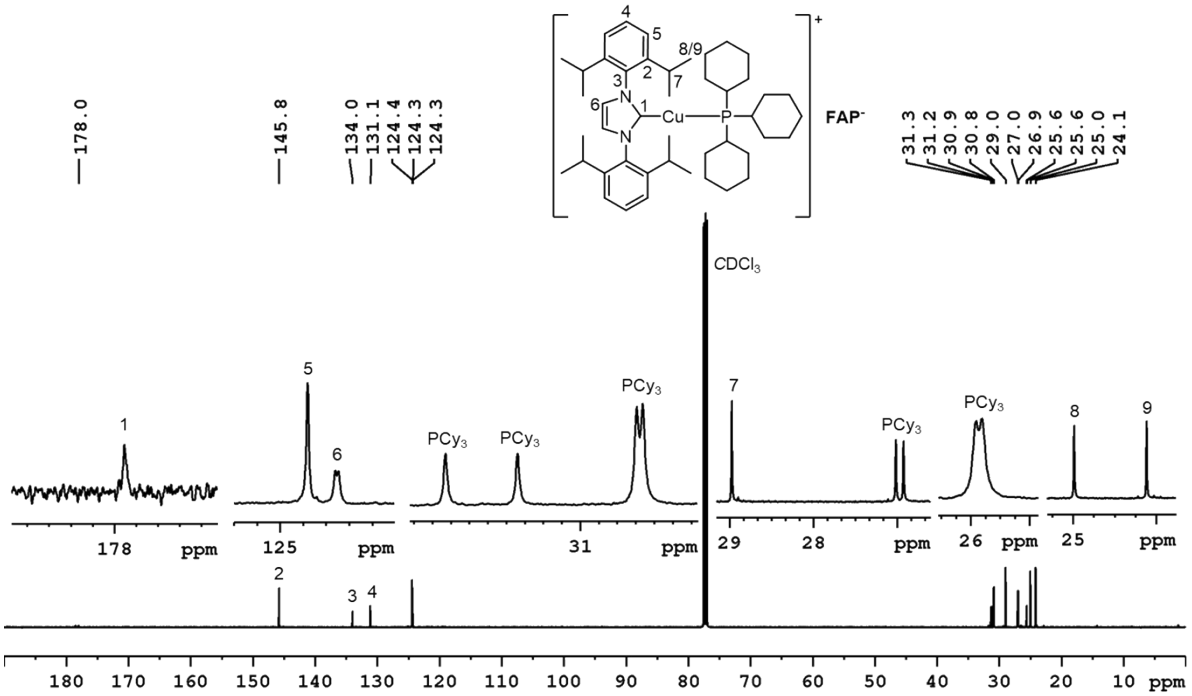

Figure S51. $^{13}C\{^{1}H\}$ NMR spectrum (100.6 MHz) of **9** recorded in $CDCl_3$.

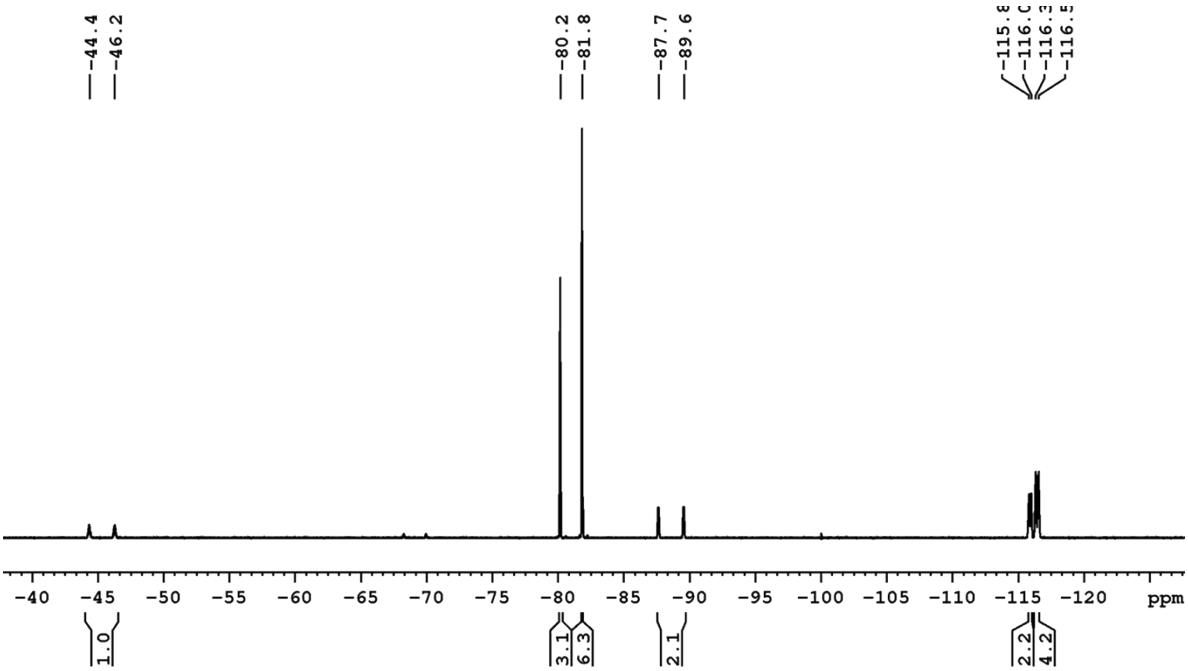

Figure S52. ^{19}F NMR spectrum (470.5 MHz) of **9** recorded in $CDCl_3$.

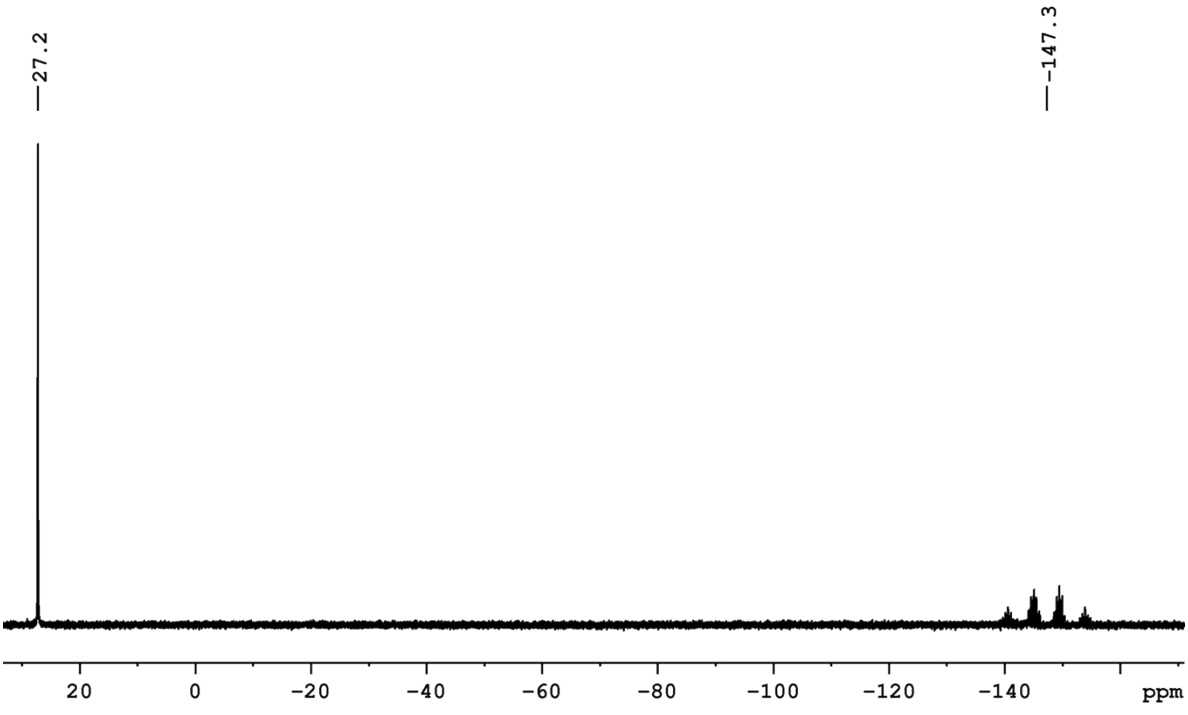

Figure S53. ^{31}P NMR spectrum (202.4 MHz) of **9** recorded in $CDCl_3$.

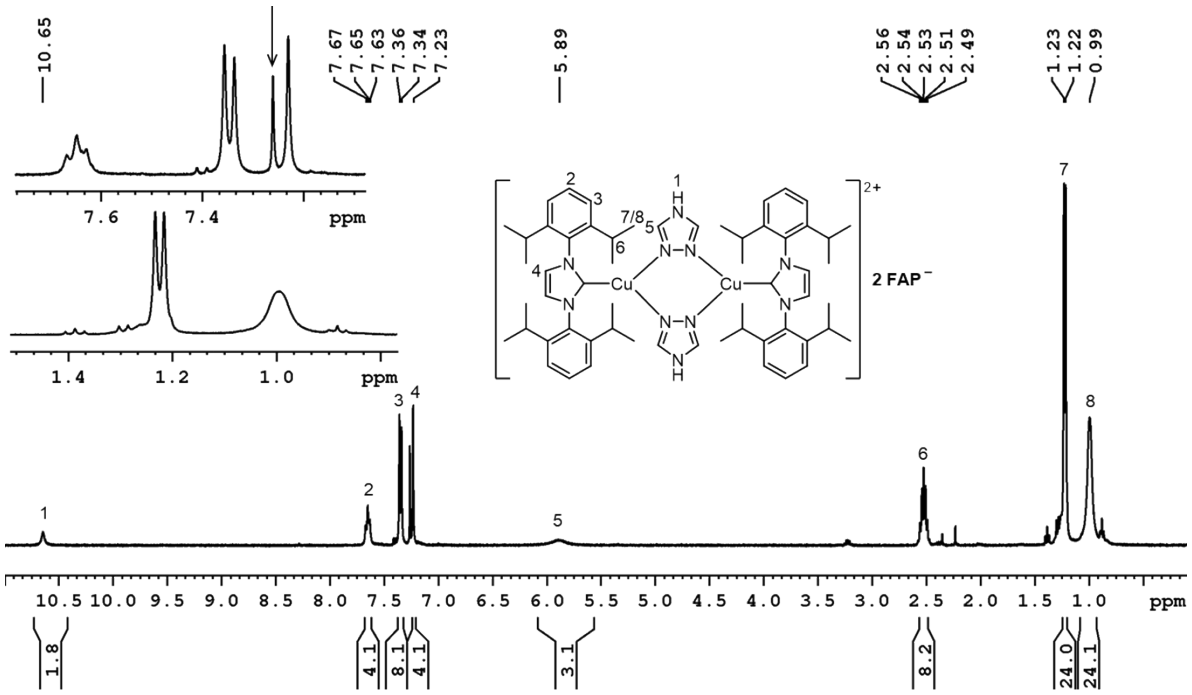

Figure S54. ^{1}H NMR spectrum (400.1 MHz) of **10** recorded in $CDCl_3$.

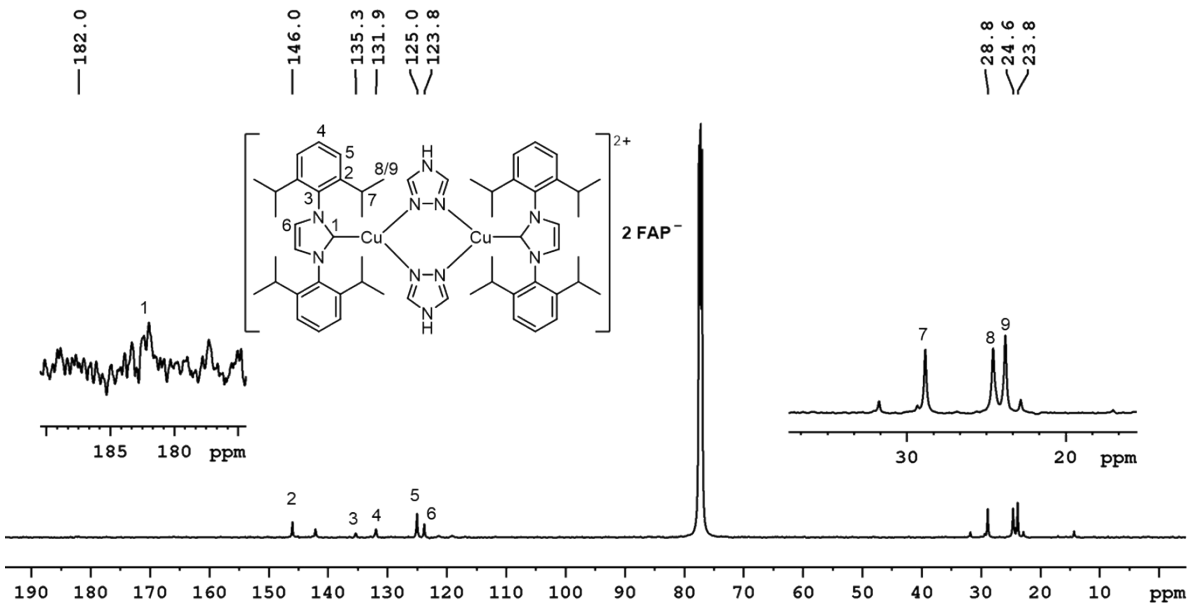

Figure S55. $^{13}C\{^{1}H\}$ NMR spectrum (125.8 MHz) of **10** recorded in $CDCl_3$.

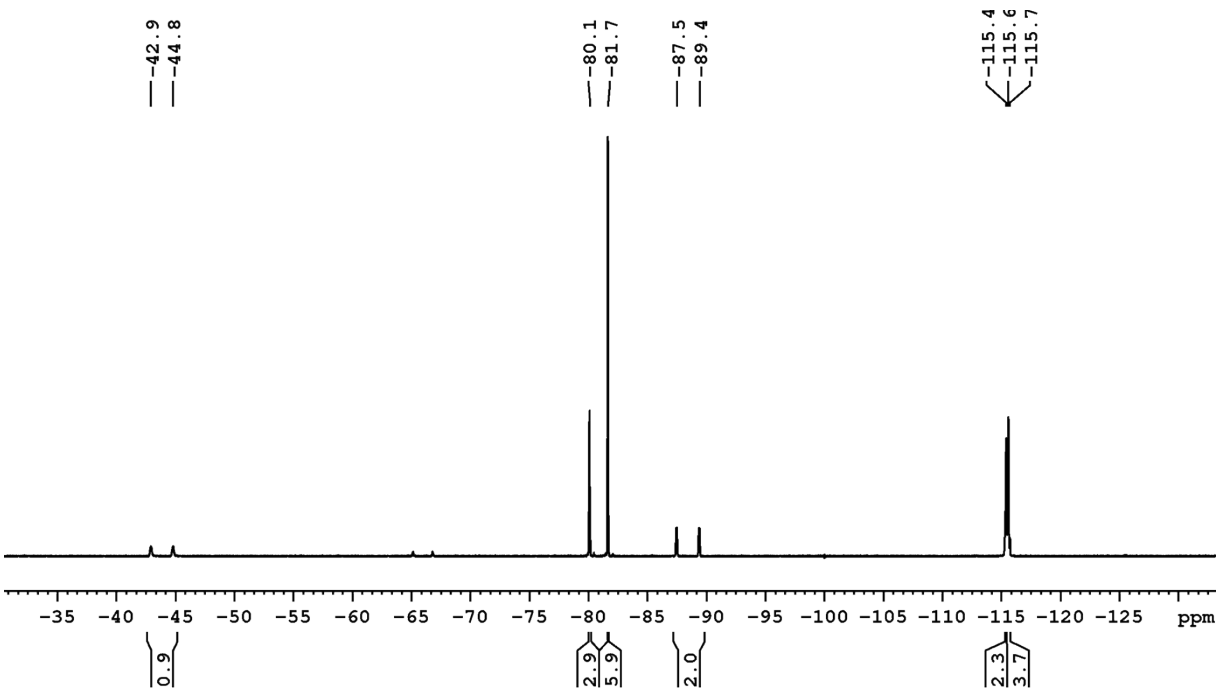

Figure S56. ^{19}F NMR spectrum (470.5 MHz) of **10** recorded in $CDCl_3$.

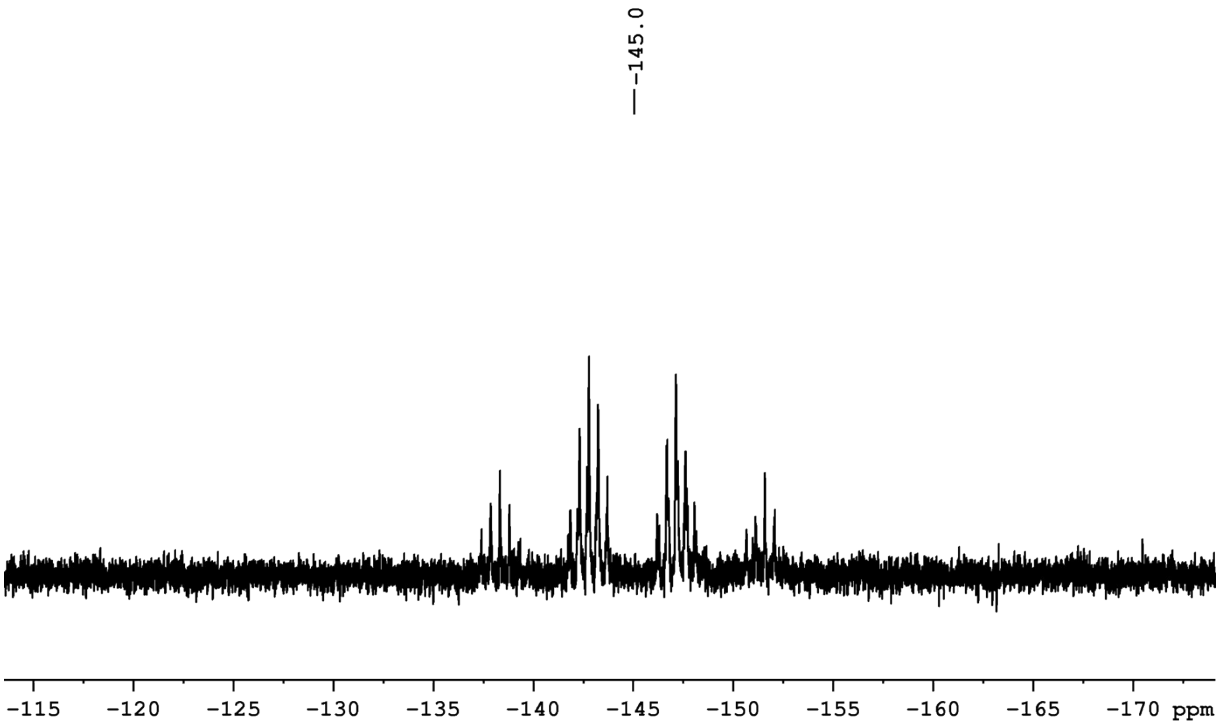

Figure 57. ^{31}P NMR spectrum (202.4 MHz) of **10** recorded in $CDCl_3$.

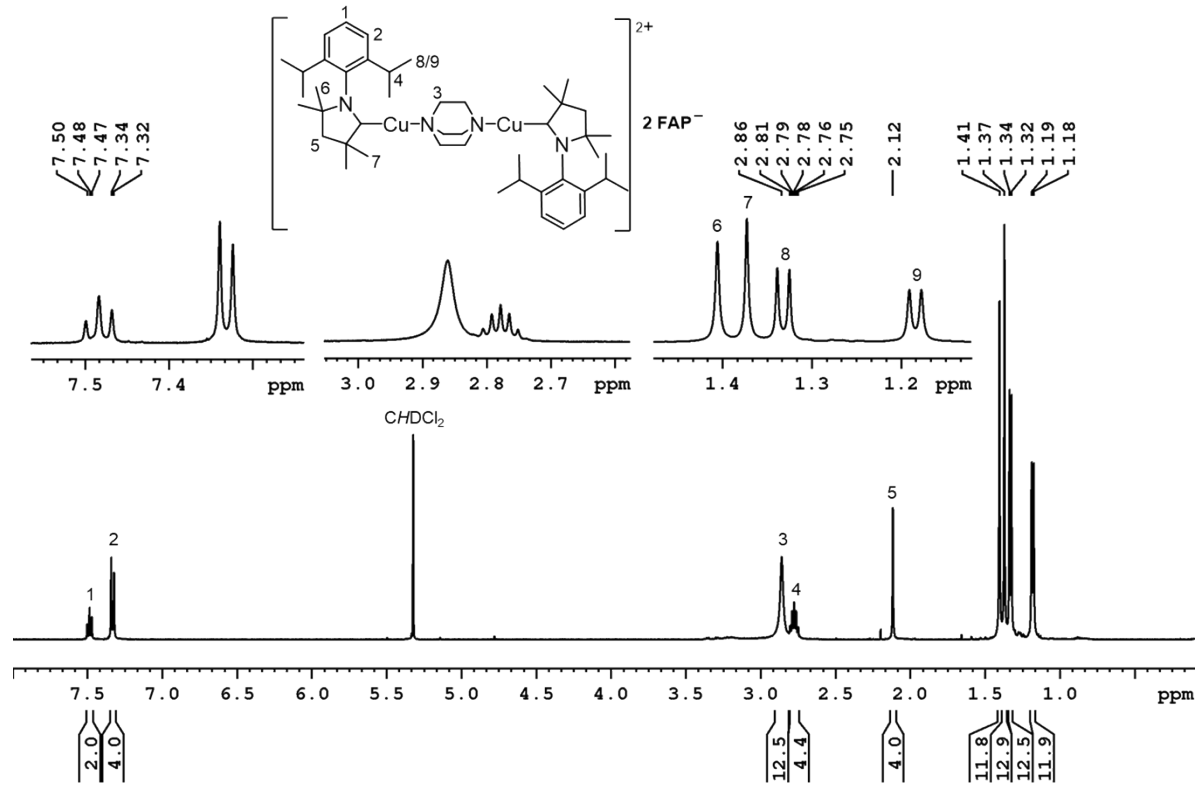

Figure S58. ^{1}H NMR spectrum (500.1 MHz) of **11** recorded in CD_2Cl_2.

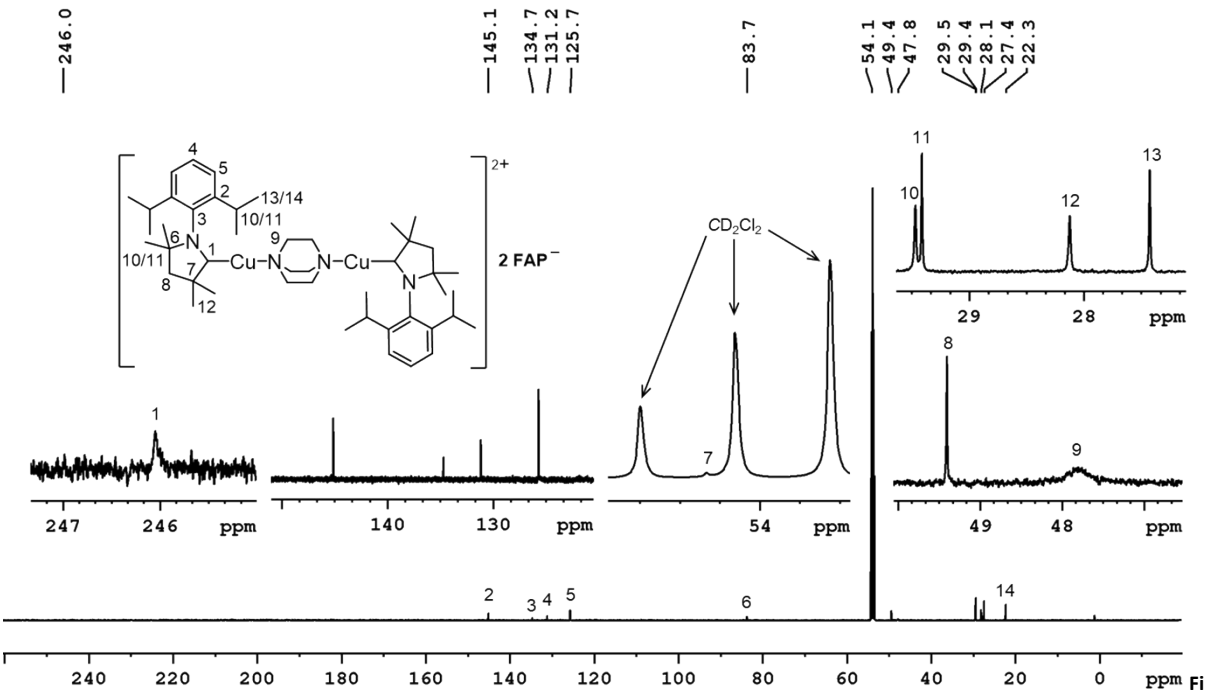

gure S59. $^{13}C\{^{1}H\}$ NMR spectrum (125.8 MHz) of **11** recorded in CD_2Cl_2.

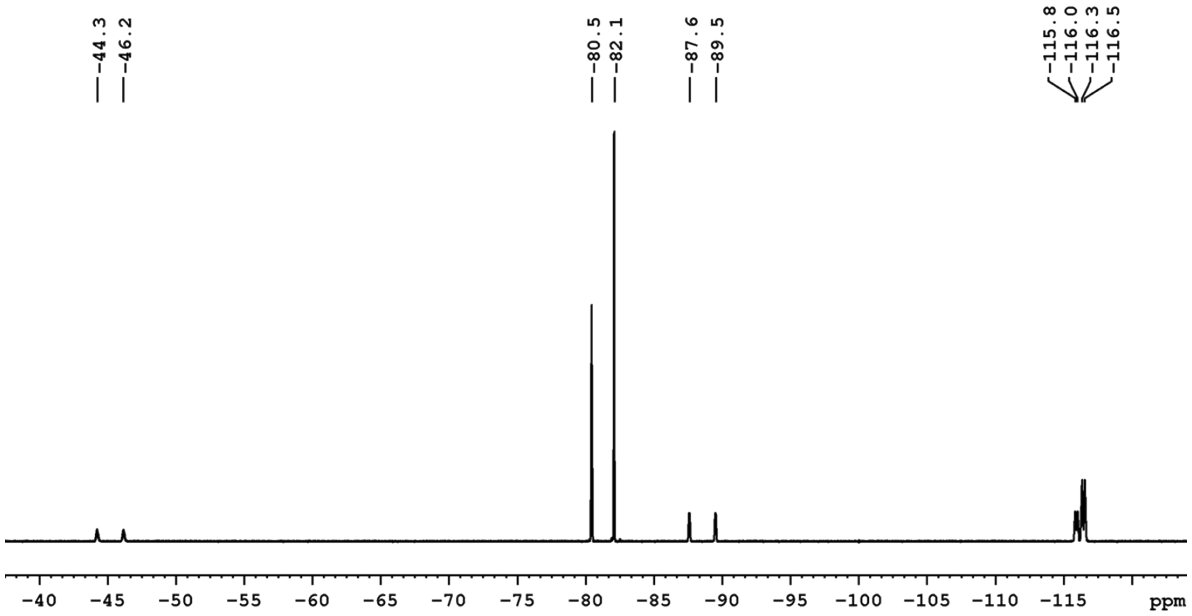

Figure S60. ^{19}F NMR spectrum (470.5 MHz) of **11** recorded in CD_2Cl_2.

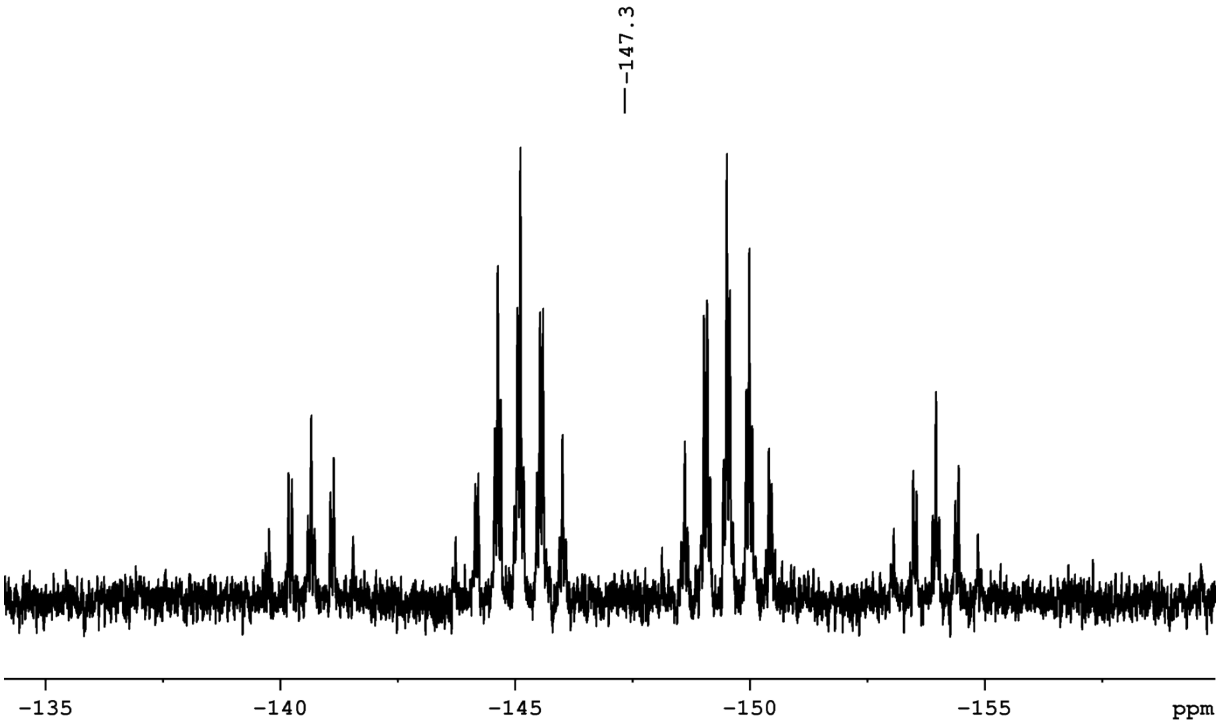

Figure S61. ^{31}P NMR spectrum (202.4 MHz) of **11** recorded in CD_2Cl_2.

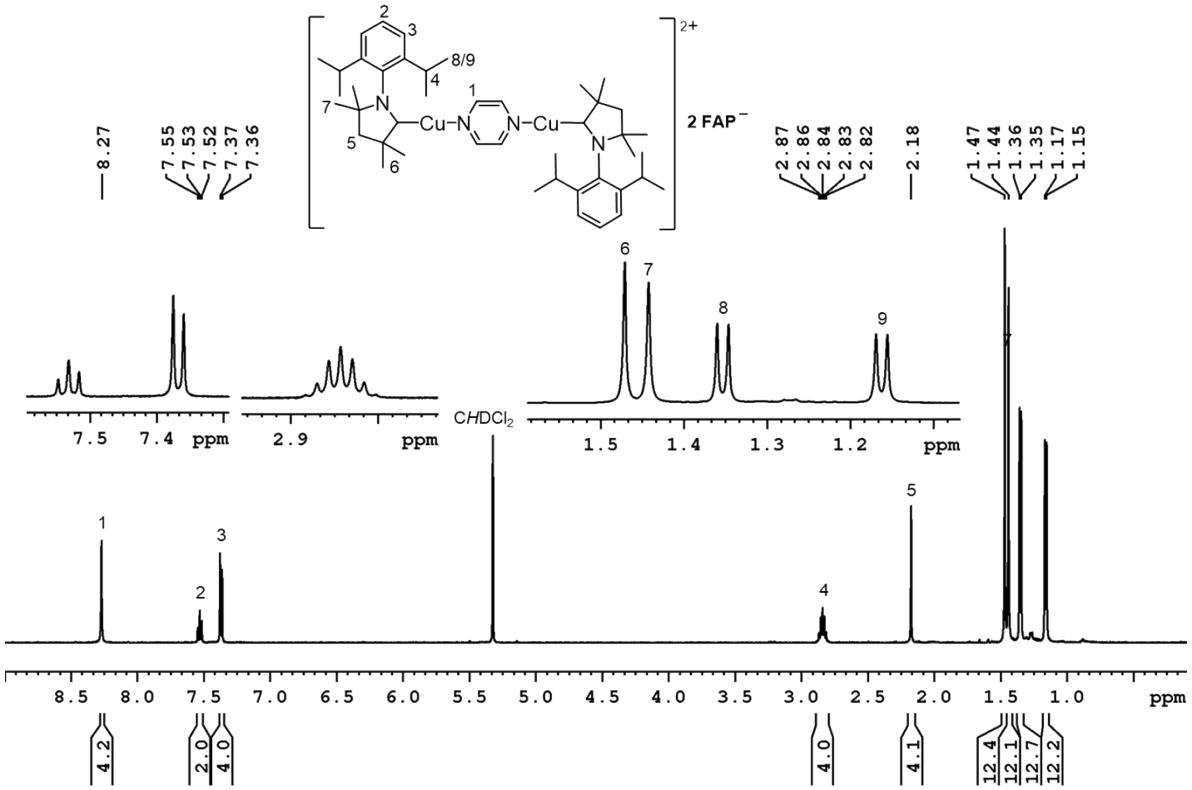

Figure S62. ^{1}H NMR spectrum (500.1 MHz) of **12** recorded in CD_2Cl_2.

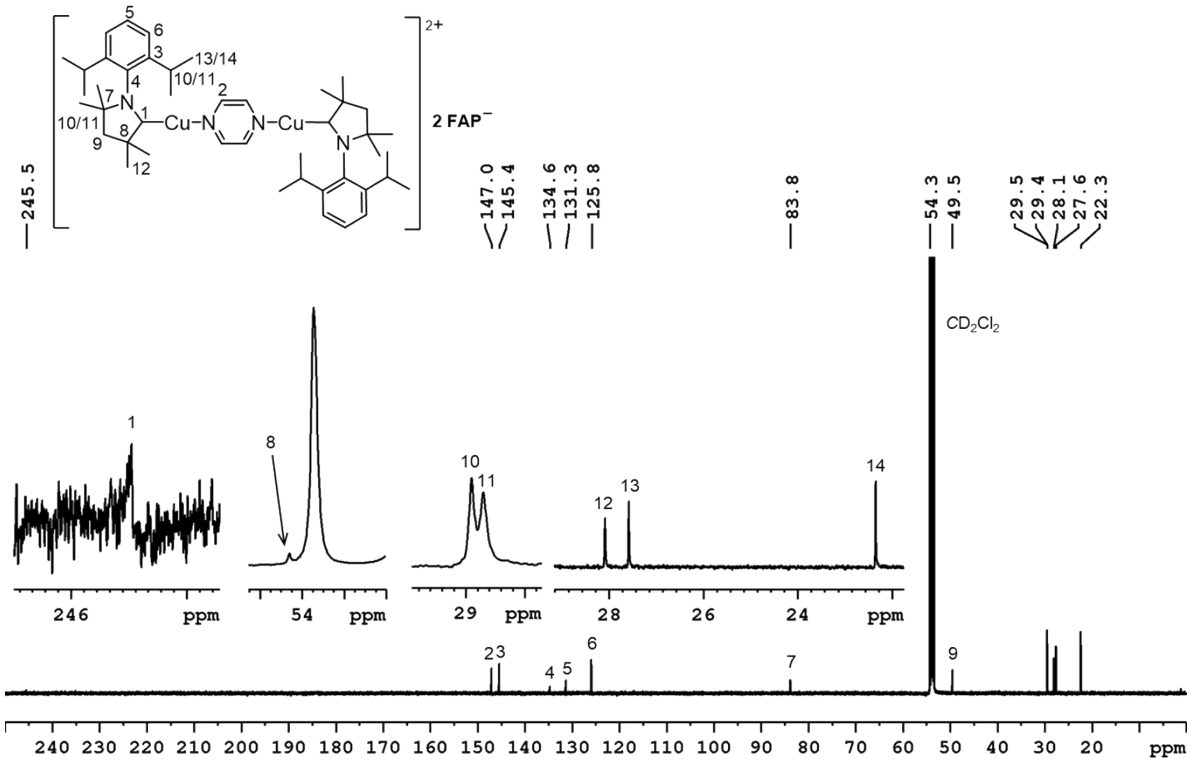

Figure S63. $^{13}C\{^{1}H\}$ NMR spectrum (125.8 MHz) of **12** recorded in CD_2Cl_2.

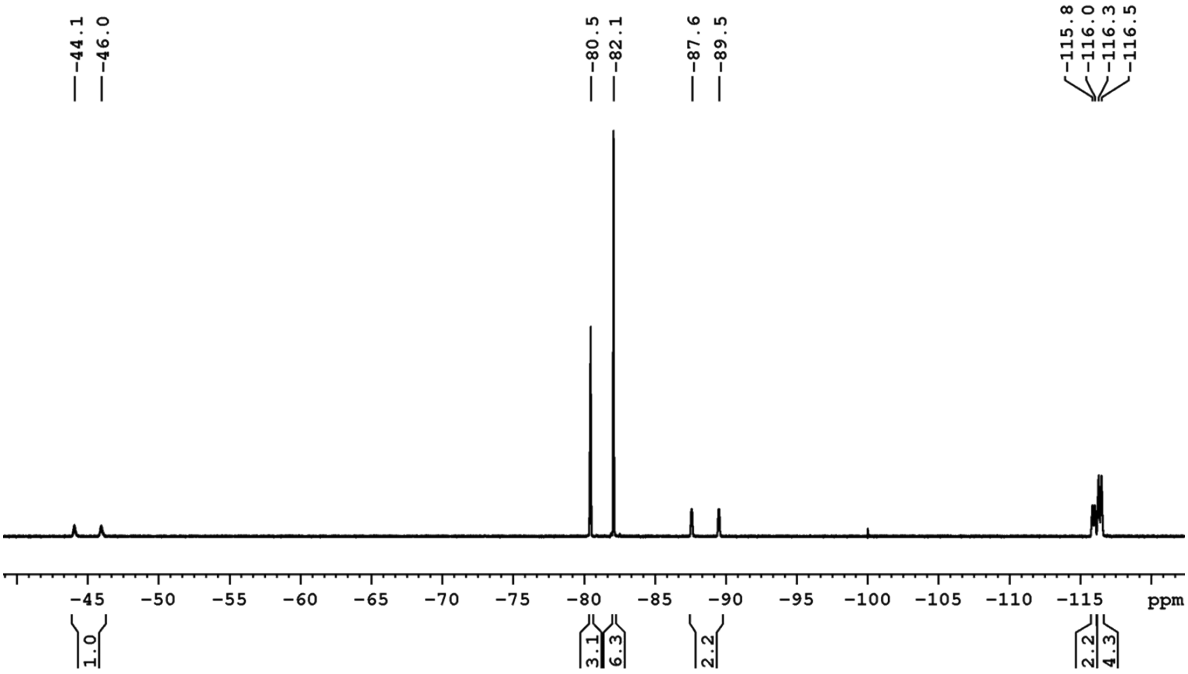

Figure S64. ^{19}F NMR spectrum (470.5 MHz) of **12** recorded in CD_2Cl_2.

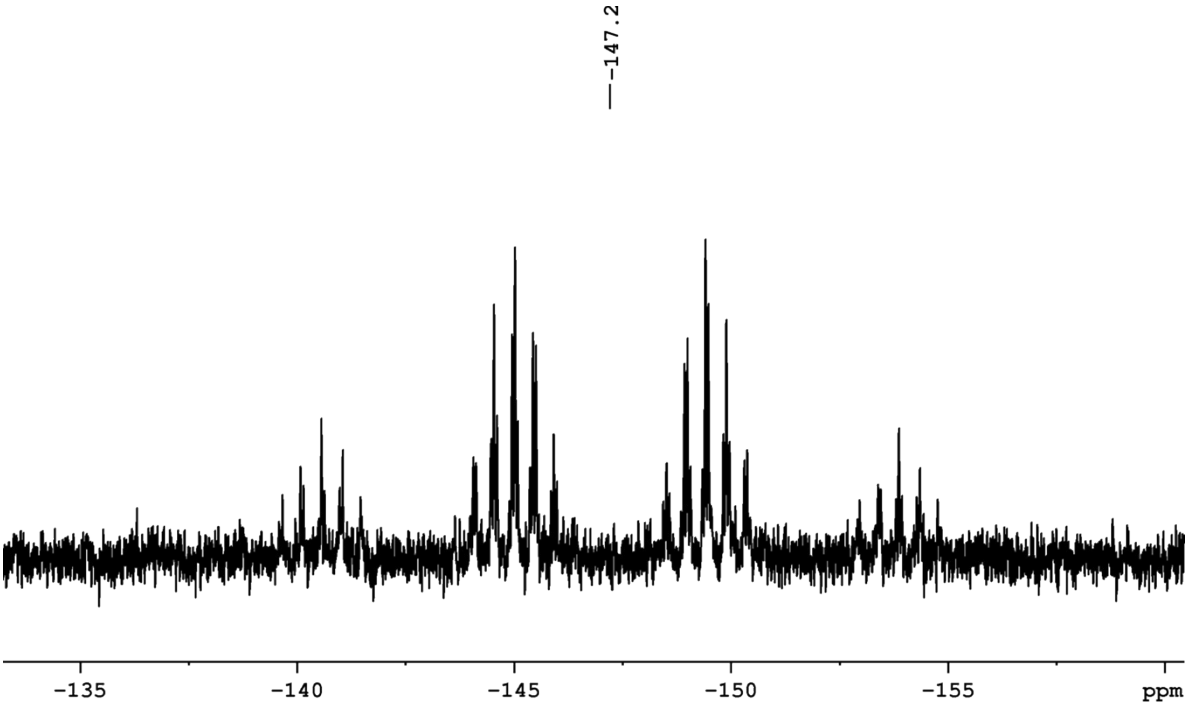

Figure S65. ^{31}P NMR spectrum (202.4 MHz) of **12** recorded in CD_2Cl_2.

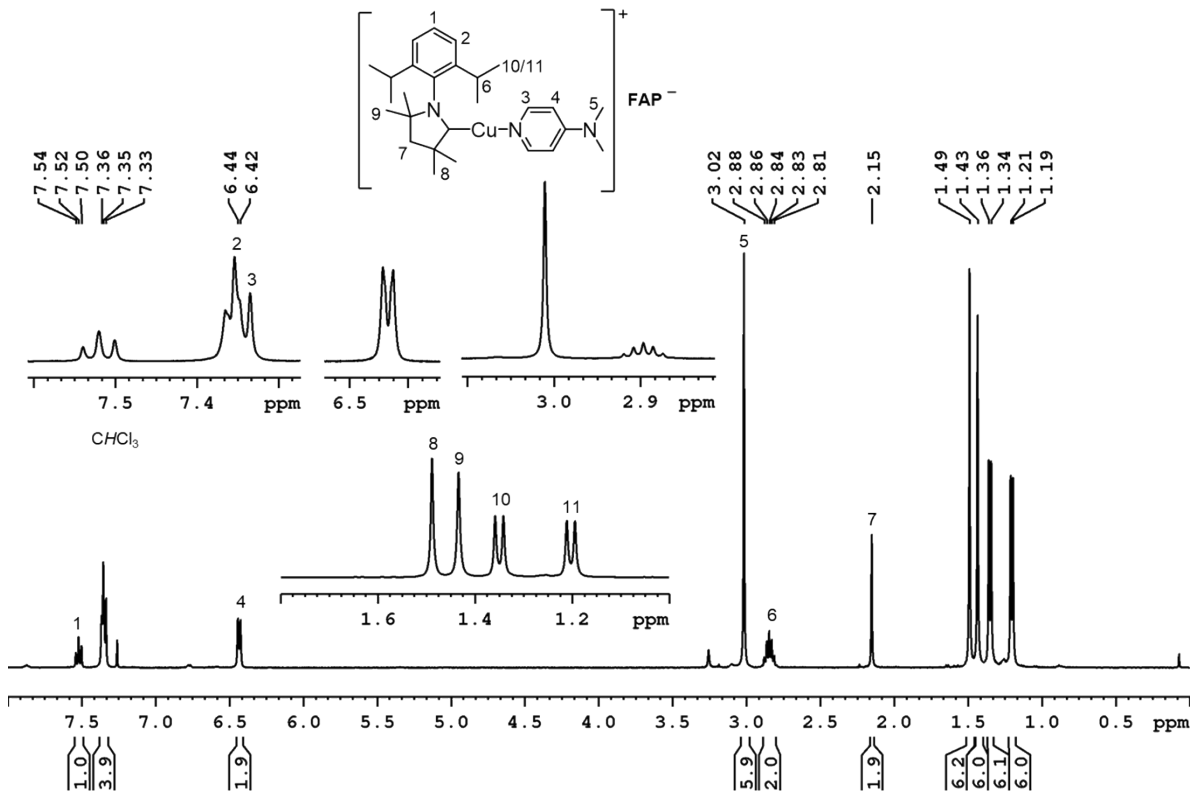

Figure S66. ^{1}H NMR spectrum (500.1 MHz) of **13** recorded in $CDCl_3$.

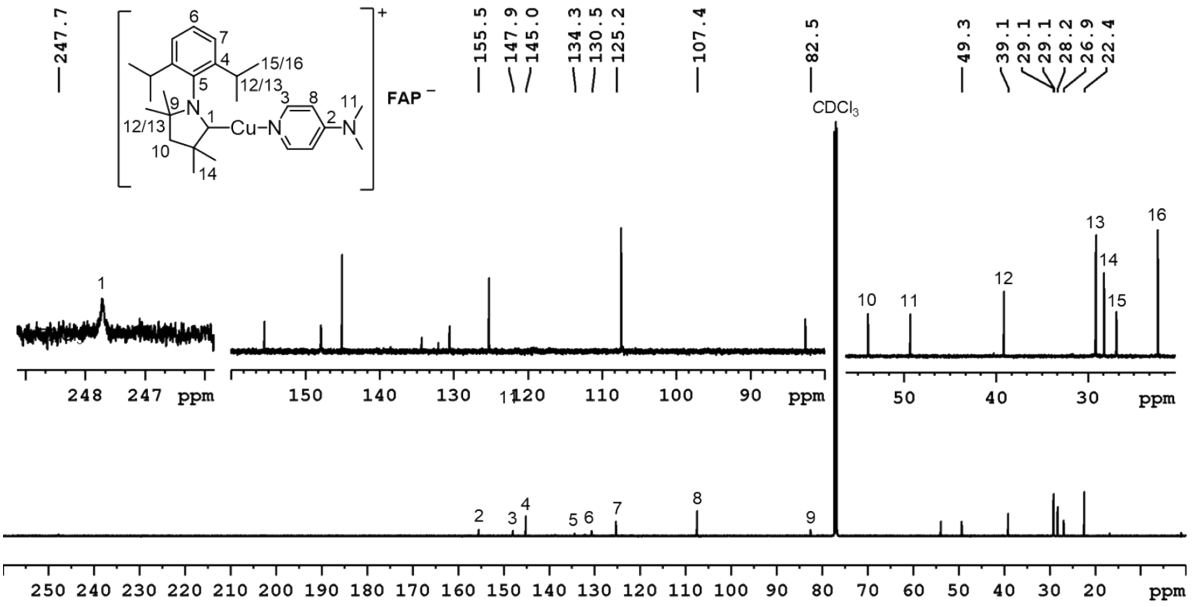

Figure S67. $^{13}C\{^{1}H\}$ NMR spectrum (125.8 MHz) of **13** recorded in $CDCl_3$.

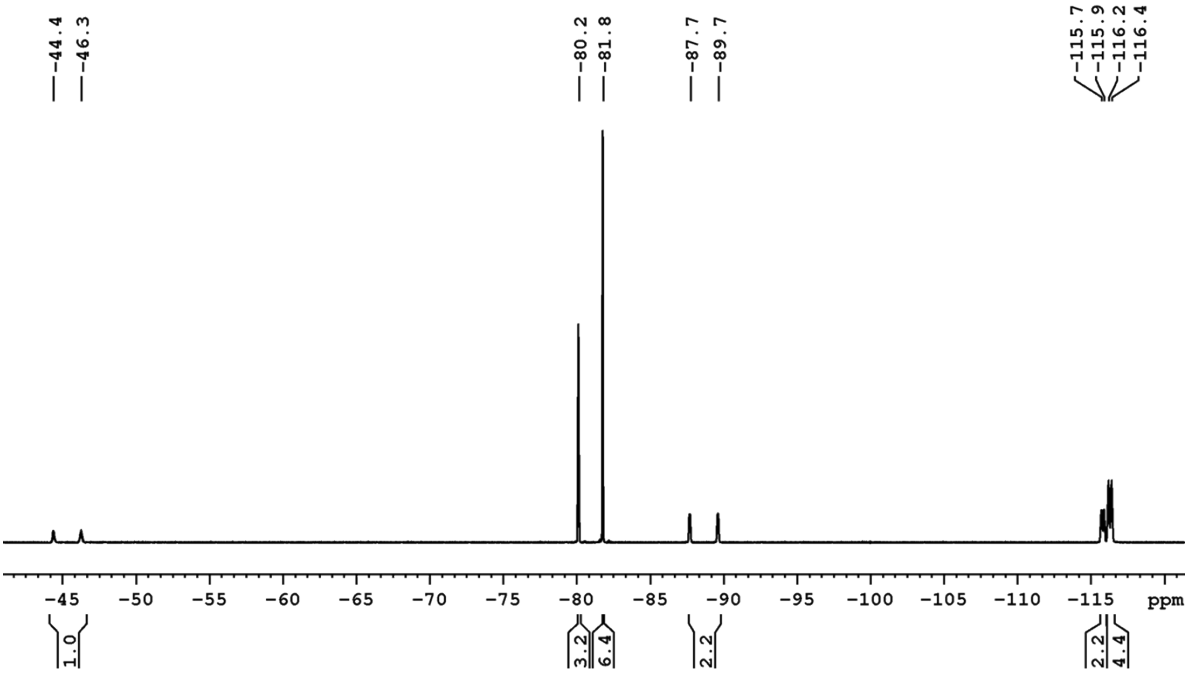

Figure S68. ^{19}F NMR spectrum (470.5 MHz) of **13** recorded in $CDCl_3$.

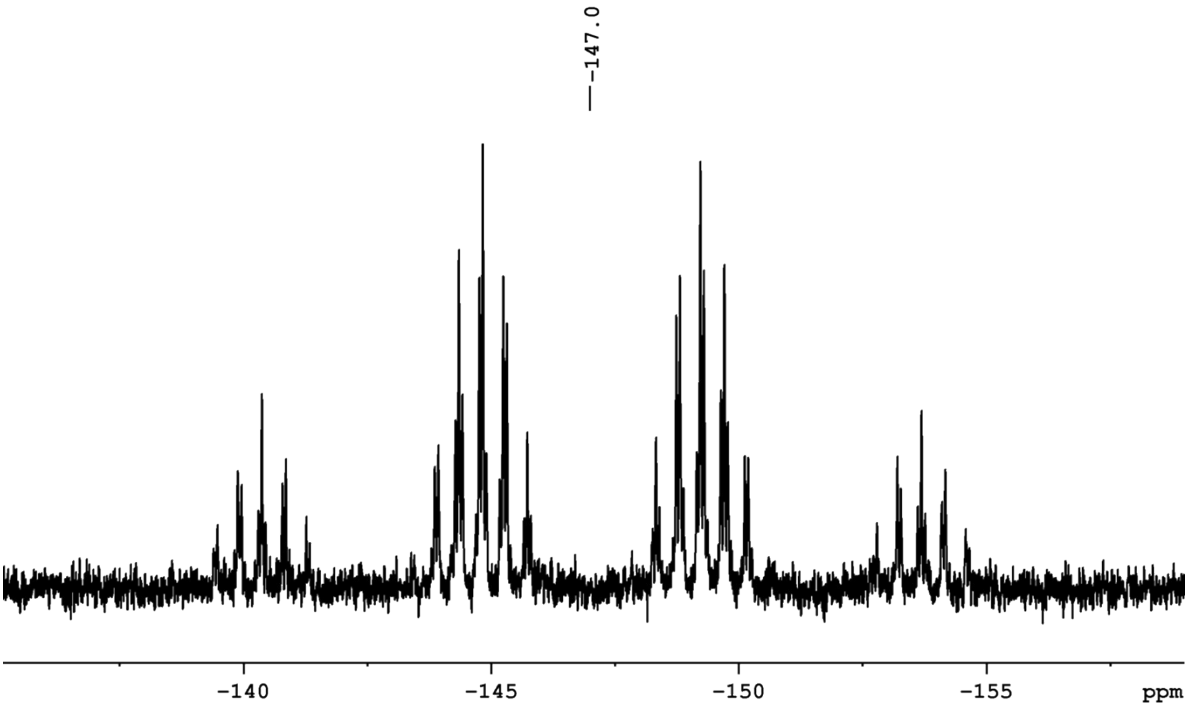

Figure S69. ^{31}P NMR spectrum (202.4 MHz) of **13** recorded in $CDCl_3$.

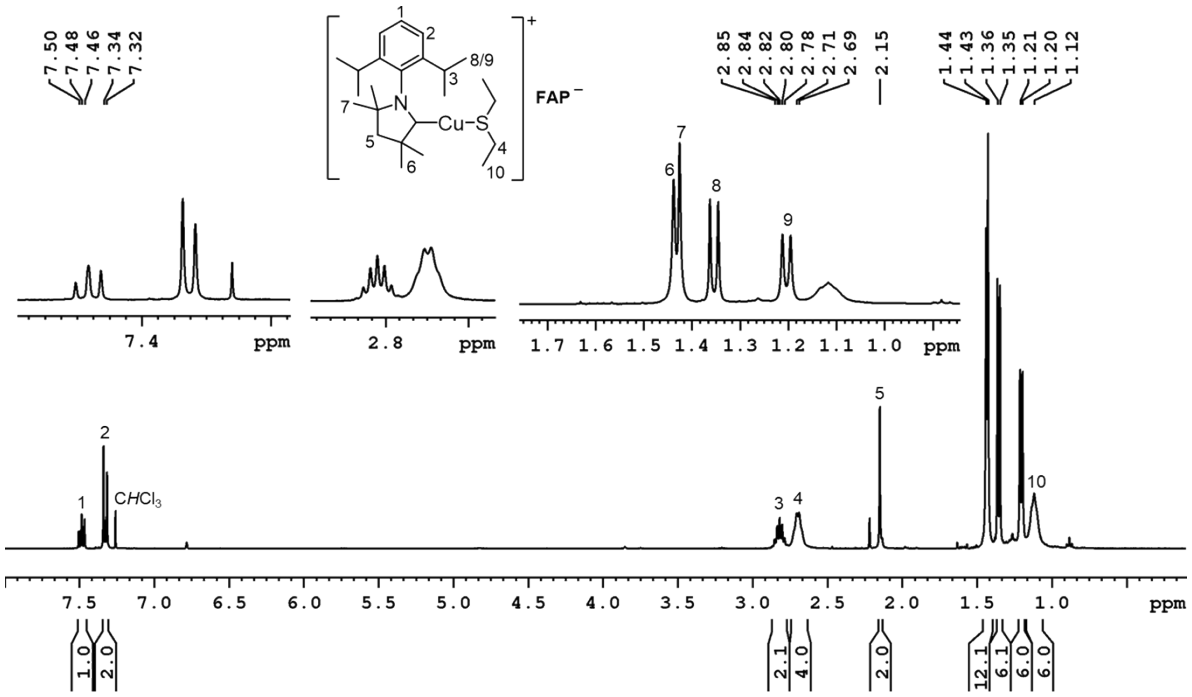

Figure S70. ^{1}H NMR spectrum (400.1 MHz) of **14** recorded in $CDCl_3$.

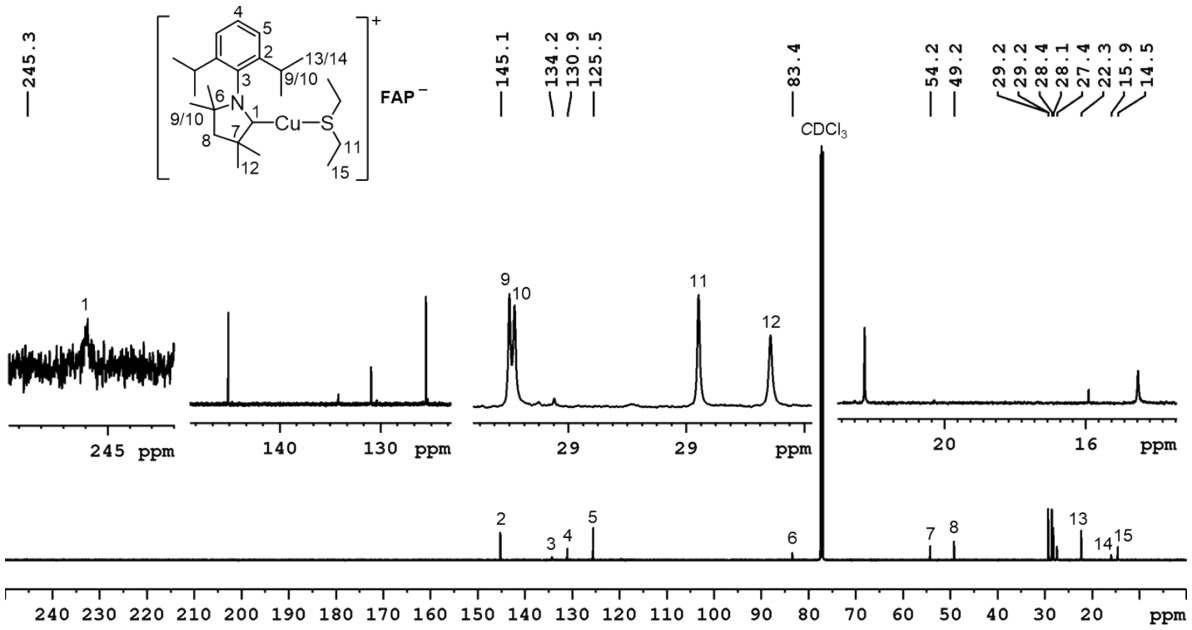

Figure S71. $^{13}C\{^{1}H\}$ NMR spectrum (100.6 MHz) of **14** recorded in $CDCl_3$.

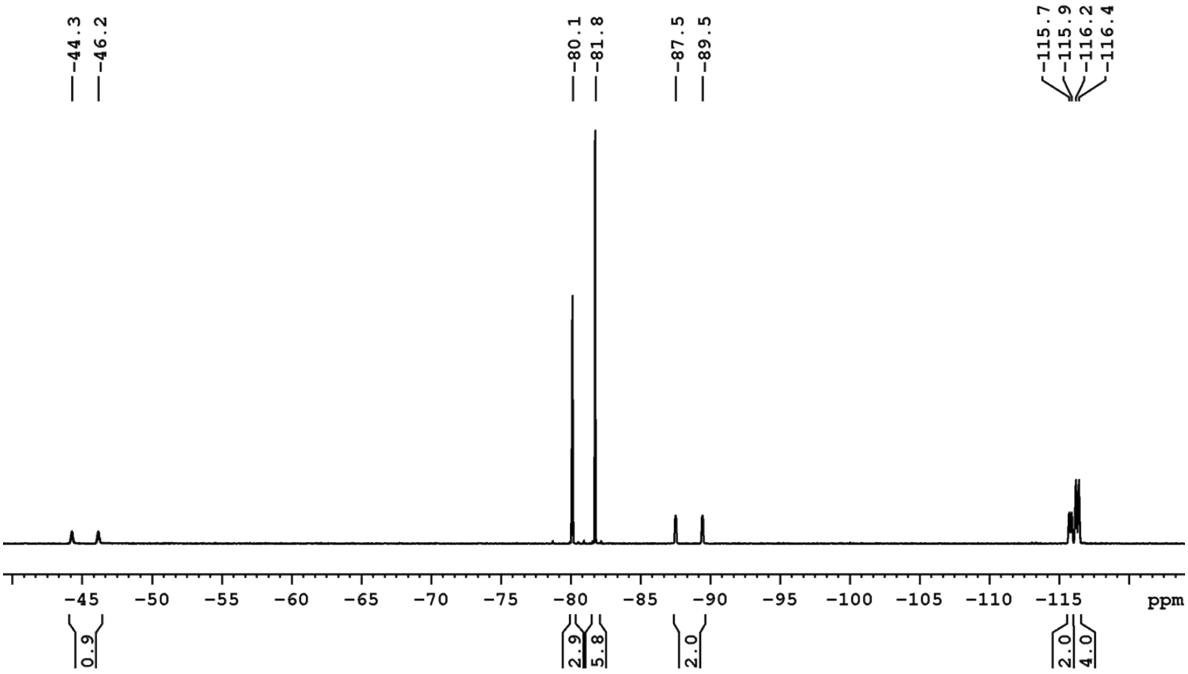

Figure S72. ^{19}F NMR spectrum (470.5 MHz) of **14** recorded in $CDCl_3$.

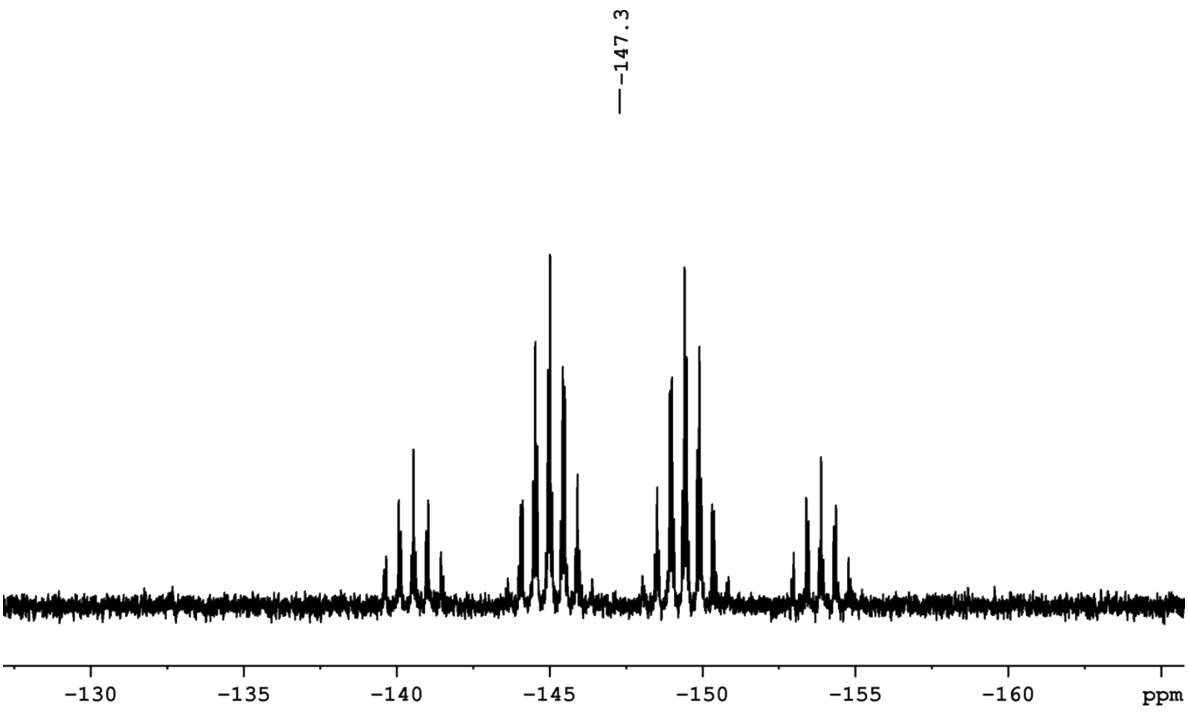

Figure S73. ^{31}P NMR spectrum (202.4 MHz) of **14** recorded in $CDCl_3$.

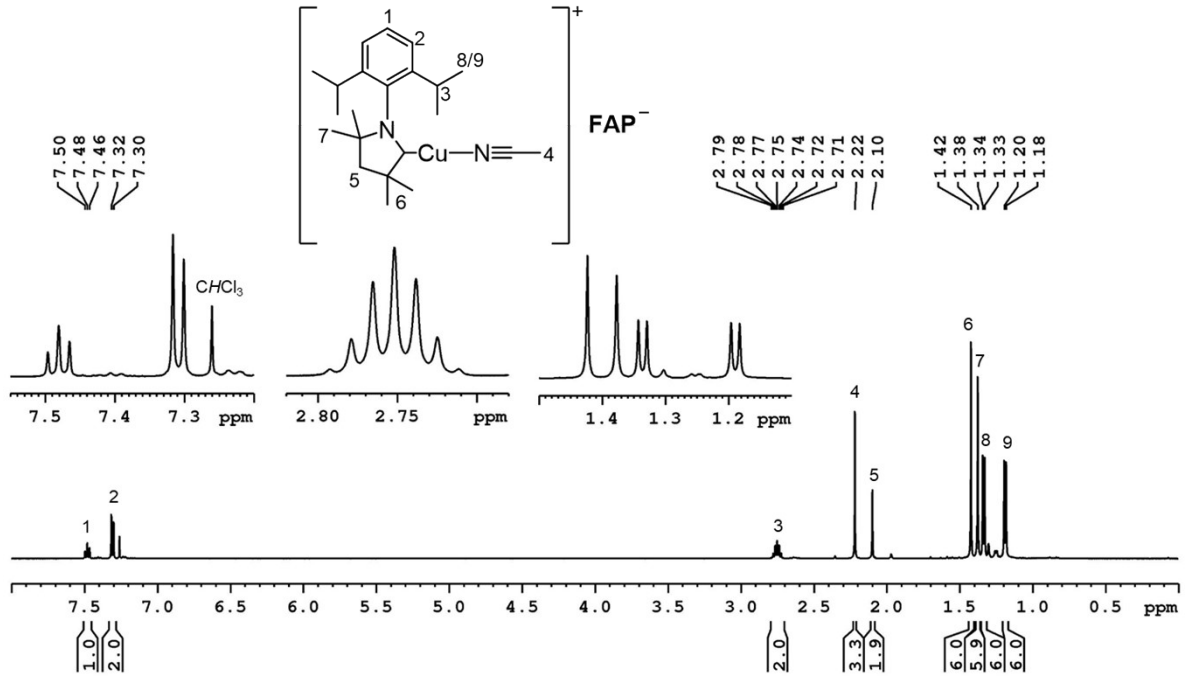

Figure S74. ^{1}H NMR spectrum (500.1 MHz) of **15** recorded in $CDCl_3$.

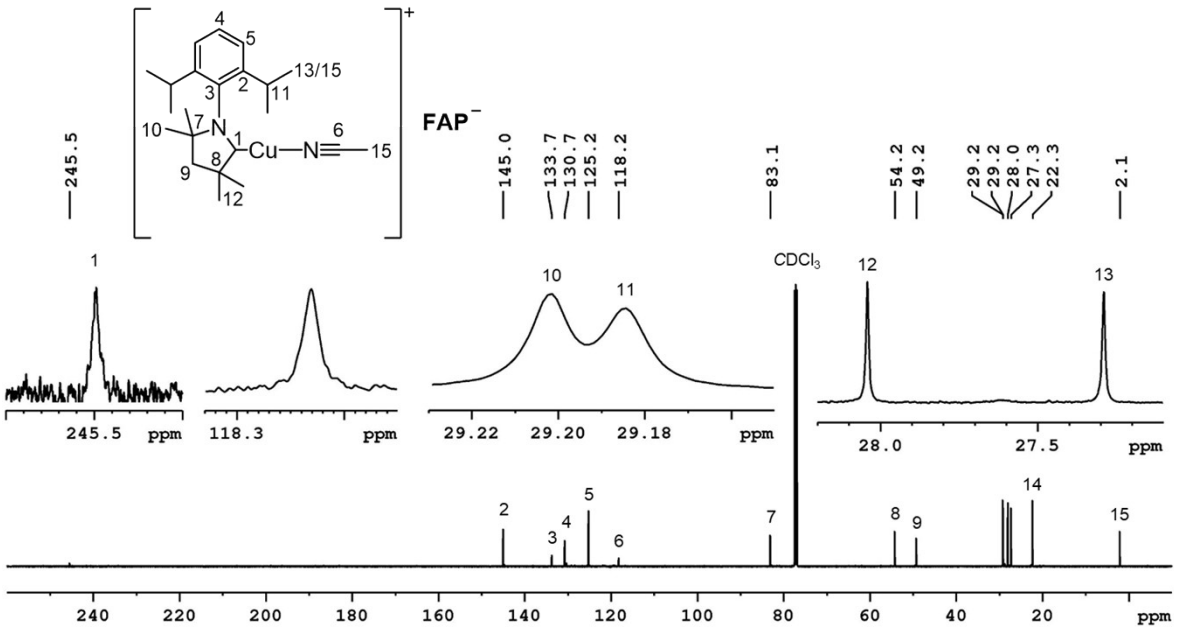

Figure S75. $^{13}C\{^{1}H\}$ NMR spectrum (125.8 MHz) of **15** recorded in $CDCl_3$.

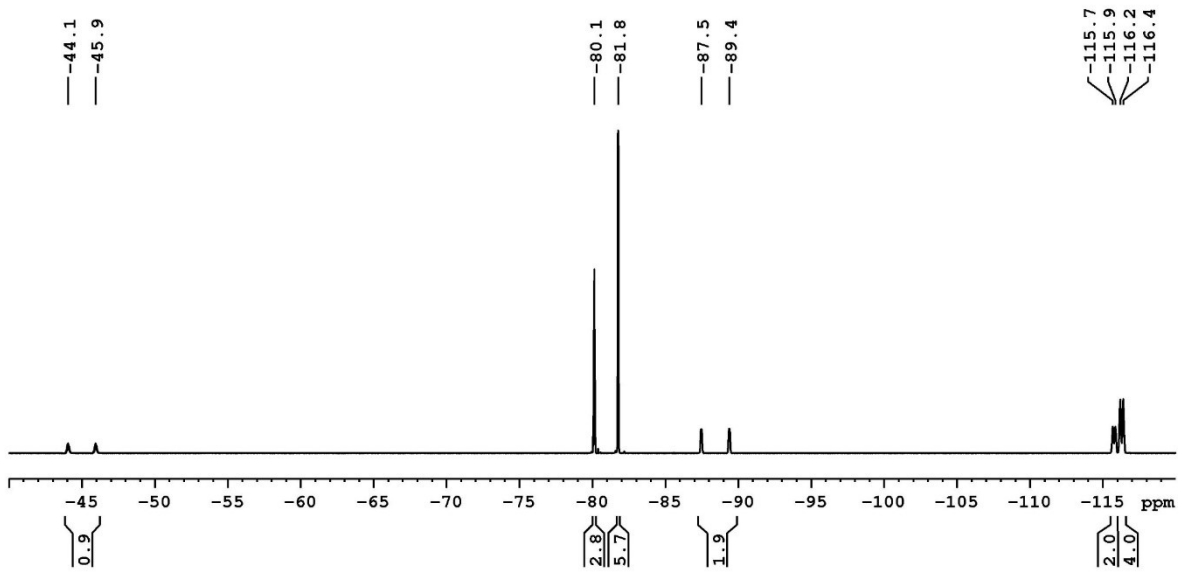

Figure S76. ^{19}F NMR spectrum (470.5 MHz) of **15** recorded in $CDCl_3$.

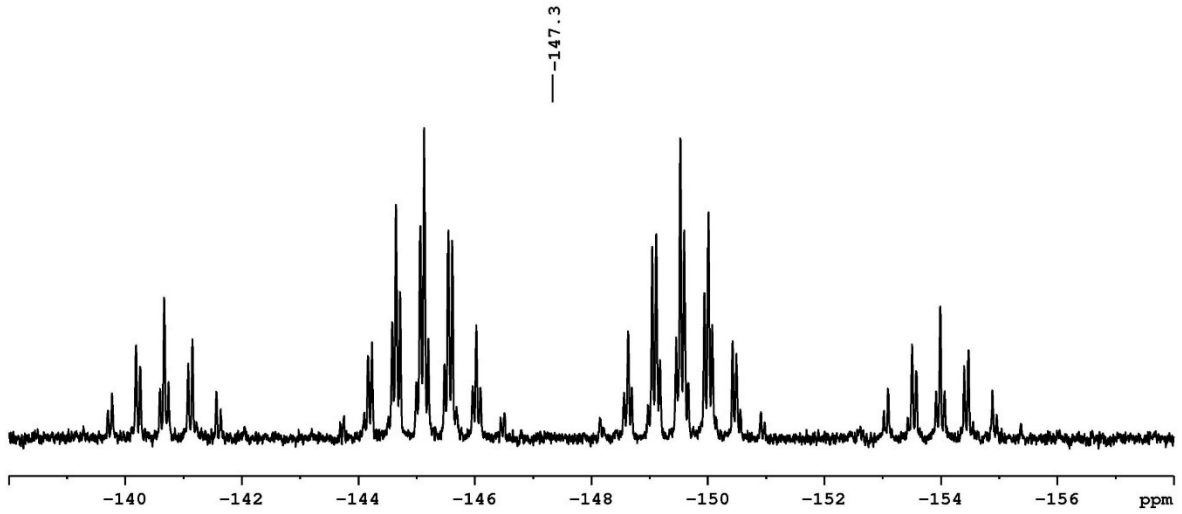

Figure S77. ^{31}P NMR spectrum (202.4 MHz) of **15** recorded in $CDCl_3$.

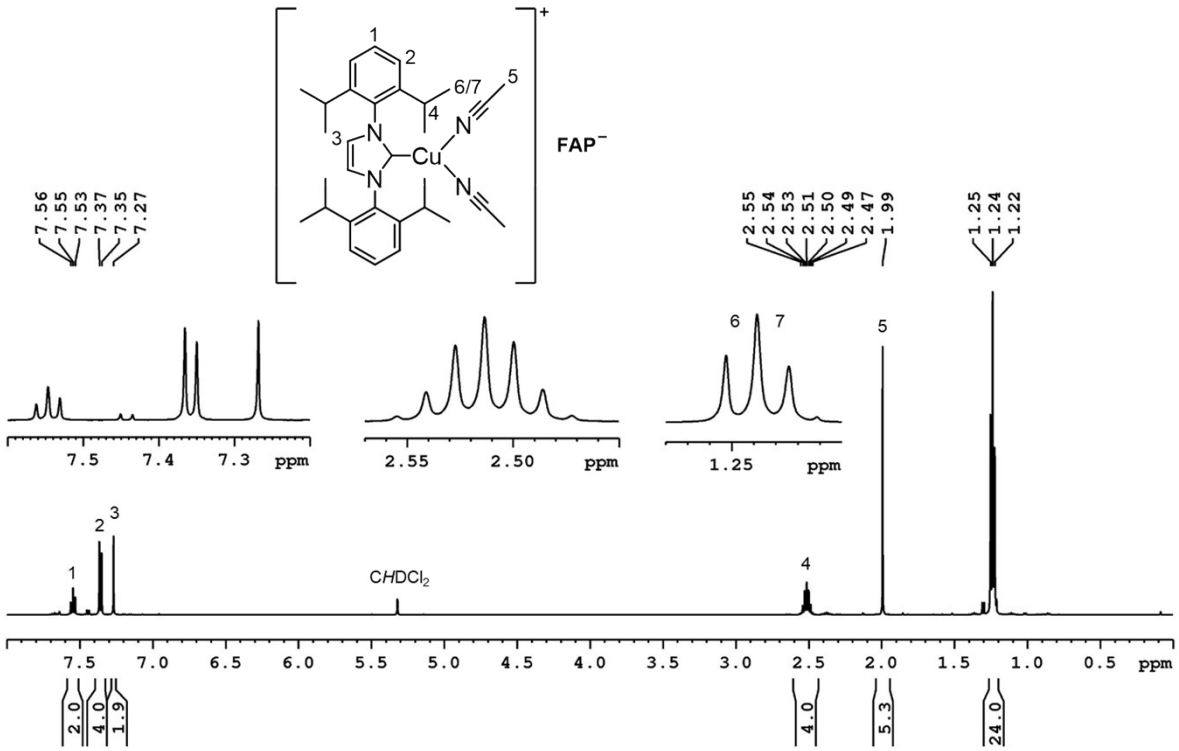

Figure S78. ^{1}H NMR spectrum (500.1 MHz) of **16** recorded in $CDCl_3$.

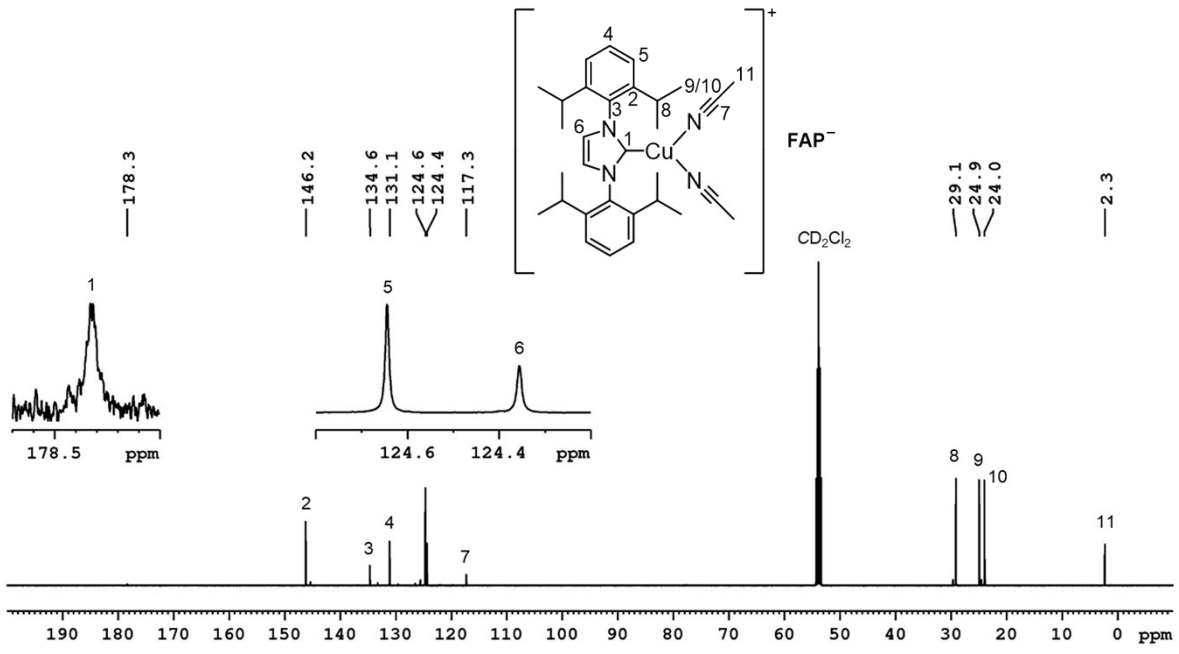

Figure S79. $^{13}C\{^{1}H\}$ NMR spectrum (125.8 MHz) of **16** recorded in CD_2Cl_2.

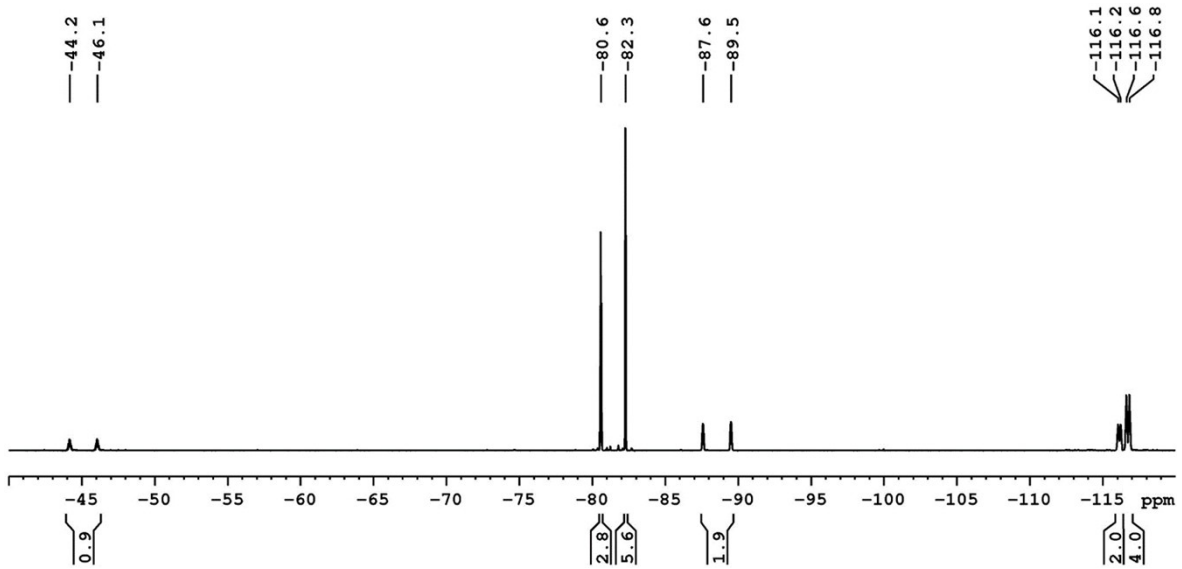

Figure S80. ^{19}F NMR spectrum (470.5 MHz) of **16** recorded in CD_2Cl_2.

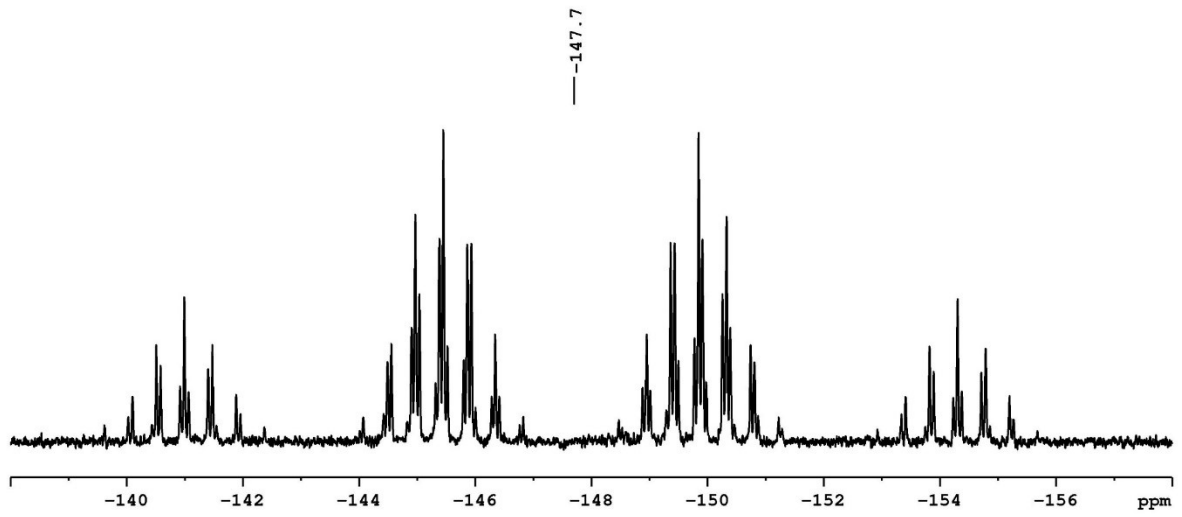

Figure S81. ^{31}P NMR spectrum (202.4 MHz) of **16** recorded in CD_2Cl_2.

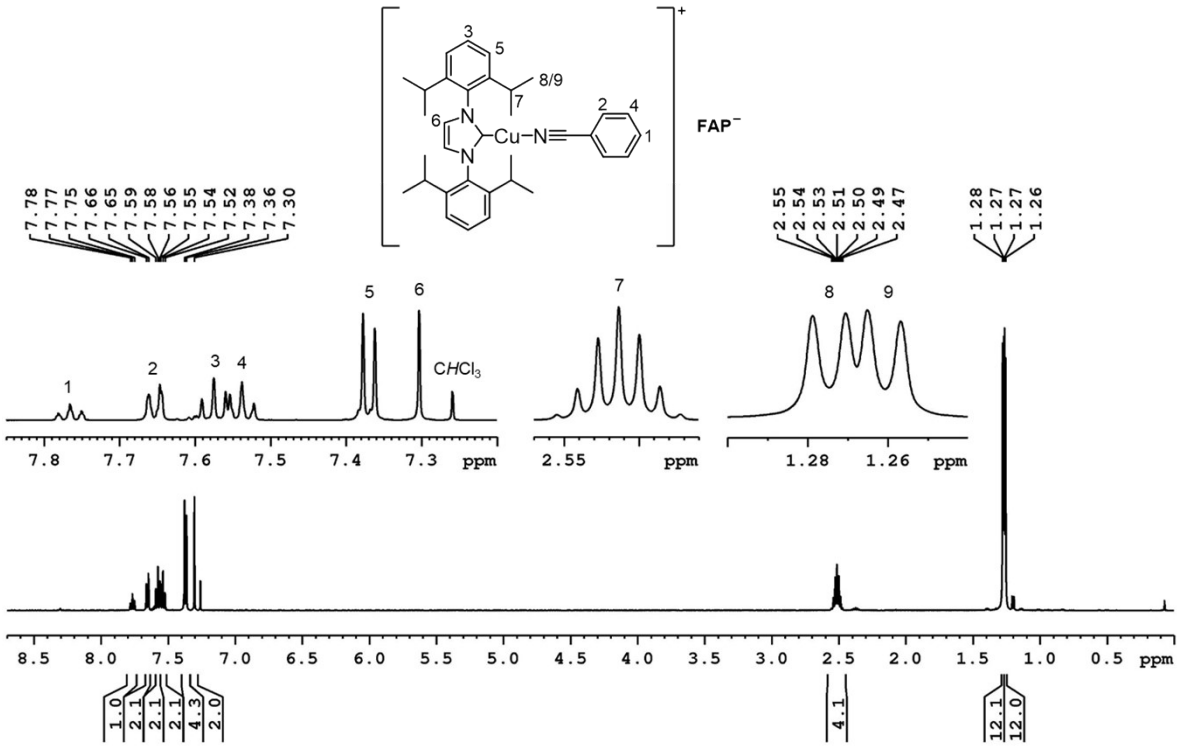

Figure S82. ^{1}H NMR spectrum (500.1 MHz) of **17** recorded in $CDCl_3$.

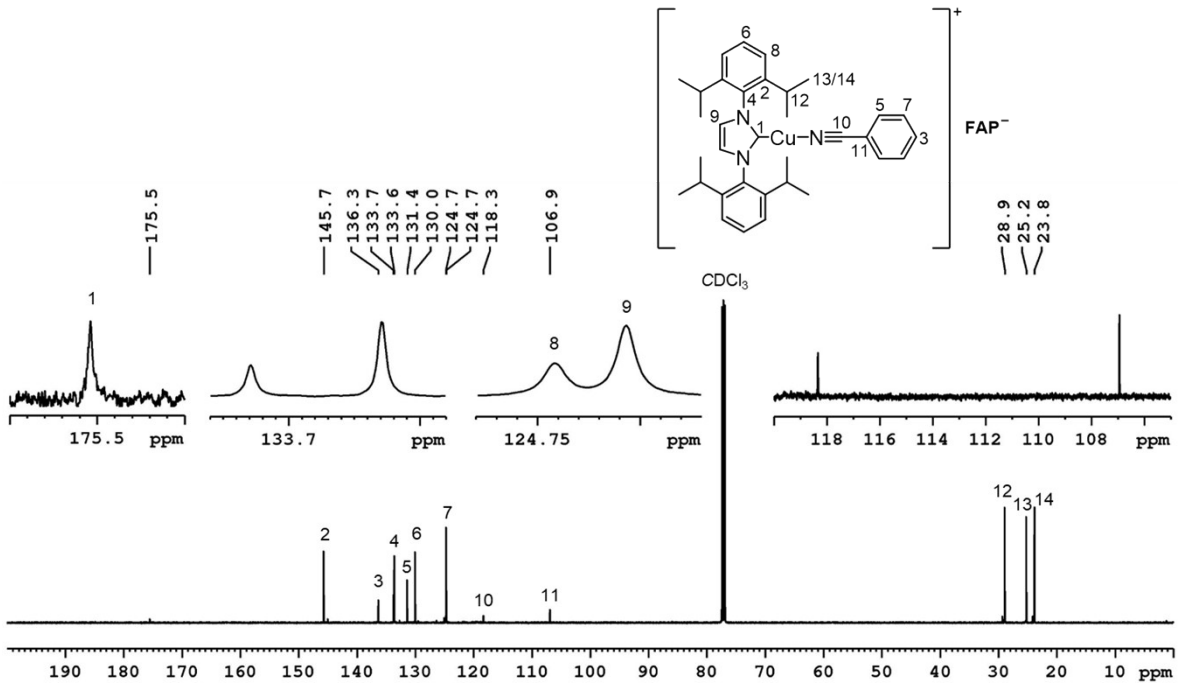

Figure S83. $^{13}C\{^{1}H\}$ NMR spectrum (125.8 MHz) of **17** recorded in $CDCl_3$.

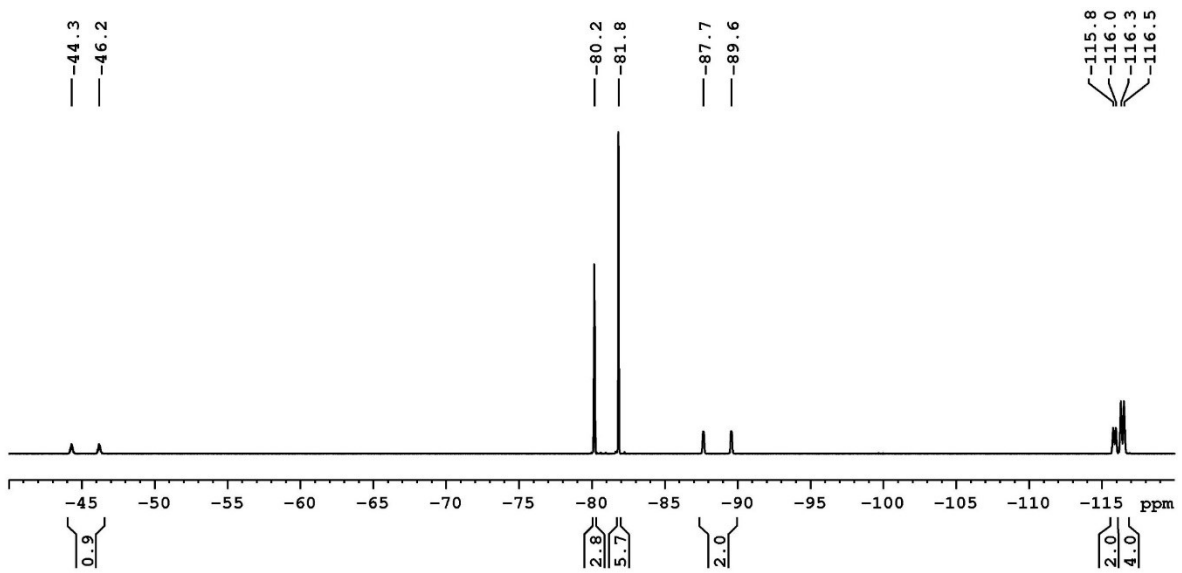

Figure S84. ^{19}F NMR spectrum (470.5 MHz) of **17** recorded in $CDCl_3$.

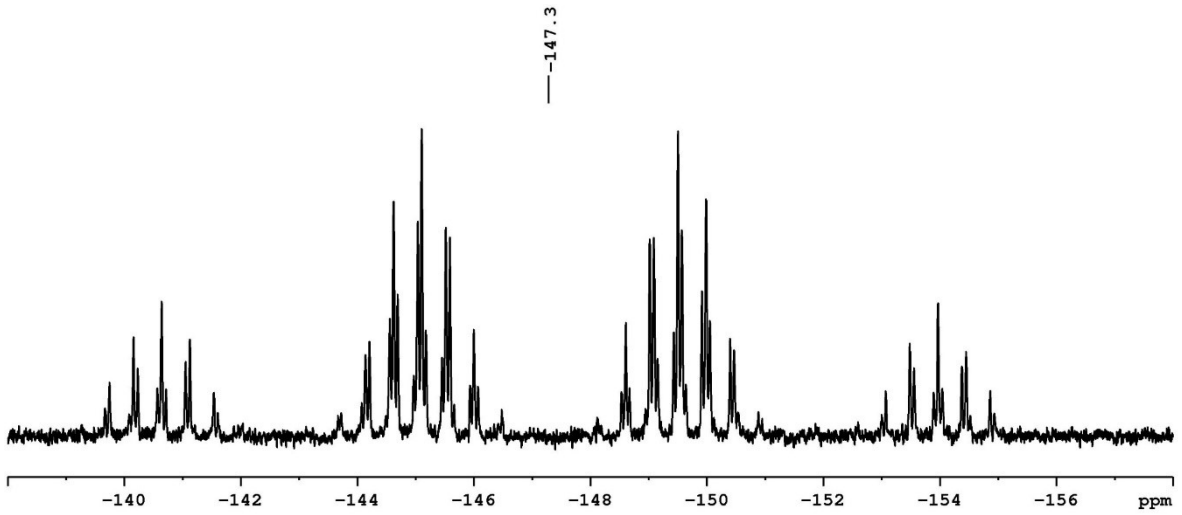

Figure S85. ^{31}P NMR spectrum (202.4 MHz) of **17** recorded in $CDCl_3$.

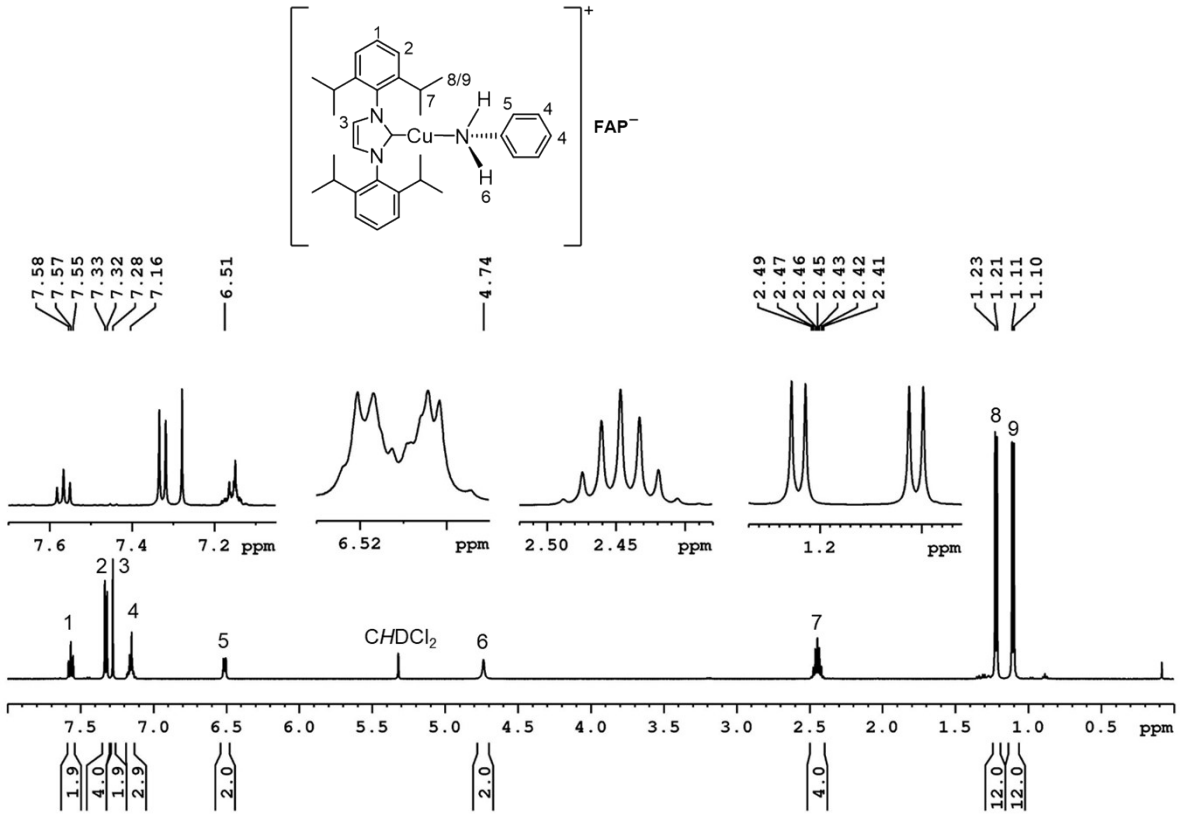

Figure S86. ^{1}H NMR spectrum (500.1 MHz) of **18** recorded in CD_2Cl_2.

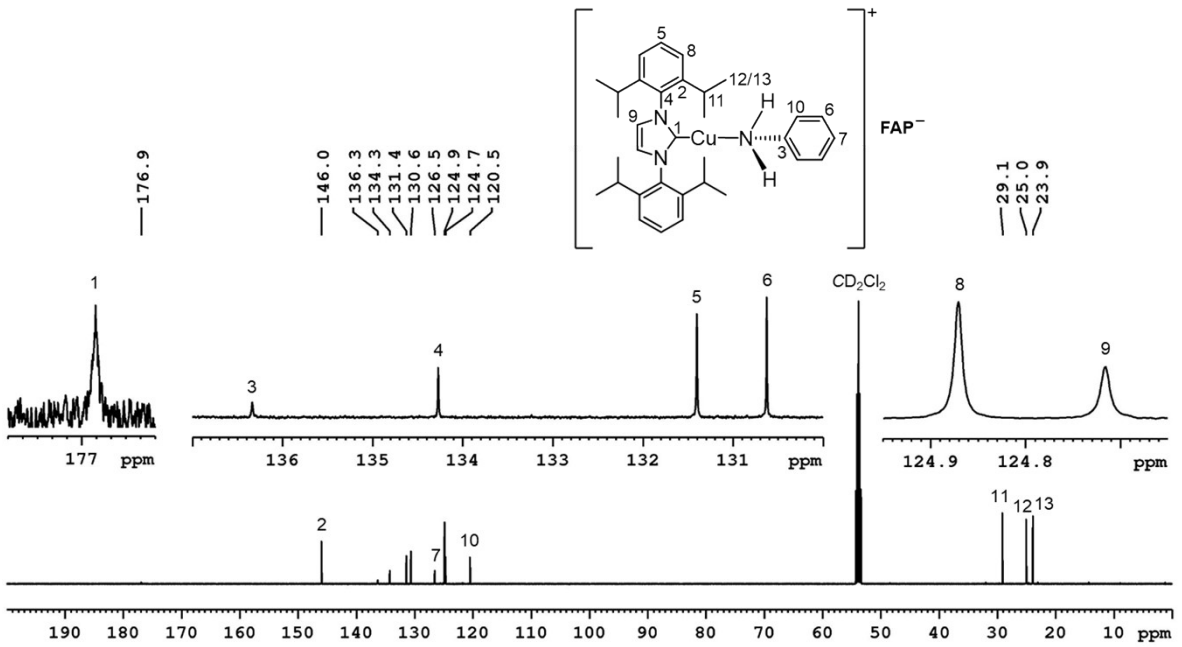

Figure S87. $^{13}C\{^{1}H\}$ NMR spectrum (125.8 MHz) of **18** recorded in CD_2Cl_2.

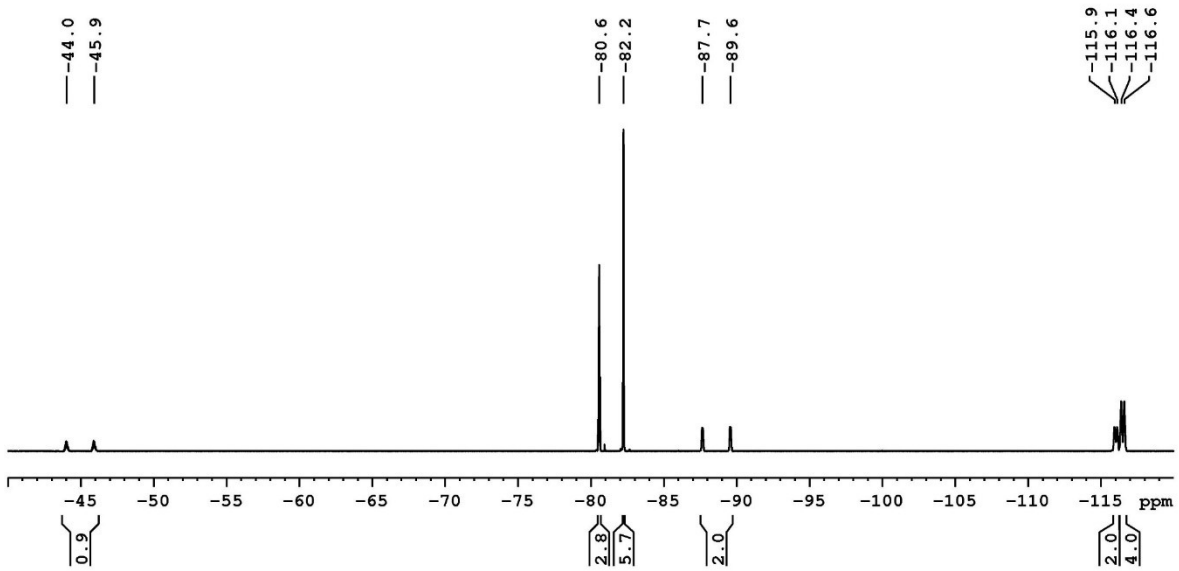

Figure S88. ^{19}F NMR spectrum (470.5 MHz) of **18** recorded in CD_2Cl_2.

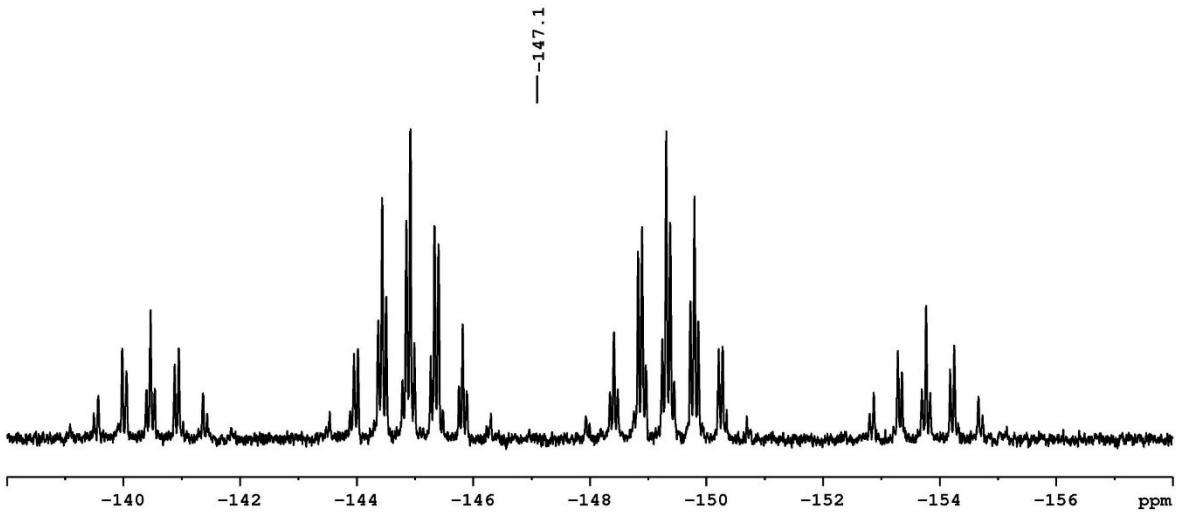

Figure S89. ^{31}P NMR spectrum (202.4 MHz) of **18** recorded in CD_2Cl_2.

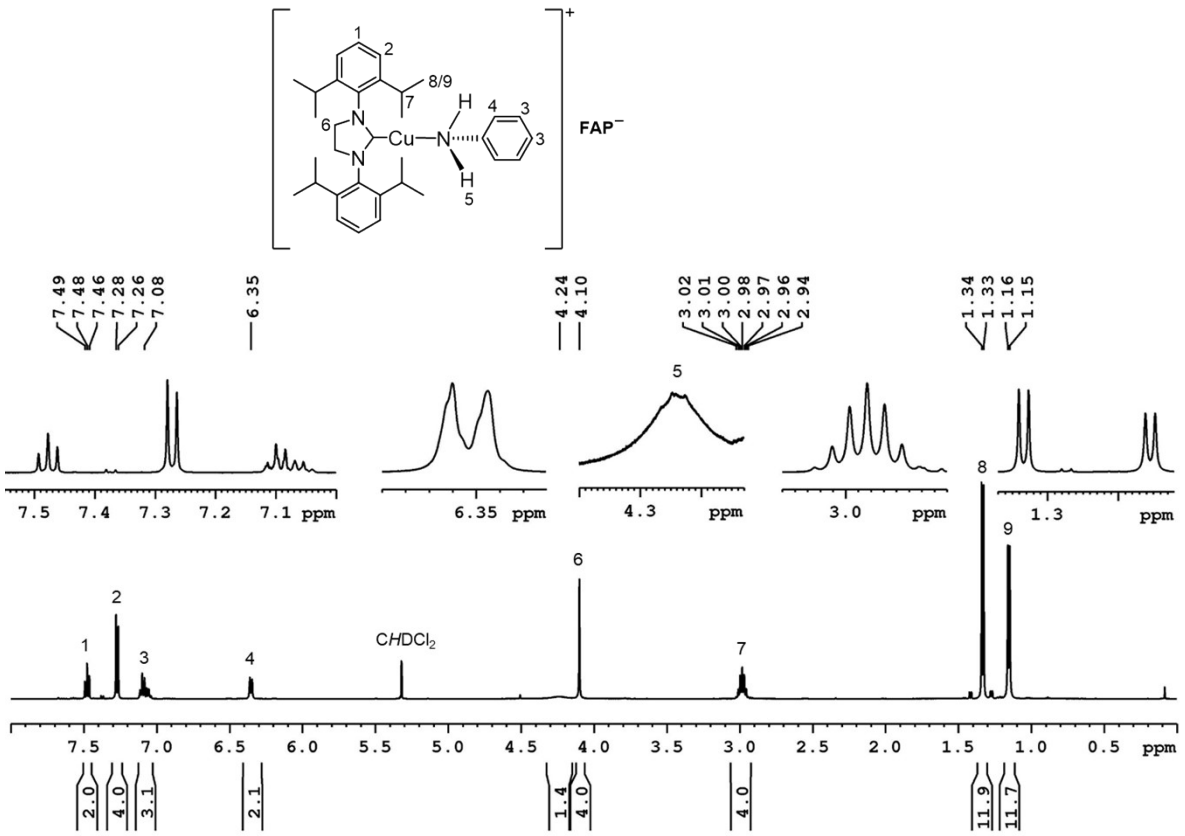

Figure S90. ^{1}H NMR spectrum (500.1 MHz) of **19** recorded in CD_2Cl_2.

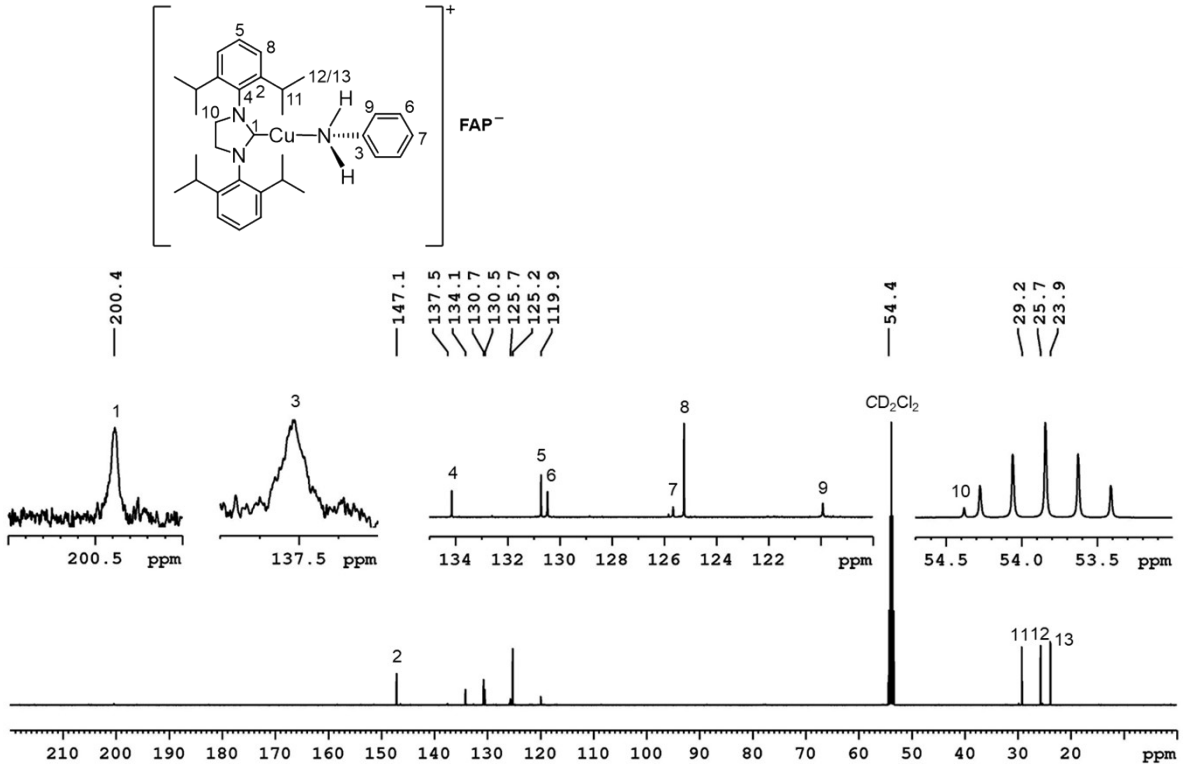

Figure S91. $^{13}C\{^{1}H\}$ NMR spectrum (125.8 MHz) of **19** recorded in CD_2Cl_2.

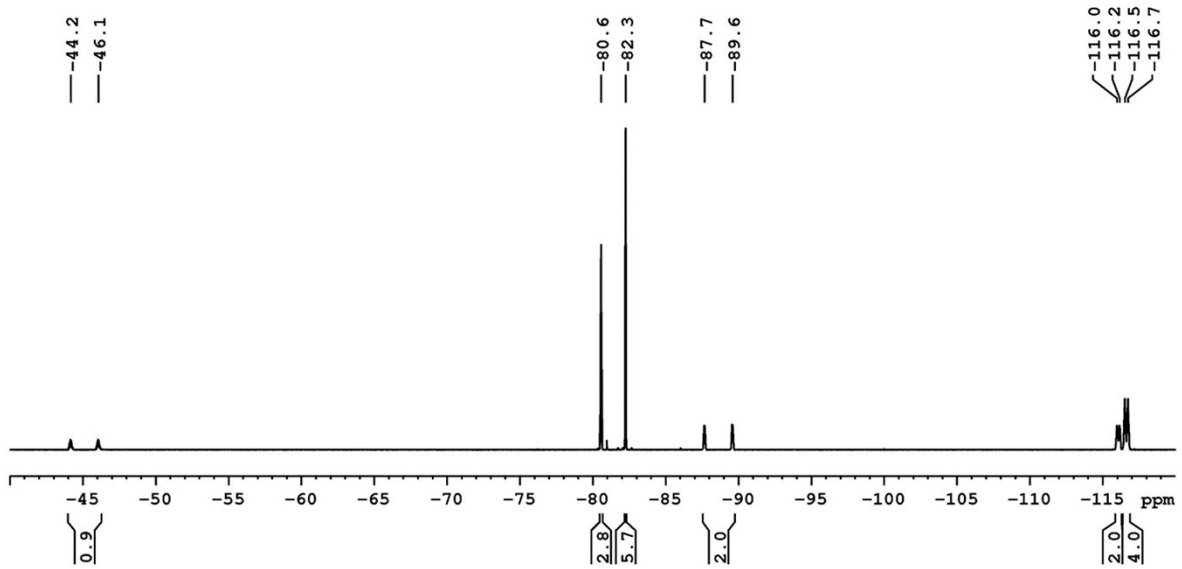

Figure S92. ^{19}F NMR spectrum (470.5 MHz) of **19** recorded in CD_2Cl_2.

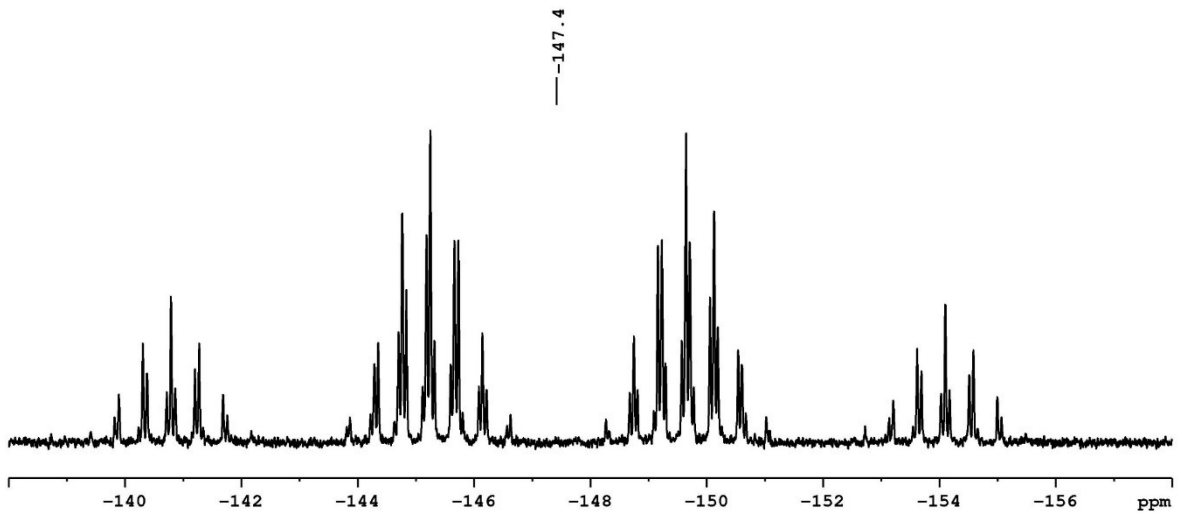

Figure S93. ^{31}P NMR spectrum (202.4 MHz) of **19** recorded in CD_2Cl_2.

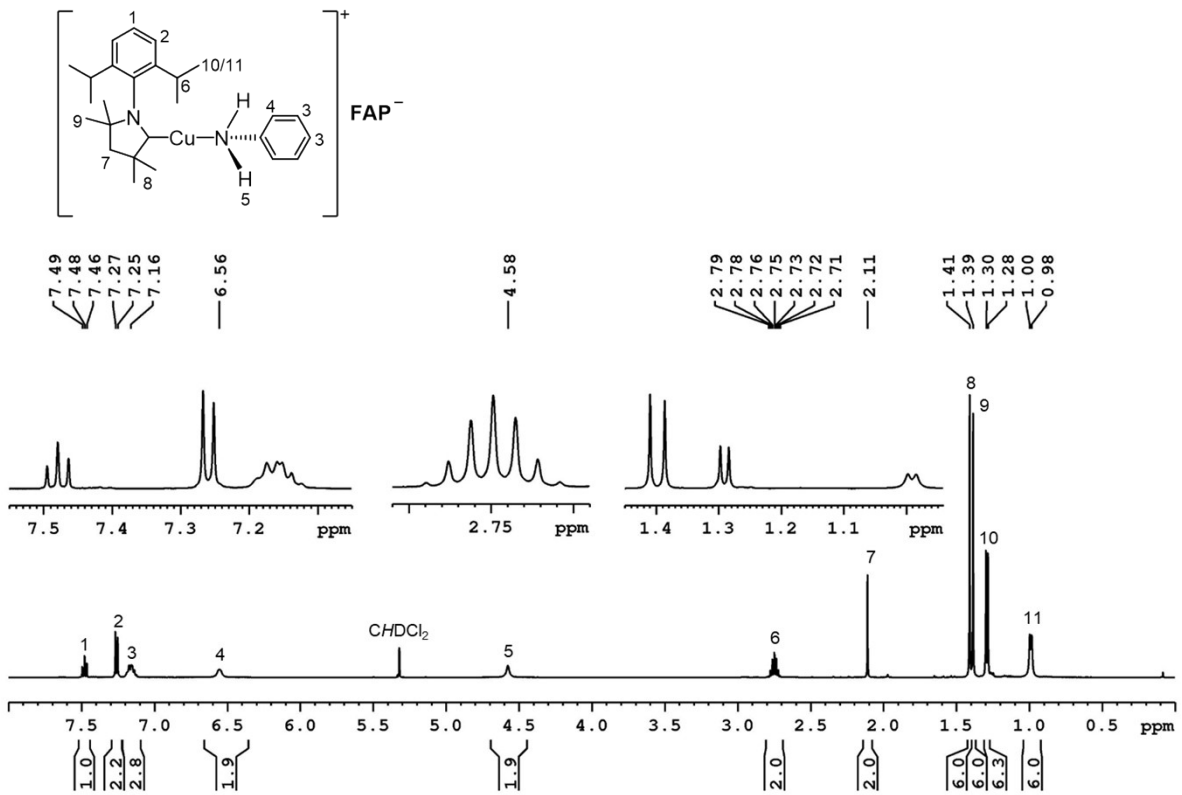

Figure S94. ^{1}H NMR spectrum (500.1 MHz) of **20** recorded in CD_2Cl_2.

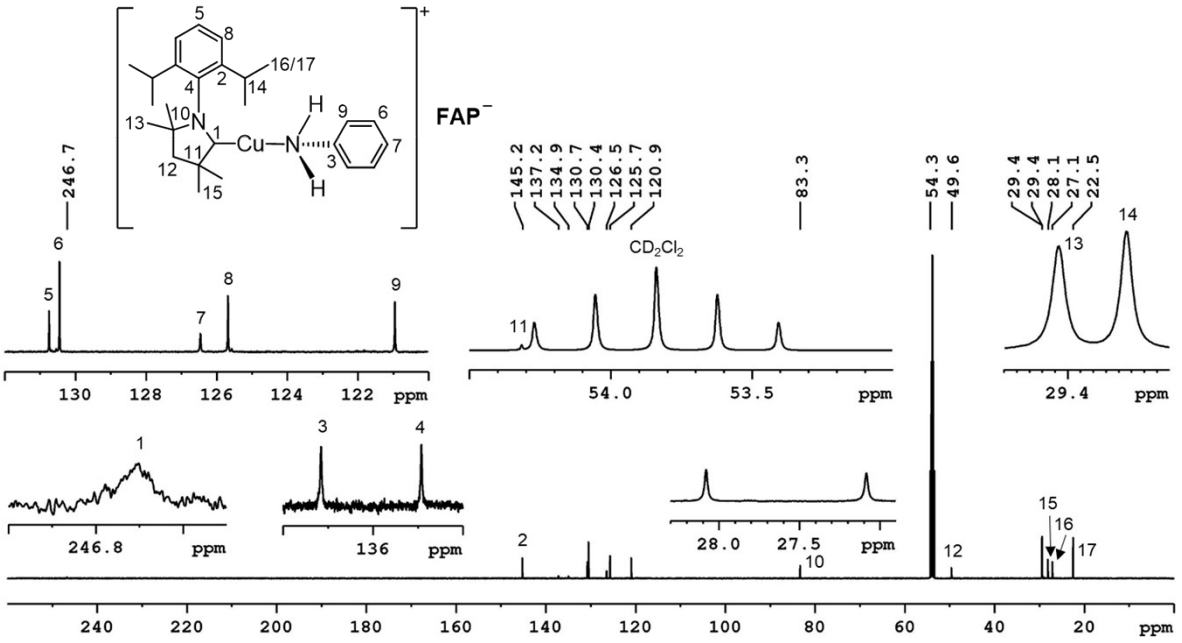

Figure S95. $^{13}C\{^{1}H\}$ NMR spectrum (125.8 MHz) of **20** recorded in CD_2Cl_2.

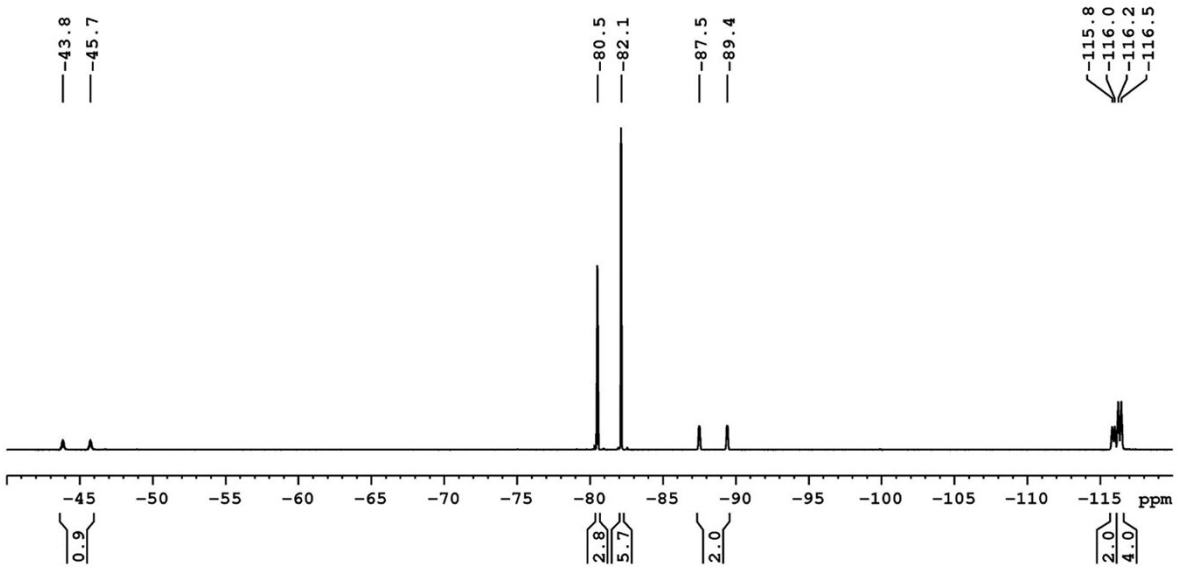

Figure S96. ^{19}F NMR spectrum (470.5 MHz) of **20** recorded in CD_2Cl_2.

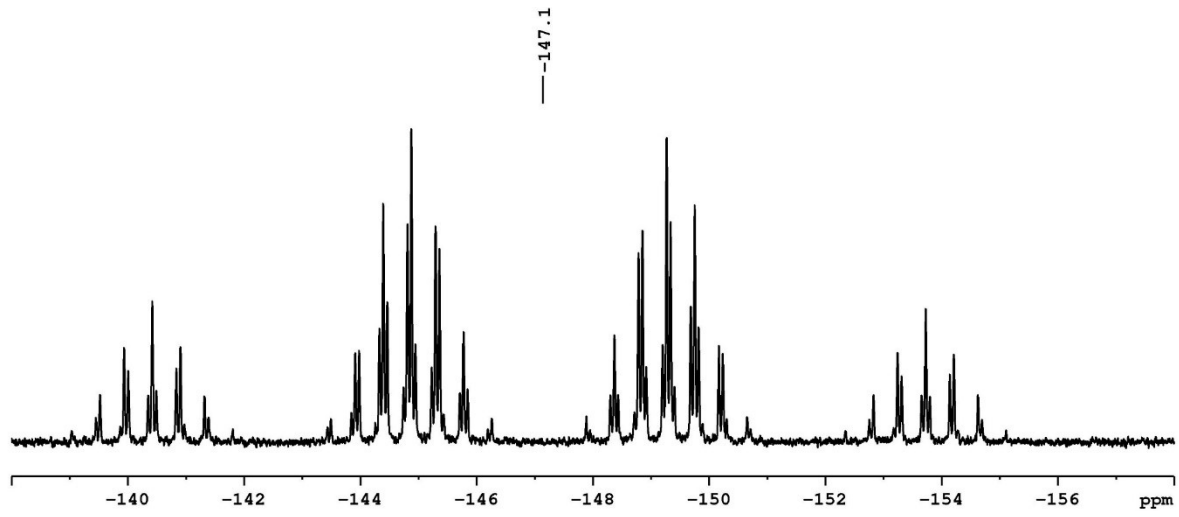

Figure S97. ^{31}P NMR spectrum (202.4 MHz) of **20** recorded in CD_2Cl_2.

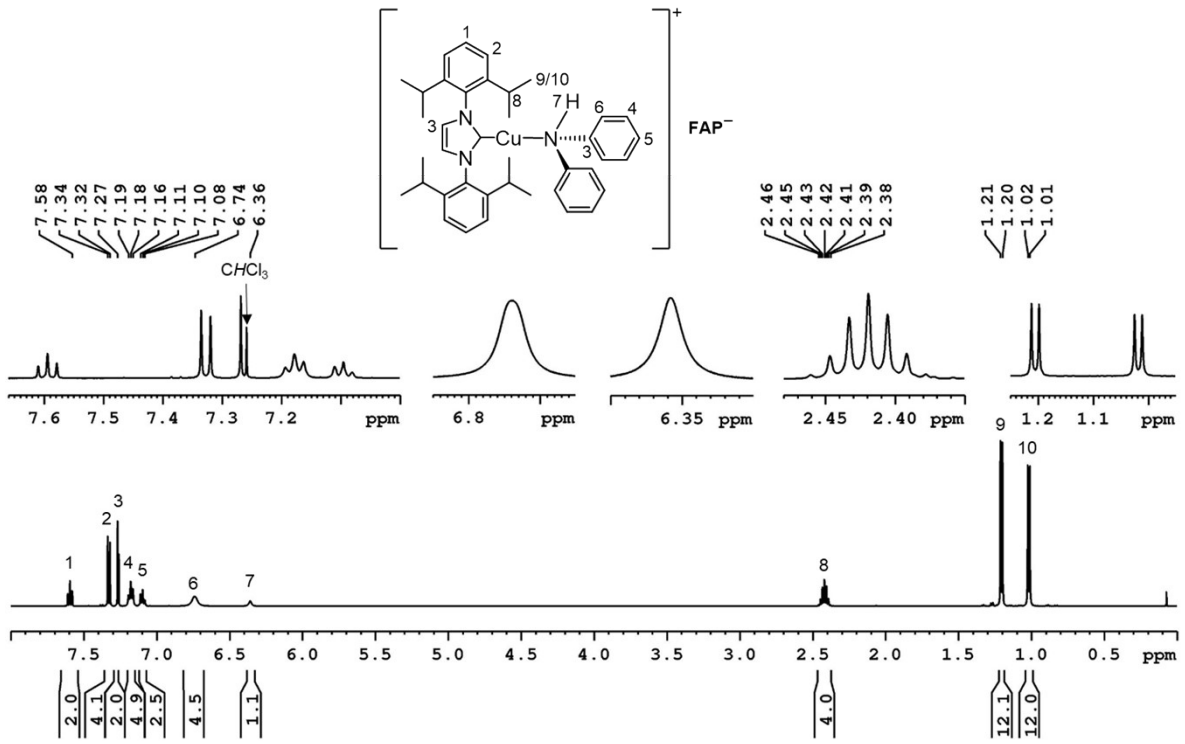

Figure S98. ^{1}H NMR spectrum (500.1 MHz) of **21** recorded in $CDCl_3$.

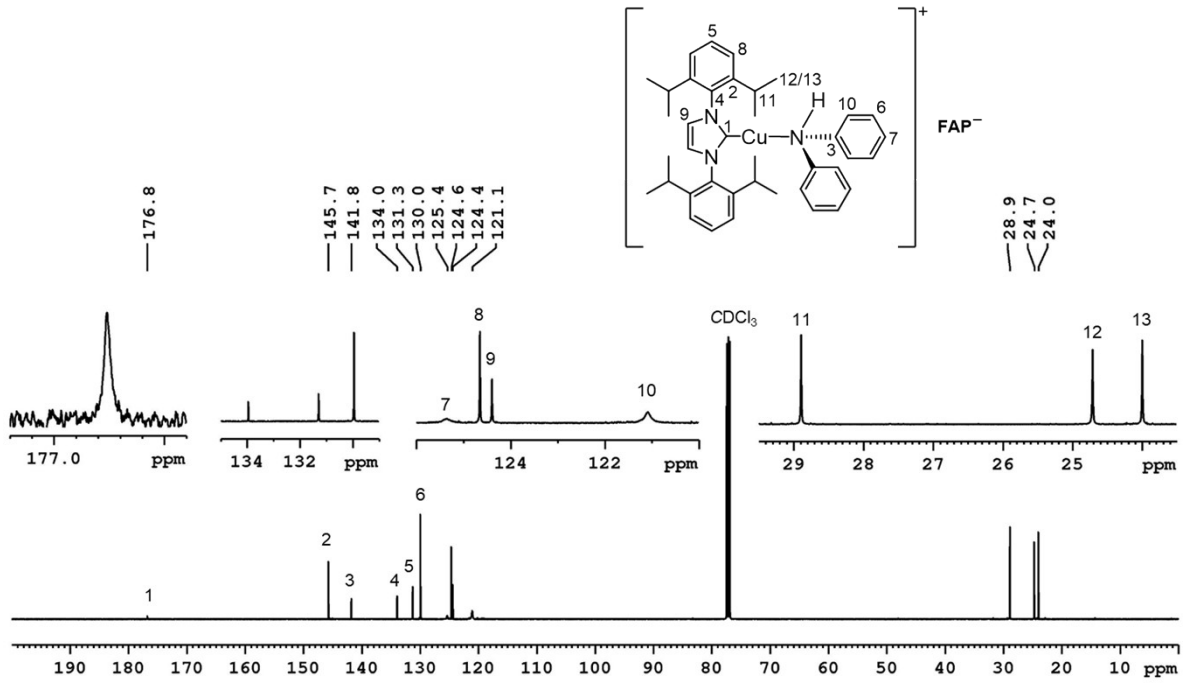

Figure S99. $^{13}C\{^{1}H\}$ NMR spectrum (125.8 MHz) of **21** recorded in $CDCl_3$.

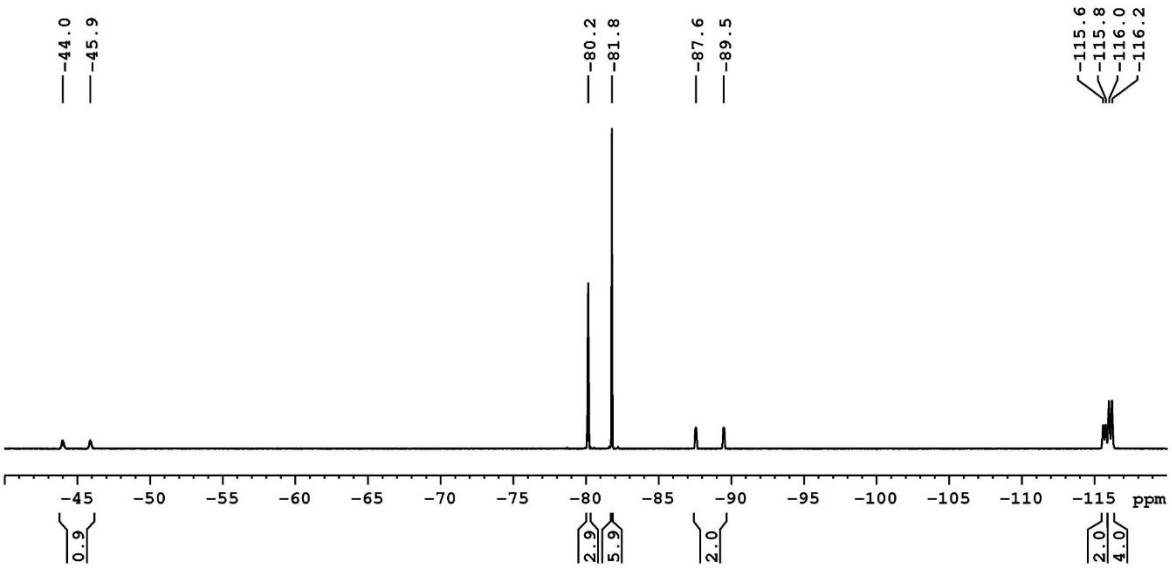

Figure S100. ^{19}F NMR spectrum (470.5 MHz) of **21** recorded in $CDCl_3$.

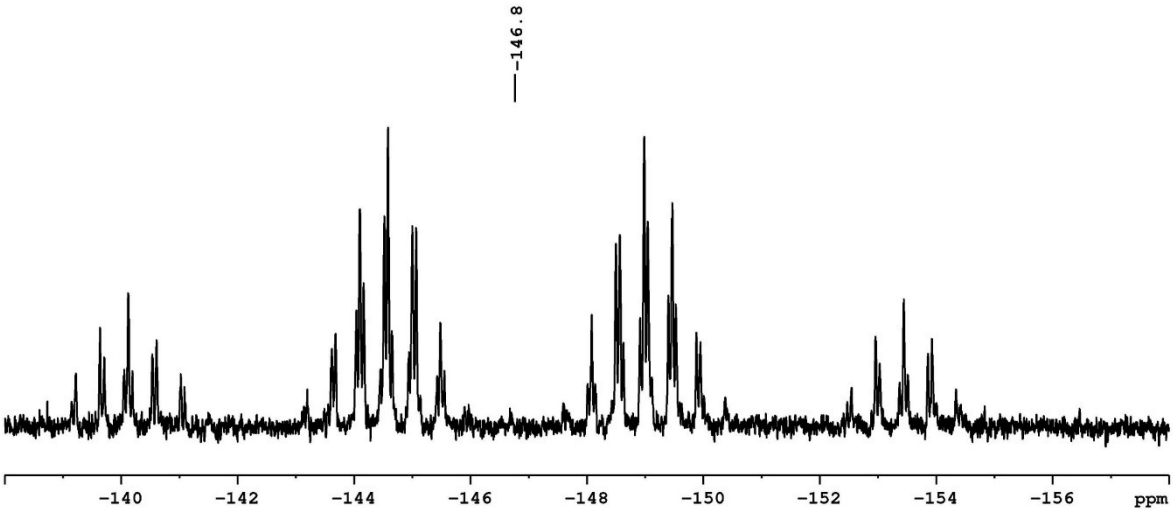

Figure S101. ^{31}P NMR spectrum (202.4 MHz) of **21** recorded in $CDCl_3$.

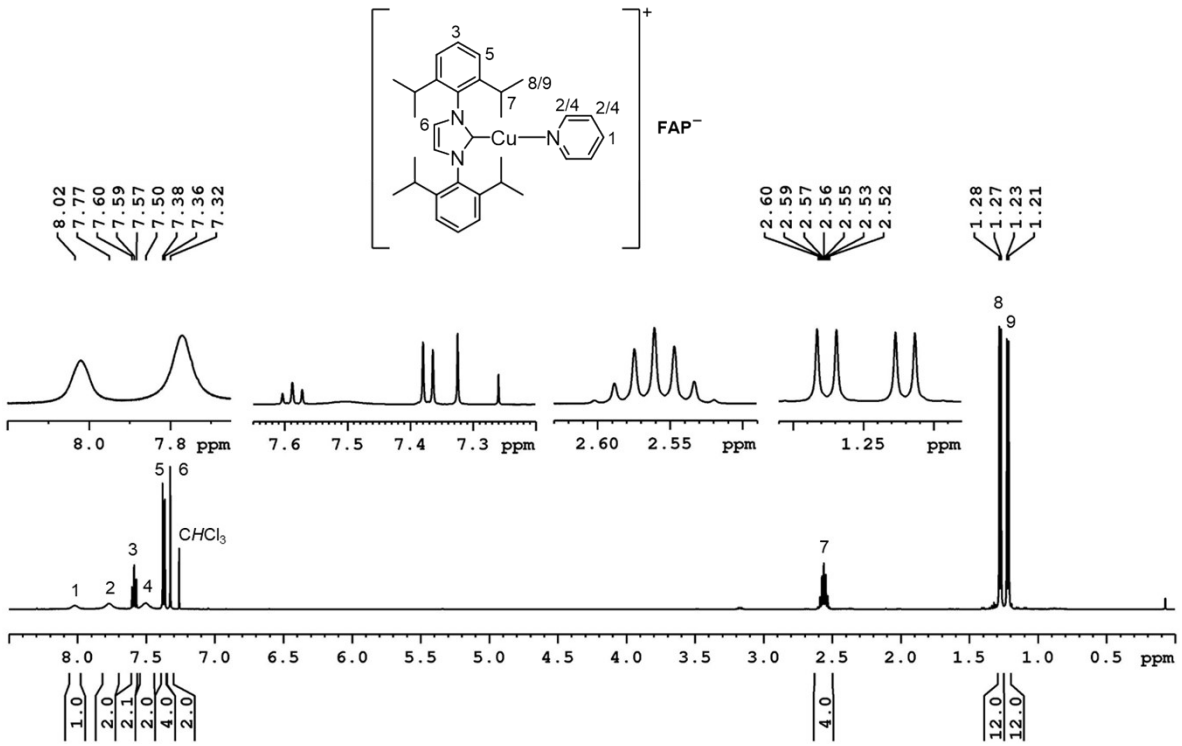

Figure S102. ^{1}H NMR spectrum (500.1 MHz) of **22** recorded in $CDCl_3$.

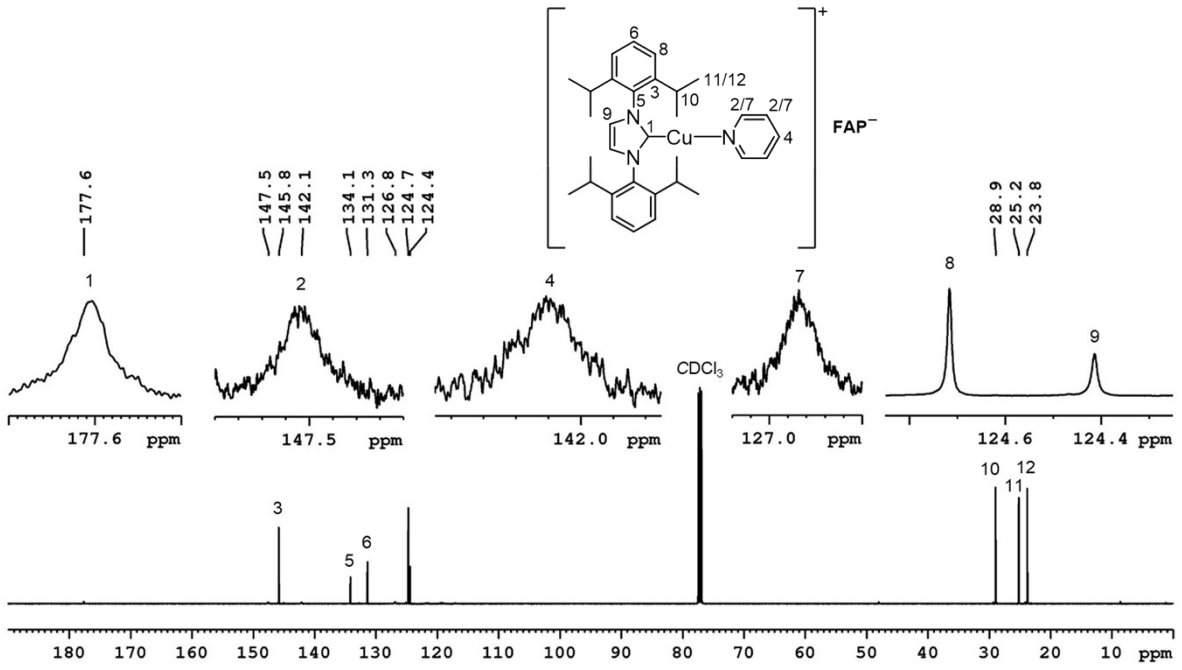

Figure S103. $^{13}C\{^{1}H\}$ NMR spectrum (125.8 MHz) of **22** recorded in $CDCl_3$.

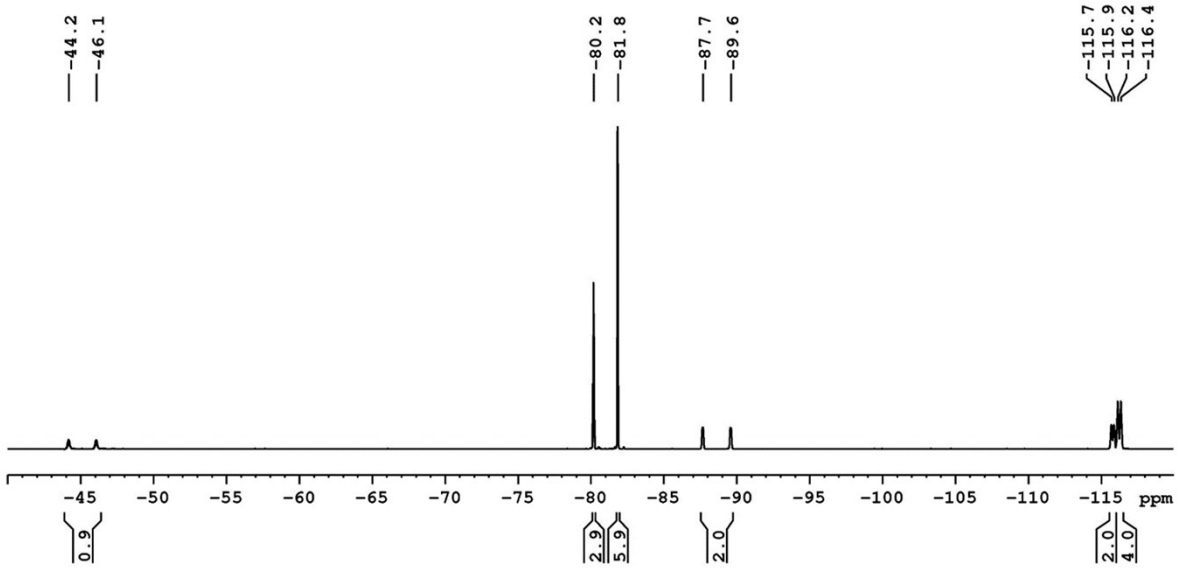

Figure S104. ^{19}F NMR spectrum (470.5 MHz) of **22** recorded in $CDCl_3$.

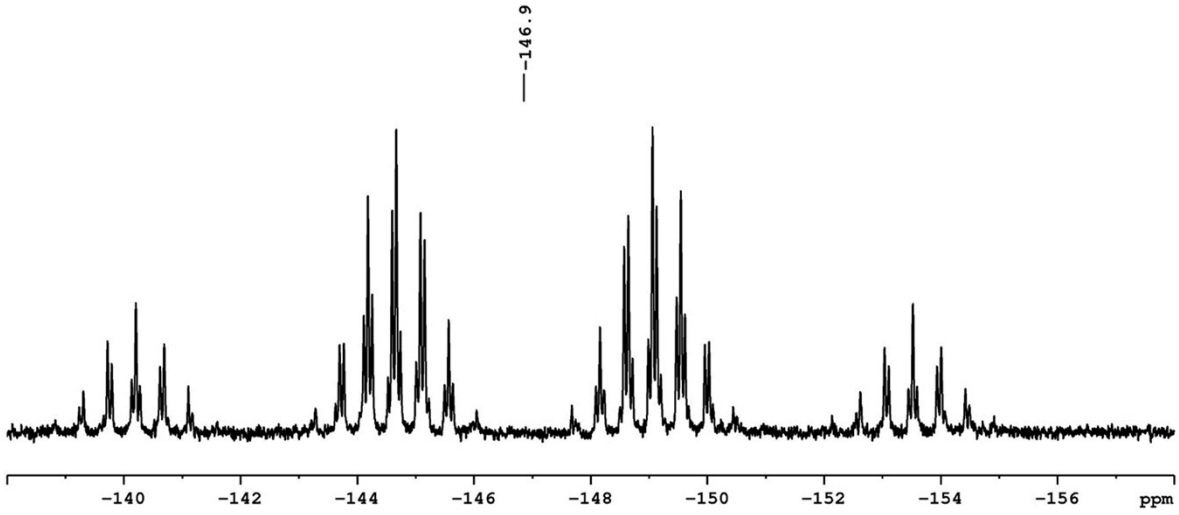

Figure S105. ^{31}P NMR spectrum (202.4 MHz) of **22** recorded in $CDCl_3$.

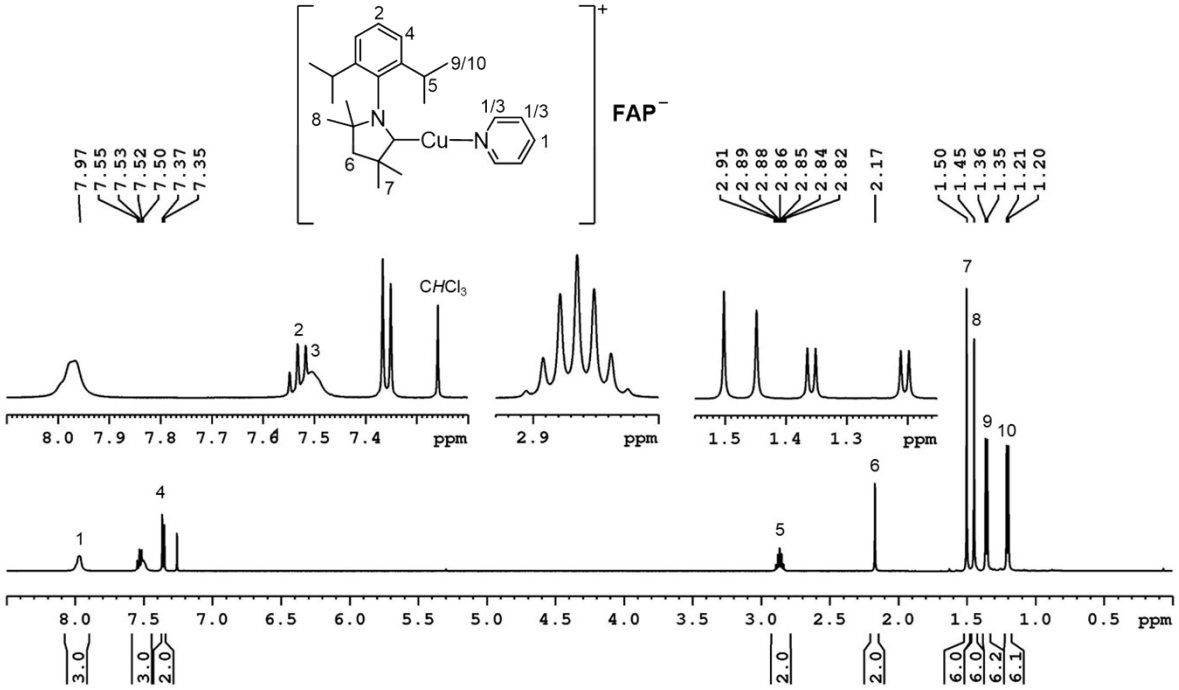

Figure S106. ^{1}H NMR spectrum (500.1 MHz) of **23** recorded in $CDCl_3$.

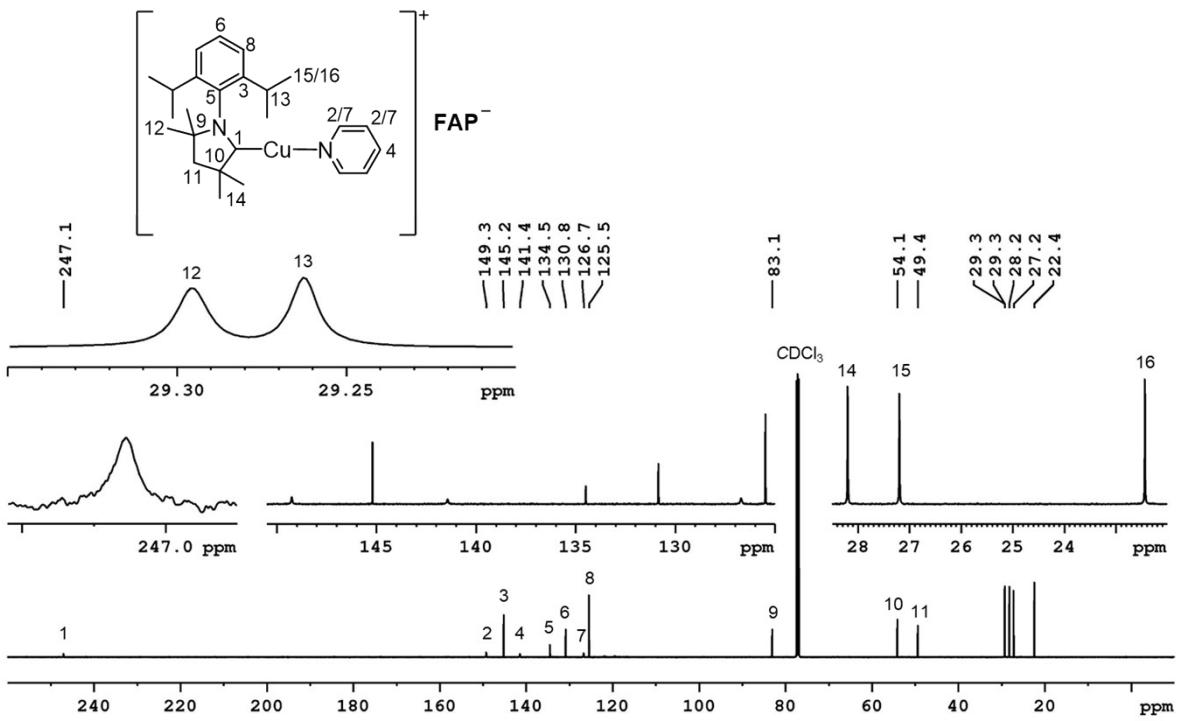

Figure S107. $^{13}C\{^{1}H\}$ NMR spectrum (125.8 MHz) of **23** recorded in $CDCl_3$.

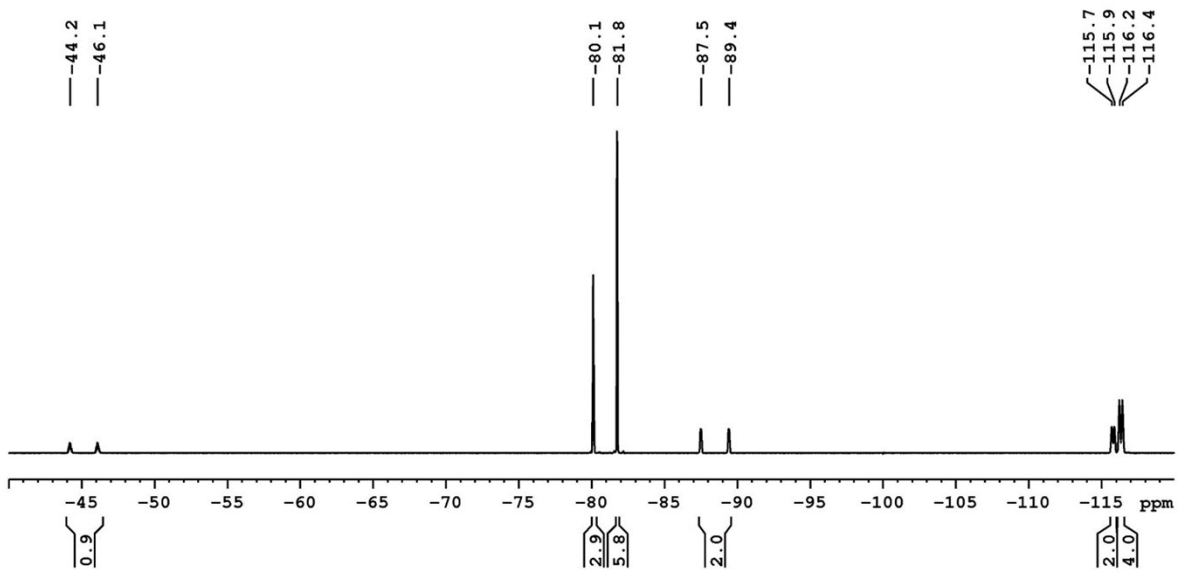

Figure S108. ^{19}F NMR spectrum (470.5 MHz) of **23** recorded in $CDCl_3$.

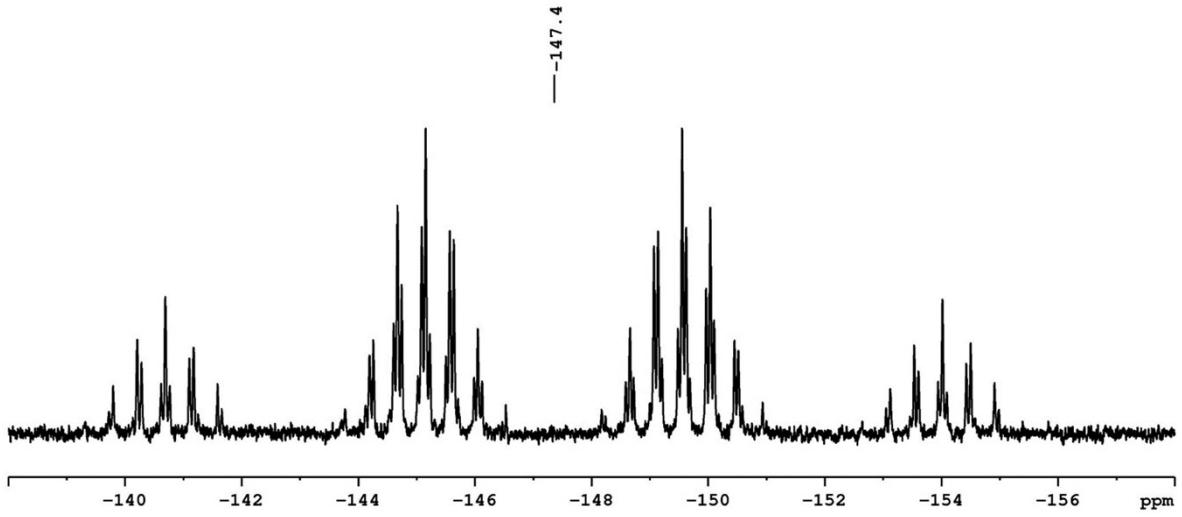

Figure S109. ^{31}P NMR spectrum (202.4 MHz) of **23** recorded in $CDCl_3$.

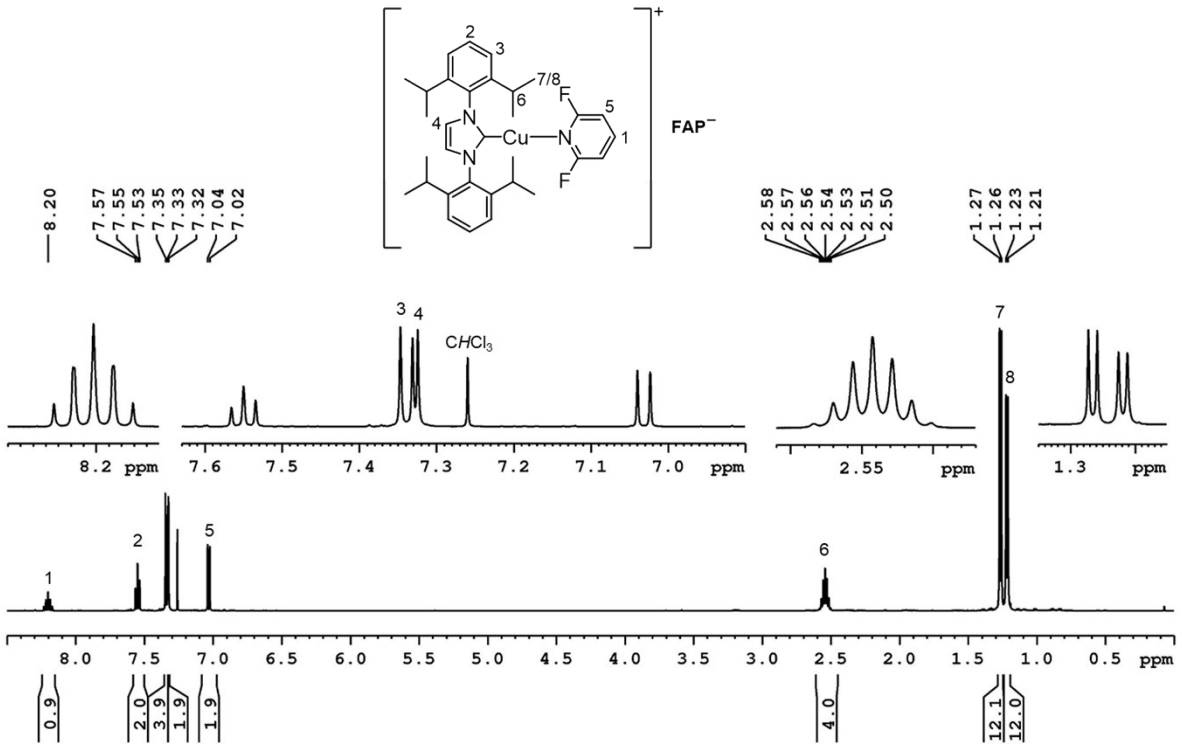

Figure S110. ^{1}H NMR spectrum (500.1 MHz) of **24** recorded in $CDCl_3$.

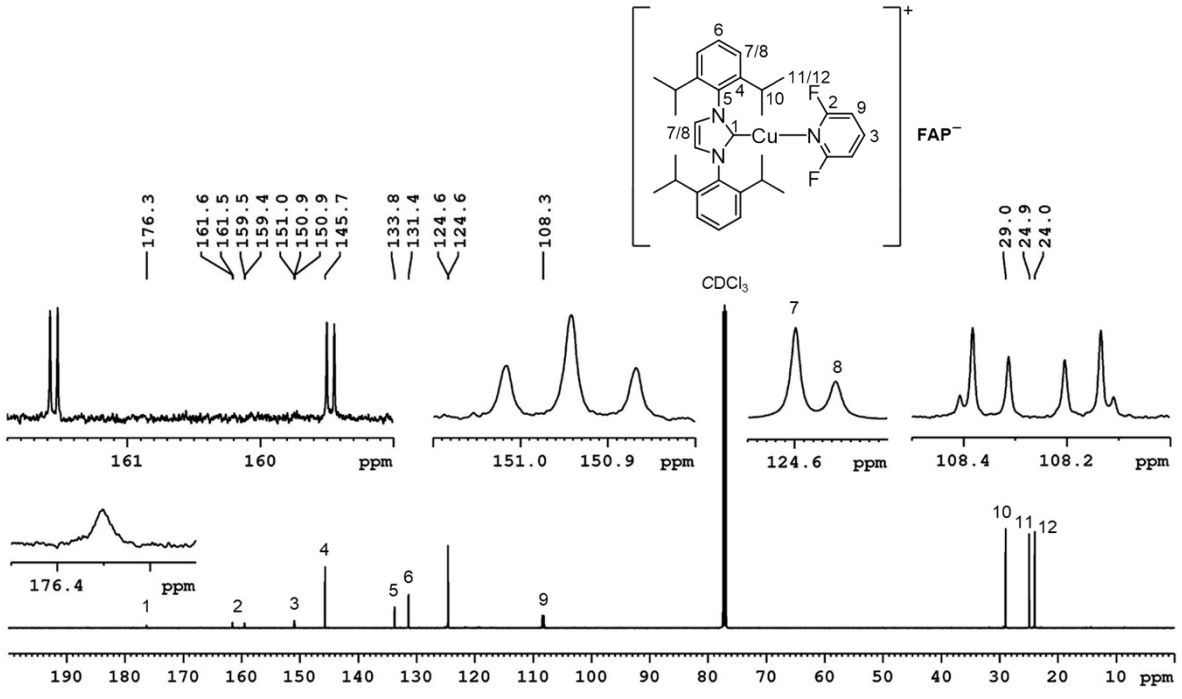

Figure S111. $^{13}C\{^{1}H\}$ NMR spectrum (125.8 MHz) of **24** recorded in $CDCl_3$.

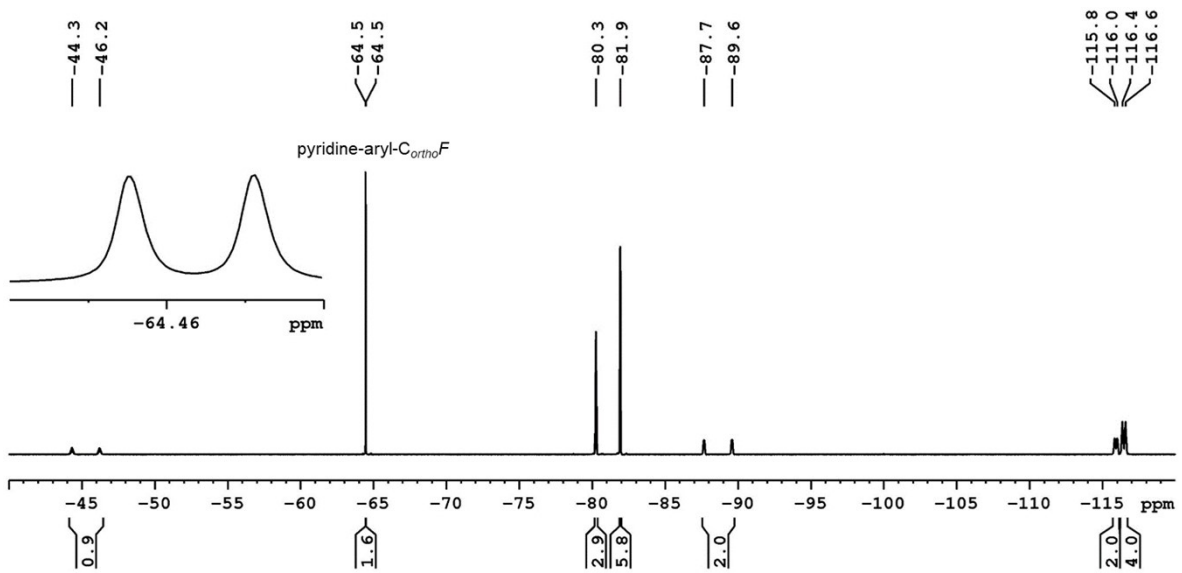

Figure S112. ^{19}F NMR spectrum (470.5 MHz) of **24** recorded in $CDCl_3$.

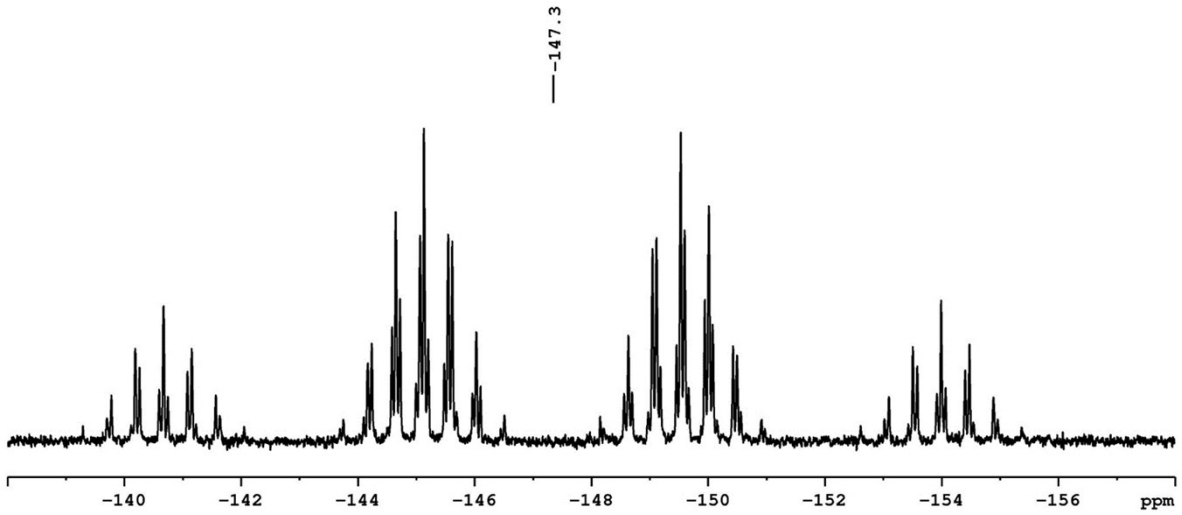

Figure S113. ^{31}P NMR spectrum (202.4 MHz) of **24** recorded in $CDCl_3$.

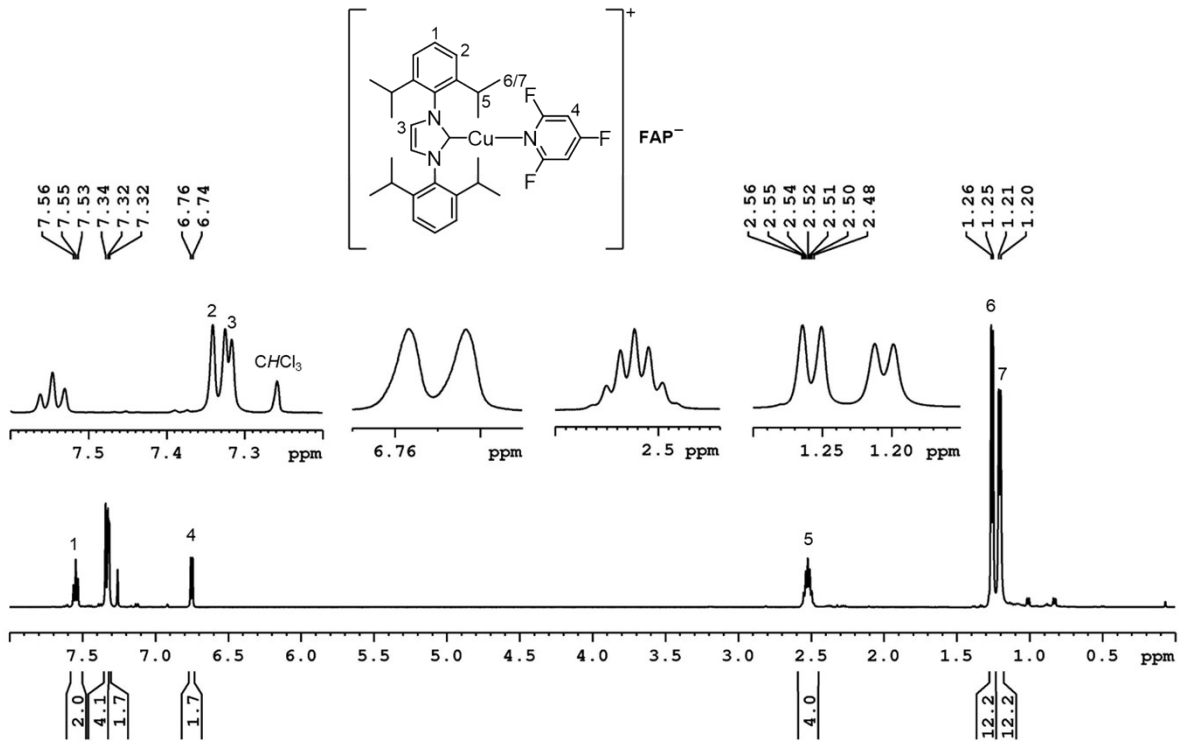

Figure S114. ^{1}H NMR spectrum (500.1 MHz) of **25** recorded in $CDCl_3$.

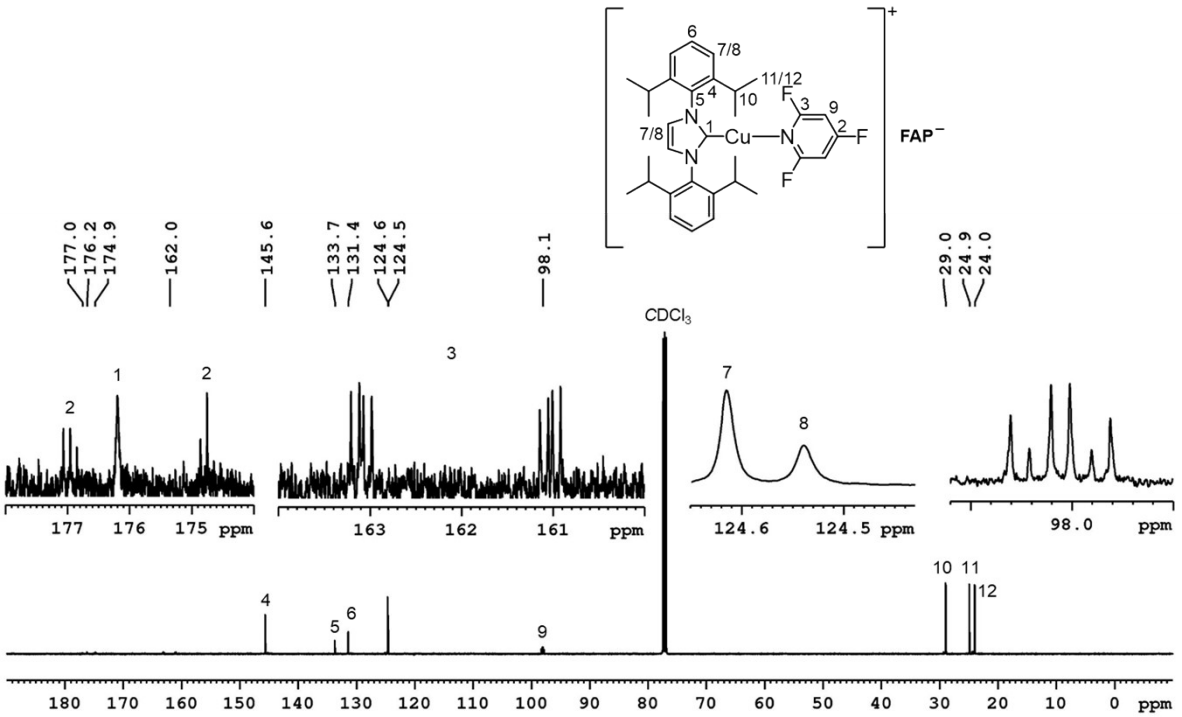

Figure S115. $^{13}C\{^{1}H\}$ NMR spectrum (125.8 MHz) of **25** recorded in $CDCl_3$.

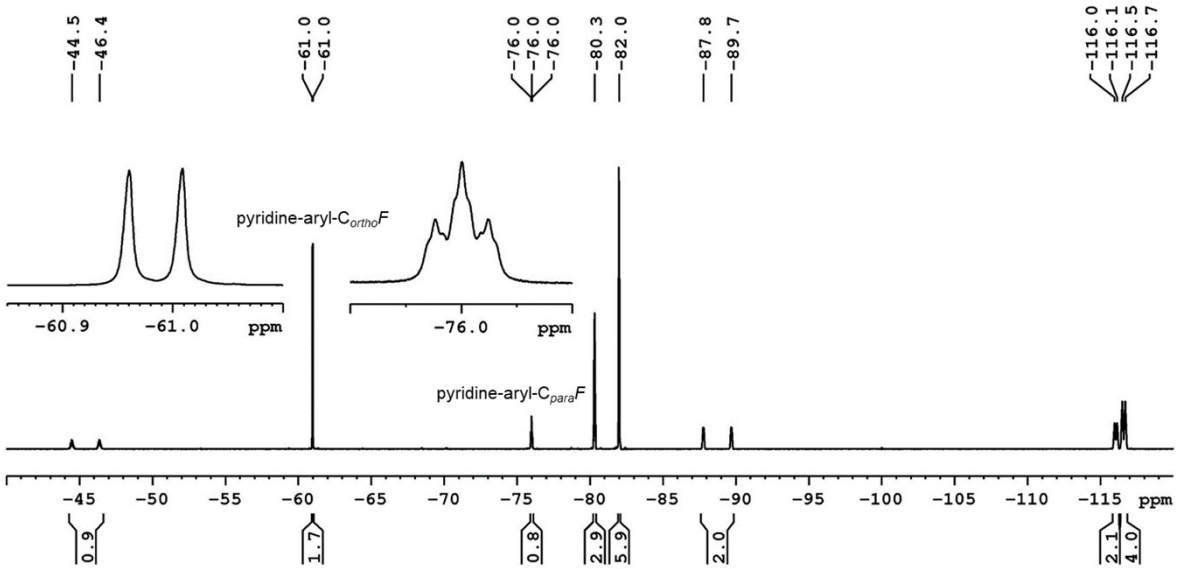

Figure S116. ^{19}F NMR spectrum (470.5 MHz) of **25** recorded in $CDCl_3$.

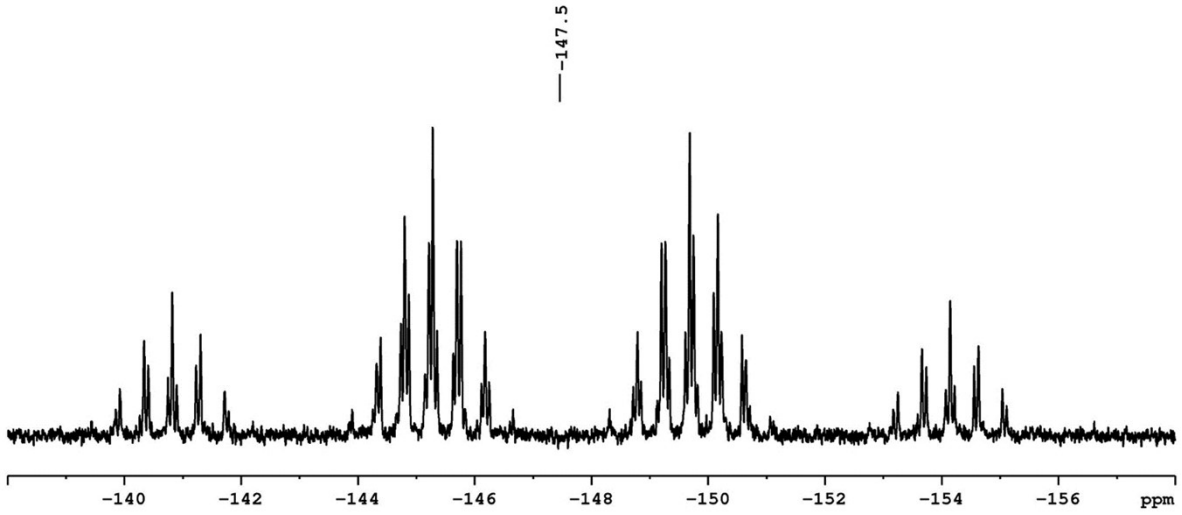

Figure S117. ^{31}P NMR spectrum (202.4 MHz) of **25** recorded in $CDCl_3$.

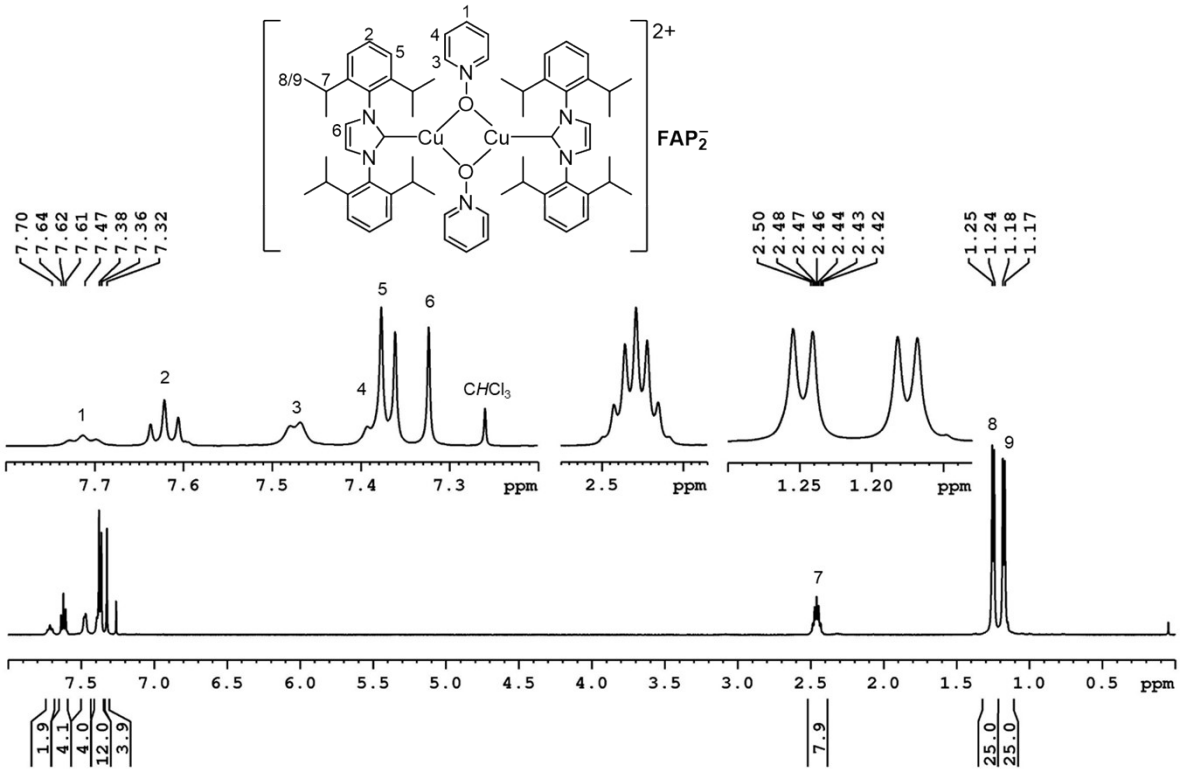

Figure S118. ^{1}H NMR spectrum (400.1 MHz, 236.5 K) of **26** recorded in $CDCl_3$.

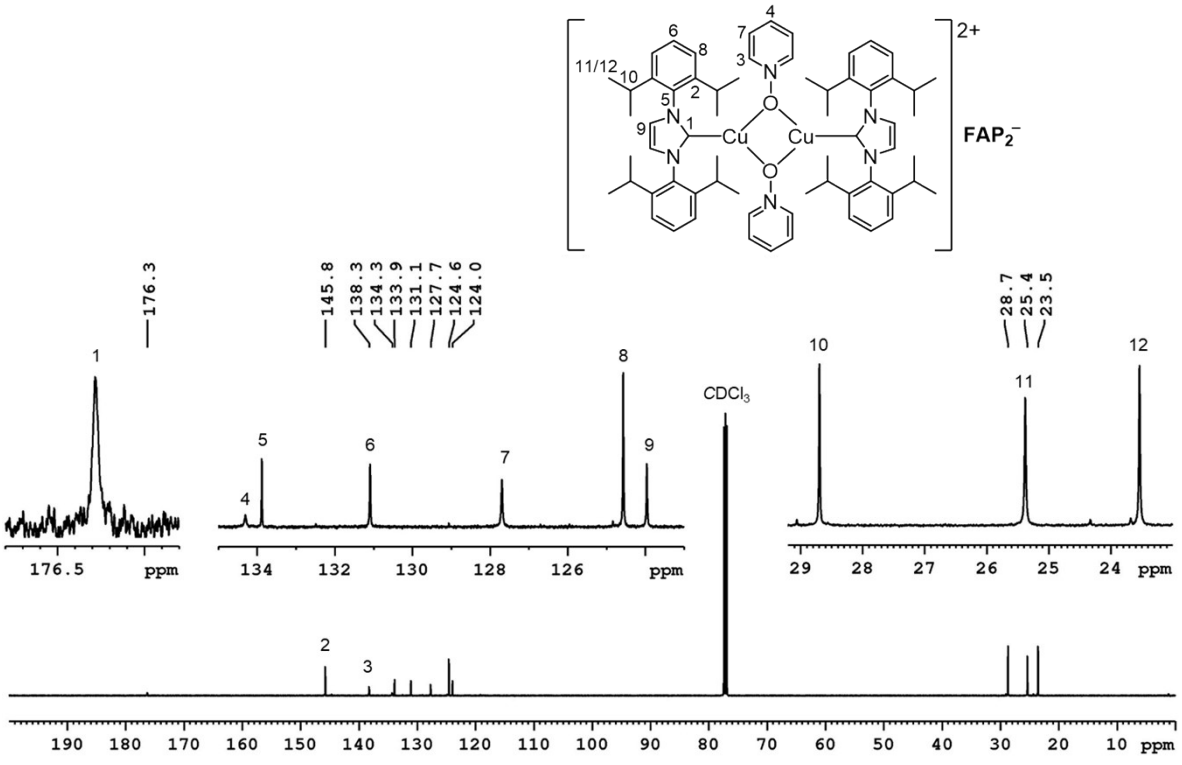

Figure S119. $^{13}C\{^{1}H\}$ NMR spectrum (100.6 MHz, 236.5 K) of **26** recorded in $CDCl_3$.

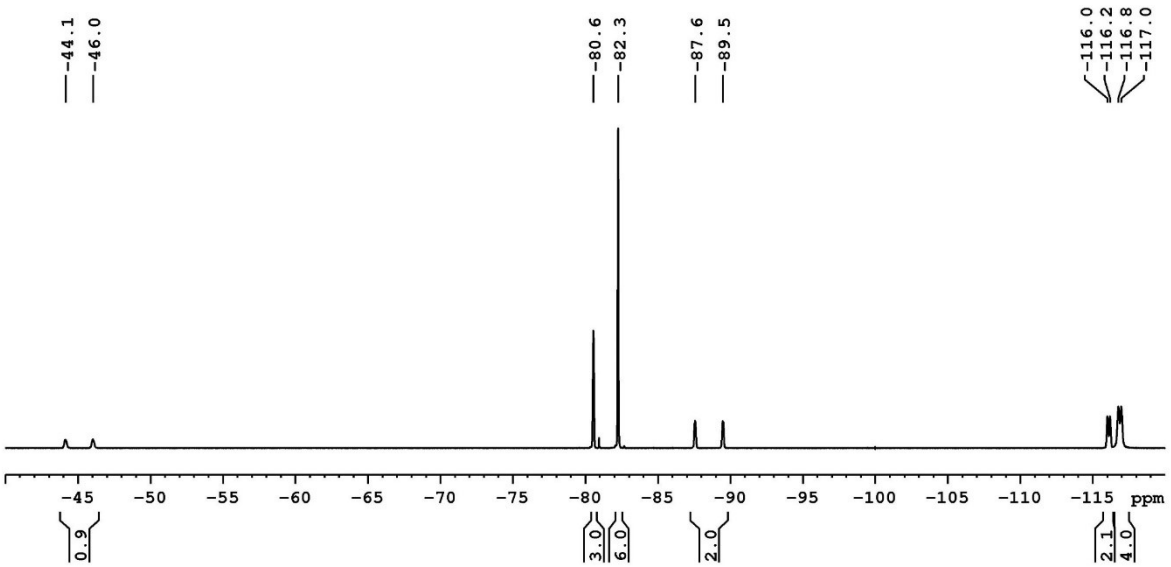

Figure S120. ^{19}F NMR spectrum (470.5 MHz) of **26** recorded in CD_2Cl_2.

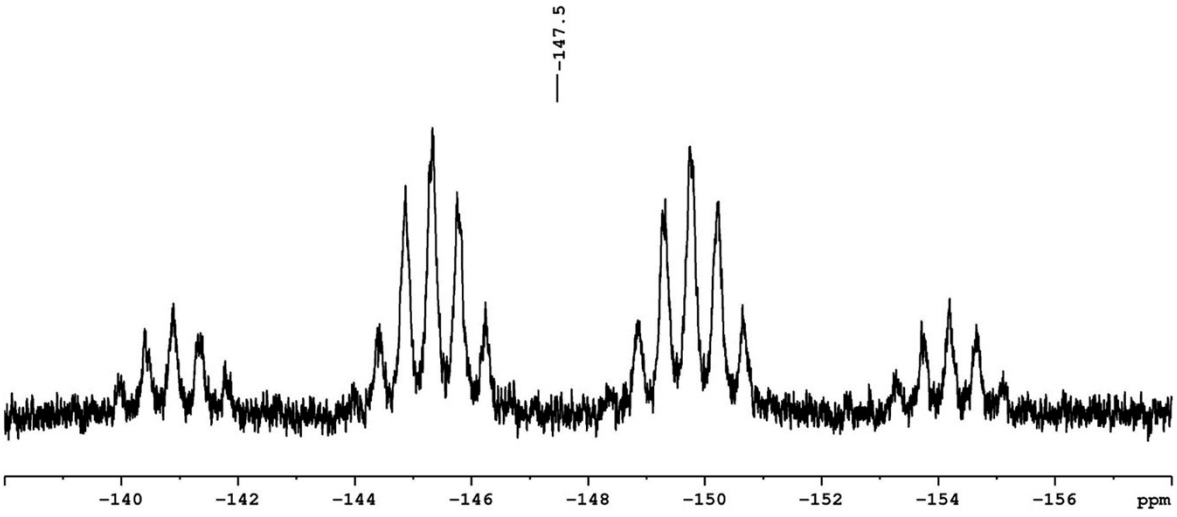

Figure S121. ^{31}P NMR spectrum (202.4 MHz) of **26** recorded in CD_2Cl_2.

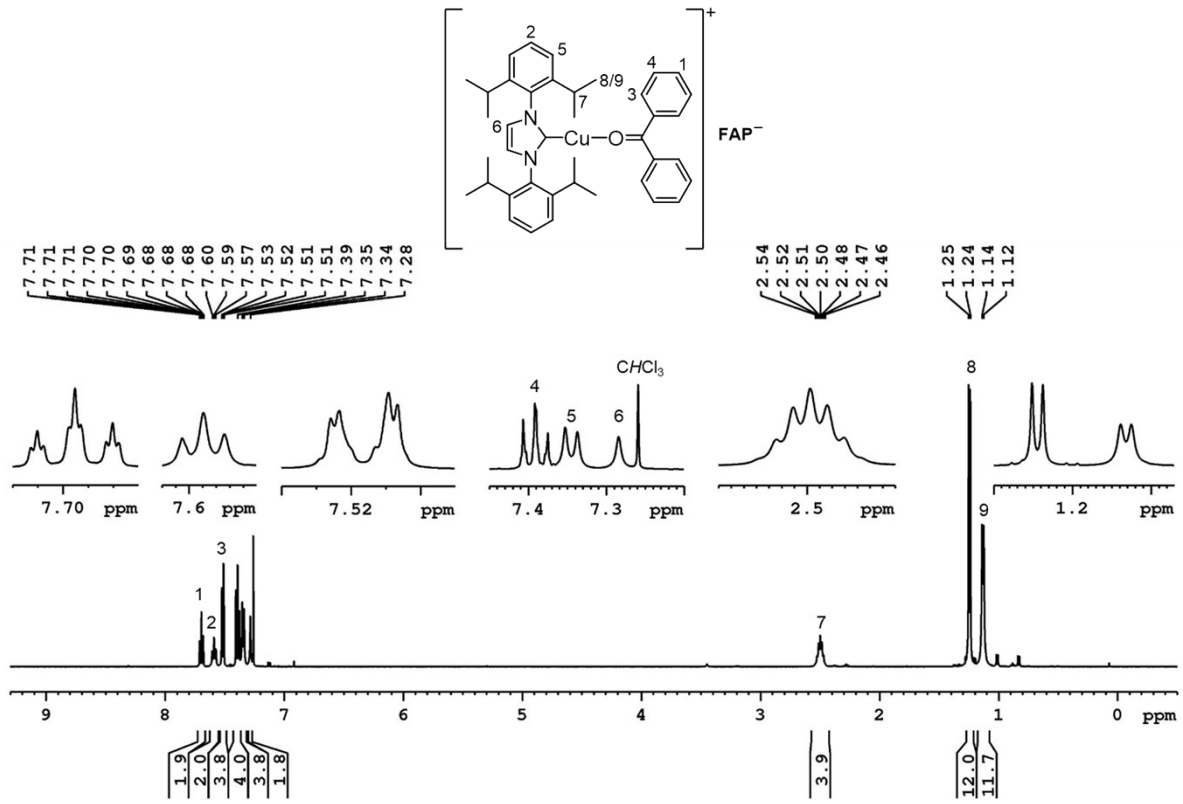

Figure S122. ^{1}H NMR spectrum (500.1 MHz) of **27** recorded in $CDCl_3$.

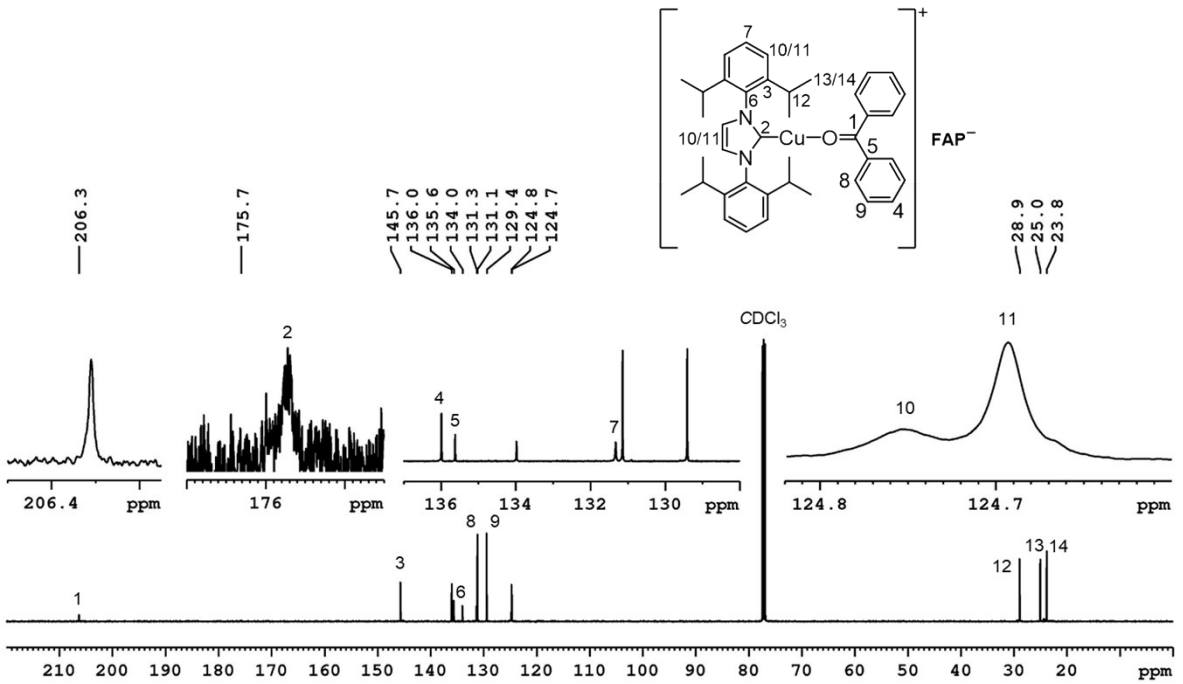

Figure S123. $^{13}C\{^{1}H\}$ NMR spectrum (125.8 MHz) of **27** recorded in $CDCl_3$.

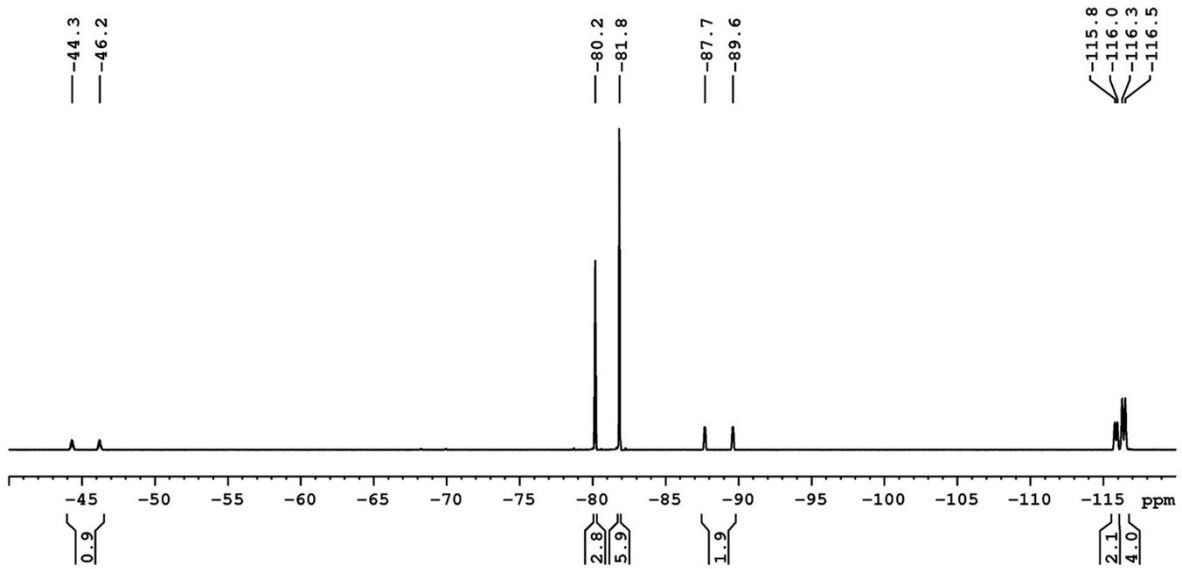

Figure S124. ^{19}F NMR spectrum (470.5 MHz) of **27** recorded in $CDCl_3$.

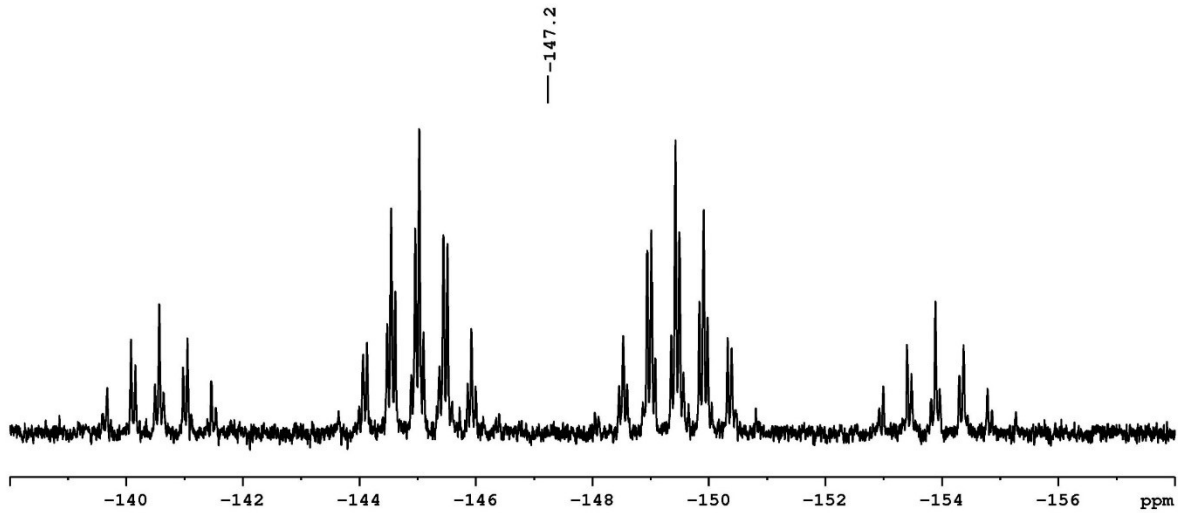

Figure S125. ^{31}P NMR spectrum (202.4 MHz) of **27** recorded in $CDCl_3$.

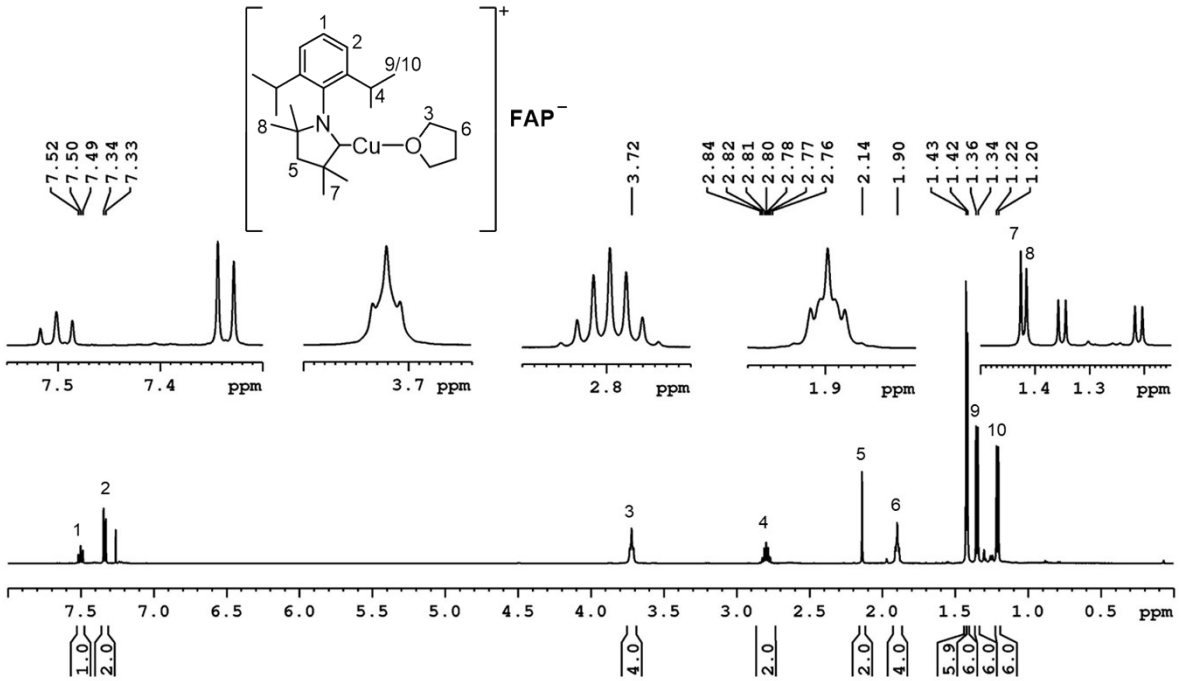

Figure S126. ^{1}H NMR spectrum (500.1 MHz) of **28** recorded in $CDCl_3$.

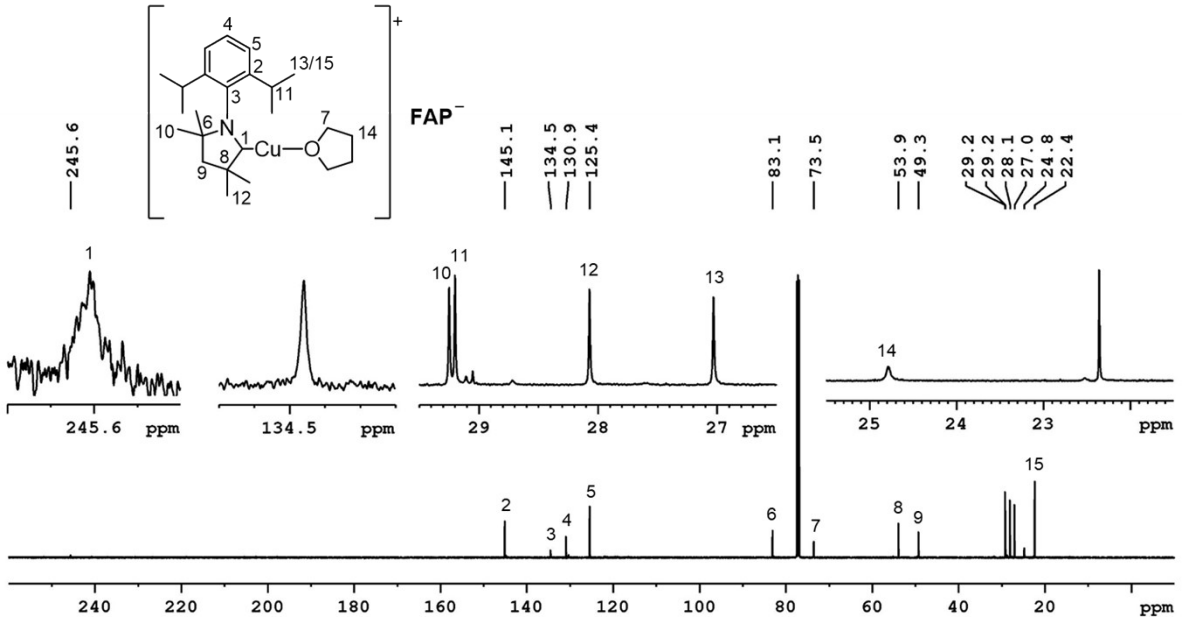

Figure S127. $^{13}C\{^{1}H\}$ NMR spectrum (125.8 MHz) of **28** recorded in $CDCl_3$.

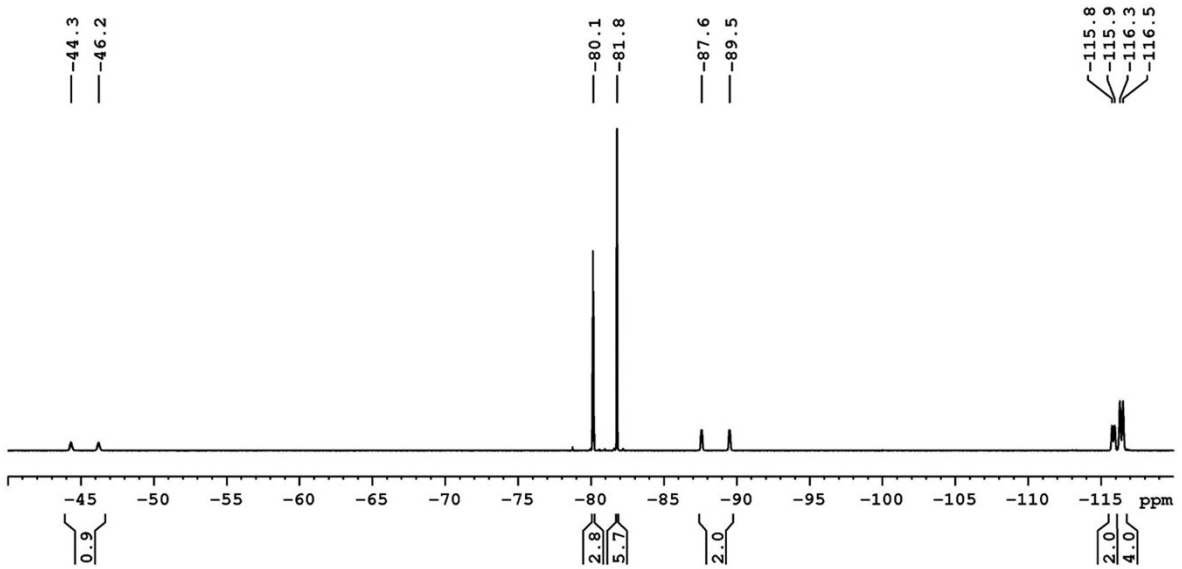

Figure S128. ^{19}F NMR spectrum (470.5 MHz) of **28** recorded in $CDCl_3$.

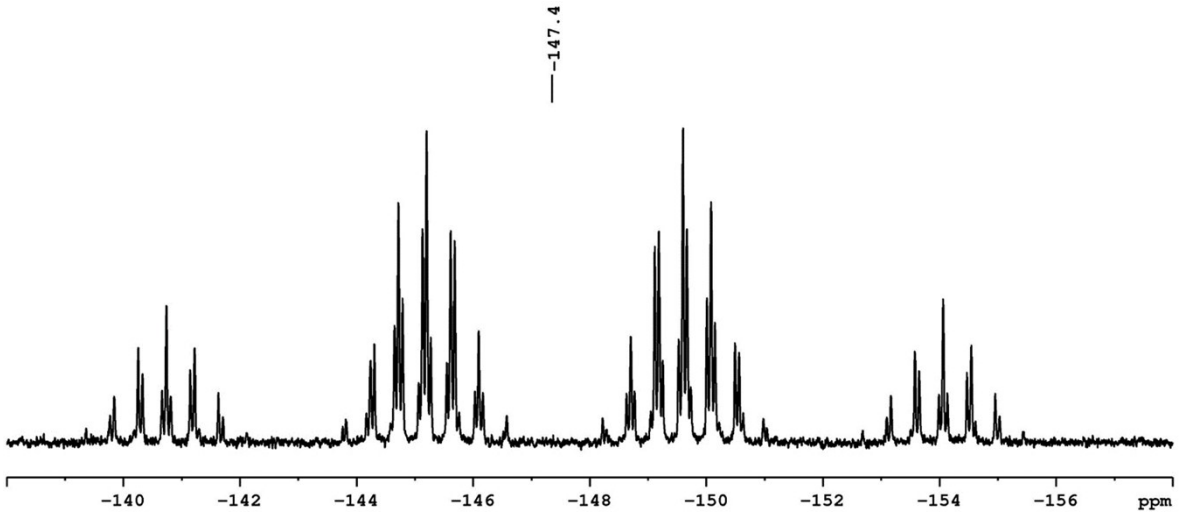

Figure S129. ^{31}P NMR spectrum (202.4 MHz) of **28** recorded in $CDCl_3$.

References

(1) Sheldrick, G. SHELXT - Integrated Space-Group and Crystal-Structure Determination. *Acta Crystallogr., Sect. A: Found Chrstallogr* **2015,** *71* (1), 3−8.